CORRELATIONS BETWEEN SPINAL DEFORMITY AND BACK MUSCLE STIFFNESS DISTRIBUTION

CHENG LOK KAN

M.Phil

The Hong Kong Polytechnic University

2017

The Hong Kong Polytechnic University

Interdisciplinary Division of Biomedical Engineering

Correlations between Spinal Deformity and Back Muscle Stiffness Distribution

Cheng Lok Kan

A thesis submitted in partial fulfillment of the requirements for the degree of Master of Philosophy

June 2016

CERTIFICATE OF ORIGINALITY

I hereby declare that this thesis is my own work and that, to the best of my knowledge and belief, it reproduces no material previously published or written, nor material that has been accepted for the award of any other degree or diploma, except where due acknowledgement has been made in the text.

_____ (Signed)

Cheng Lok Kan (Name of student)

ABSTRACT OF THESIS

"Correlations between Spinal Deformity and Back Muscle Stiffness Distribution"

Submitted by Cheng Lok Kan

For the degree of Master of Philosophy

At The Hong Kong Polytechnic University

In April 2016

Asymmetry of para-spinal muscle properties such as muscle activity, morphology and histology are often related to the etiology of idiopathic scoliosis (IS). Changes of these properties change can also lead to a change in muscle stiffness. However, very few studies attempted to investigate the para-spinal muscle stiffness distribution and asymmetry in either normal or IS population. Therefore, this study aimed to systematically document the para-spinal muscle stiffness distribution along and across the spine of normal subjects and idiopathic scoliosis subjects with objective indentation measurement. The significances of this study were to demonstrate if there was any para-spinal muscle stiffness imbalance existed in normal subjects and IS patients.

In this study, a manual indentation system was developed and verified to perform muscle stiffness measurements. The system was comprised of a load cell and an electromagnetic spatial sensor to measure force applied to muscle and the subsequent deformation. Measurement results obtained were highly comparable with a standard mechanical testing machine (R^2=.9903, p=.001) and had excellent intra- and inter-operator reliability (both ICC>0.9).

Para-spinal muscle stiffness of normal subjects including male (n=13) and female (n=20) was measured separately at 1.5 cm (n=22) and 3 cm (n=11) contralateral to the spinous processes of T3, T7, T11 and L4 vertebral levels in relaxed standing. To test the system's repeatability, nine of the normal subjects underwent another measurement at the same locations of T3 and L4 one day after the first measurement. The measurements were reproducible (ICC >0.8). Para-spinal muscle stiffness measurement was also taken on IS subjects (n=25; male=7; female=18) separately at 1.5 cm (n=13) and 3 cm (n=12) contralateral to the spinous process of vertebrae at the level of upper end, apex and lower end of the largest curvature as well as the T3, T7, T11 and L4. Both the measurements on normal and IS subjects adopted the same protocol.

The average para-spinal muscle stiffness was found to be significantly larger along the left hand side of the normal spine ($p<.05$). The imbalance diminished when separation from spinous process increased from 1.5 cm to 3 cm. Muscle stiffness at T7 and T11 was demonstrated to be significantly larger than that at T3 and L4 in the normal subjects. Regardless of apex location in the scoliosis subjects, the muscle stiffness distributions between left and right side, along the spine and at different separations from spinous process were similar to the results of normal subjects.

When para-spinal muscle stiffness of scoliosis subjects was analyzed according to the apex location, para-spinal muscles on convex side of the lumbar curve and on concave side of the thoracic curve were observed to have larger stiffness but did not show significant difference with the lateral side except at location of 1.5 cm at lower end of thoracic curve. Para-spinal muscle stiffness along lumbar curve gradually reduced from upper end towards the lower end. While along the thoracic curve, muscle stiffness increased then decreased with the largest value at the apex level. Para-spinal

muscle stiffness at the same spine regions of the normal and scoliosis subjects were compared. Muscle stiffness at the concave side of the left lumbar curve was lower than the right lumbar spine of the normal spine while muscle stiffness at the concave side of the right thoracic curve was larger than the left thoracic of the normal subjects.

The main findings of this study can be summarized as follows. First, average para-spinal muscle stiffness was larger on the left hand side of normal subjects in relaxed standing posture. Para-spinal muscle stiffness imbalance between left and right hand sides could be associated with a pre-existed vertebral rotation in the normal subjects but the cause of muscle stiffness change was uncertain. Second, para-spinal muscle stiffness imbalance observed across and along the spine in relaxed standing might be normal and irrelevant to the existence of scoliosis. Finally, inconsistent relationships between para-spinal muscle stiffness at concavity of different scoliosis apex locations and the same spinal region in normal spine suggested para-spinal muscles might play more than one role in the cause and development of scoliosis.

PUBLICATIONS ARISING FROM THE THESIS

Conference proceedings

1. Connie LK CHENG and Yong-Ping ZHENG. Development of a manual indentation system for objective assessment of back muscle stiffness, BME 2014 Conference, Hong Kong, Dec, 2014.

2. Connie LK CHENG and YP Zheng, Para-spinal muscle stiffness distribution on normal subjects in standing position, Fourteenth International Tissue Elasticity Conference, Verona, Italy, pp 64, Sept 2015.

Journal paper being prepared for submission

1. Connie LK CHENG and Yong-Ping ZHENG. Para-spinal muscle stiffness distribution on normal subjects in standing position. Being prepared for submission.

ACADEMIC AWARD

1. Hong Kong Medical and Healthcare Industries Association (HKMHDIA), Student Research Award 2013-2014, 2nd Runner-up.

ACKNOWLEDGEMENTS

Taking this opportunity, I would like to express my gratitude to all those who had provided help during my study. There are a lot of people I would like to thank whose names cannot be completely listed out here.

Much of my thank goes to my supervisor Prof. Yong-ping Zheng who gave me an opportunity to be a part of his research team. His tremendous support in knowledge, experience and resources has guided me through each obstacle in the past few years. I believe what I learnt here will continue to brighten my future.

Special appreciation also goes to Mr. Wong Ming Sun and his staff for sharing their professional knowledge in manual therapy as well as providing help in recruiting participants.

Part of the credit for the success of this study goes to former and present colleagues of Prof. Zheng's team and other staff and fellow research students in the department for their technical support and honest opinion.

Not to mention all the participants in my study for their precious time and effort. Without their participation in all the measurements, this study could not have succeeded.

Last but not least, my friends and family for their unconditional support during this journey.

TABLE OF CONTENTS

CERTIFICATE OF ORIGINALITY ..... **I**
ABSTRACT OF THESIS ..... **II**
PUBLICATIONS ARISING FROM THE THESIS ..... **V**
ACADEMIC AWARD ..... **VI**
ACKNOWLEDGEMENTS ..... **VII**
TABLE OF CONTENTS ..... **VIII**
LIST OF ABBREVIATIONS ..... **XI**
LIST OF FIGURES ..... **XII**
LIST OF TABLES ..... **XVIII**
CHAPTER 1 INTRODUCTION **1**
1.1. Background **1**
1.2. Objectives **5**
1.3. Dissertation outline **6**
CHAPTER 2 LITERATURE REVIEW **7**
2.1. Spine anatomy—Bones **7**
2.2. Spine anatomy—Muscles **9**
2.3. Introduction of scoliosis **12**
2.4. Introduction of idiopathic scoliosis **14**
2.5. Current medical management for IS patients **17**
2.6. Alternative treatment for IS **22**
2.7. Concept of IS development in manual therapy **24**
2.8. Previous studies on para-spinal muscle stiffness imbalance in scoliosis **29**
2.9. Presence of para-spinal muscle asymmetry in scoliosis **31**
2.9.1. Imbalance in electromyography in para-spinal muscles 32
2.9.2. Imbalance in histologic compositions in para-spinal muscles 34
2.9.3. Imbalance in morphology in para-spinal muscles 36
2.9.4. Summary on studies in para-spinal muscle imbalance 38
2.10. Para-spinal muscle stiffness distribution in normal population **39**
2.11. Significance of para-spinal muscle stiffness measurement **42**
2.12. Objective evaluation methods for muscle stiffness **43**
2.12.1. Tissue compliance meter 44
2.12.2. Myotonometer® 46
2.12.3. Indentation instrumentation for research purposes 49
2.12.4. Tissue ultrasound palpation system (TUPS) 50
2.12.5. Ultrasound elastography 53
CHAPTER 3 METHODS **61**
3.1. Manual indentation system for stiffness measurement **61**

3.1.1. Hardware — Indentation probe 62
3.1.2. Software — Data acquisition 65
3.2. Calibration of indentation system — Loading on tissue 67
3.3. Calibration of indentation system — Deformation of tissue 67
3.3.1. Calibration for orientation matrix — Pivot calibration method 69
3.4. Data collection and analysis 73
3.5. Validation tests of manual indentation system performance 76
3.5.1. Validation of probe displacement measurement 77
3.5.2. Validation of Young's modulus measurement 78
3.5.3. Location dependency of measured Young's modulus to the location from the field transmitter 80
3.5.4. Intra- and inter- operator reliability of Young's modulus measurement on phantoms 81
3.6. Stiffness measurement on para-spinal muscles *in vivo* 82
3.6.1. Recruitment of normal and scoliosis subjects 82
3.6.2. Scoliosis assessment using 3D ultrasound imaging system 84
3.6.3. Young's modulus measurement on para-spinal muscles of normal subjects 88
3.6.4. Young's modulus measurement on para-spinal muscles of scoliosis subjects 90
3.7. Intra- and inter-operator reliability of Young's modulus measurement of para-spinal muscles *in vivo* 91
3.8. Statistical analysis on Young's modulus measurement *in vivo* 91
CHAPTER 4 RESULTS 93
4.1. Probe displacement measurement after calibration 93
4.2. Correlation between Young's moduli measured by the new method and the reference method 94
4.3. Location dependency of Young's modulus measurement with reference to the electromagnetic transmitter 95
4.4. Intra and inter-operator reliability of Young's modulus measurement on phantoms 96
4.5. Para-spinal muscle stiffness measured *in vivo* 97
4.6. Intra- and inter-operator reliability of para-spinal muscle stiffness measured *in vivo* 98
4.7. Normal para-spinal muscle stiffness distribution 98
4.8. Para-spinal muscle stiffness distribution in presence of scoliosis 104
4.9. Para-spinal muscle stiffness distribution along major curve of scoliosis 109
CHAPTER 5 DISCUSSION 117
5.1. Performance of the manual indentation system 117
5.2. Para-spinal muscle stiffness distribution in normal subjects 121
5.2.1. Para-spinal muscle stiffness imbalance between lateral sides 123
5.2.2. Para-spinal muscle stiffness variation between spinal regions 130
5.2.3. Para-spinal muscle stiffness variation between muscle groups 133

5.3. Para-spinal muscle stiffness distribution in scoliosis subjects 135
5.4. Limitations of the study 140
5.5. Future studies 143
CHAPTER 6 CONCLUSIONS 145
APPENDICES 148
I English version of information sheet 148
II Chinese version of information sheet 150
III English version of informed consent for participants above 18 151
IIII Chinese version of informed consent for participants above 18 152
IV English version of informed consent for parents or guardians of participants below 18 153
V Chinese version of informed consent for parents or guardians of participants below 18 154
REFERENCES 155

LIST OF ABBREVIATIONS

3D	Three dimensional
AIS	Adolescent idiopathic scoliosis
AUC	Area under curve
${}^{C}T_{R}$	Transformation matrix of spatial sensor to the center of flat-end indenter surface
EMG	Electromyography
EUS	Ultrasound elastography
ICC	Intraclass correlation coefficient
IS	Idiopathic scoliosis
MMT	Myotonometer
MT	Manual therapy
ROI	Region of interest
SPA	Spinous process angle
tCM	Tissue compliance meter
TCM	Traditional Chinese medicine
${}^{T}T_{C}$	Coordinate system with origin at center of flat-end surface indenter surface
${}^{T}T_{R}$	Transformation matrix of spatial sensor to electromagnetic field transmitter
TUPS	Tissue ultrasound palpation system

LIST OF FIGURES

Figure 2-1 Normal human spine viewed from side in sagittal plane (left) and from posterior direction in frontal plane. Thirty vertebrae are interconnected to form the spine. Spinal alignment is curved in side view and straight in back view. Figure was adopted from (NIAMS, 2015). 8

Figure 2-2 Outline of a vertebra from superior view (left). Vertebral arch is extended to the posterior side of vertebral body and connected by a pair of pedicles. The vertebrae are interconnected at the articular surfaces on the processes as shown in side view (right). Figure was adopted from ('Vertebral column', 2015). 9

Figure 2-3 The first and second layers of normal human para-spinal musculature counting from the bottommost. Multifidus of the first layer is shown on the left hand side of the spine. A portion of rotatores muscles being covered by multifidus are shown in the enlarged figure on the right. Erector spinae is the second layer and it is drawn on the right of the spine. The number and connection of para-spinal muscles are symmetrical in human body. Figure was adopted from (Anatomy human body, 2016). 11

Figure 2-4 Different types of scoliosis curve: (a) right single thoracic curve, (b) left lumbar curve, (c) right thoracolumbar curve and (d) double thoracic curve. Measurement of Cobb angle to describe the degree of deformity is also shown in (d). Figures were adopted from (NIAMS, 2015). 13

Figure 2-5 The chance of scoliosis progression with the progression factor was estimated by Lonstein and Carlson(1984). The progression factor was calculated using the formula listed under the graph. The numbers next to the data points indicated the number of cases it was based on. The form of treatment indicated to patients corresponding to the percentage of progrssion incidence was also labelled on the figure. Figure was adopted from (Weiss et al., 2006). 18

Figure 2-6 Front view of a patient wearing a custom-designed rigid orthosis around the body from axilla to sacral level. Figure was adopted from (Wong et al., 2008). 18

Figure 2-7 Front view of a patient wearing SpineCor, a kind of soft brace that puts harness on the body from multiple directions. Figure was adopted from (Wong et al., 2008). 19

Figure 2-8 Radiographs in frontal and sagittal plane of a patients with severe IS before (left) and after surgical correction (right). Curvature is straightened by fusing the vertebrae together by implants which appears as the brightest rods in the post-surgical radiographs. Figure was adopted from (British Columbia Children's Hospital, 2016) 19

Figure 2-9 Examples of MT techniques used by Chinese and Western therapists. (a) Pressing-and-kneading technique and (b) rolling technique are two kinds of mobilization techniques delivered in slow velocity. (c) Pulling and (d) levered thrust are two kinds of manipulation techniques delivered in high velocity. Notice that the same treatment outcome

is achieved by slightly different MT techniques by each MT branch as shown in (c) and (d). Figures a-c were adopted from (Fan and Wu, 2014). Figure d was adopted from (Vickers and Zollman, 1999). 23

Figure 2-10 Theory of scoliosis development proposed in Traditional Chinese medicine summarized from Wei (2006). 26

Figure 2-11 Co-contraction of deep para-spinal muscles on single side e.g. multifidus and rotators, results in the collapse of the adjacent vertebrae to the same side. Figure was adopted from (Polak, 2013). 27

Figure 2-12 Muscles on the convex side of scoliosis curve are overstretched. By contracting the convex muscles and stretching the contracted muscles on the concave side using MT techniques, the curvature can be reversed and scoliosis is corrected. Figure was adopted from (Lehnert-Schroth, 1992). 27

Figure 2-13 Average penetration depths of lateral para-spinal muscles induced by tissue compliance meter under the same indentation force. Both male and female healthy subjects were measured at two postures. Lower penetration depth indicated higher muscle stiffness at that location. Figure was adopted from (Waldorf et al., 1991). 40

Figure 2-14 (a) Para-spinal muscle stiffness at different points as represented by penetration depths was plotted onto a best-fit surface according to the point's location in an x-y plane defined on the back surface. (b) The projected para-spinal muscle stiffness across the back in form of color map. Brighter color (closer to red) indicates higher muscle compliance. Figures were adopted from (Williams II et al., 2007) 41

Figure 2-15 Tissue compliance meter for measuring tissue stiffness. Force is applied onto the tissue by compressing the device perpendicularly. Level of applied force can be read from the force gauge on top while the displacement can be read from markings on the shaft. Figure was adopted from (Fischer, 1987a). 44

Figure 2-16 (a) Outlook of Myotonometer for indentation measurement. The cable on the top is connected to computer for data recording. (b) The internal structure and working principle of the probe. When the probe is pushed onto soft tissue, the reference ring remains stationary while the inner indenter extends to compress the tissue. Figure a was adopted from (Performance Analysis Laboratory, 2015). Figure b was adopted from (Leonard and Mikhailenok, 2000). 47

Figure 2-17 Tissue ultrasound palpation system measuring soft tissue stiffness on neck. The part that was touching the skin surface is the ultrasound transducer. The load cell was inserted in between the indenter and the pen-size holder. Figure was adopted from (Leung et al., 2002). 51

Figure 2-18 Summary of the operation principle and calculation method for compression elastography. When the tissue is compressed, stiffer structure deforms less and shows lower strain. Strain is calculated by the degree of deformation and represented in grey or color

scale relative to the remaining structures. Figure was adopted from (Shiina, 2014).....54

Figure 2-19 The working principle of shear wave elastography in two steps. Successive ultrasonic pulses excite multiple focused areas in muscle and induce two plane shear waves in transverse directions. The propagation velocity of the travelling waves is then monitored by ultrafast imaging. Figure was adopted from (Gennisson et al., 2013). 57

Figure 2-20 (a) A diagram depicting the vibro-ultrasound system. Shear wave is induced in muscle by a mechanical vibrator and the propagation velocity of the shear wave is monitored by an ultrasound probe connected next to the vibrator. (b) The setup for measuring thigh muscle stiffness during a series of voluntary contractions. Figures were adopted from (Wang et al., 2014).....60

Figure 3-1 The hand-held indentation probe for stiffness measurement. The electromagnetic spatial sensor was put inside a plastic plug and inserted in the top of the probe. 62

Figure 3-2 Key components of the Ascension electromagnetic spatial sensing system. (a) Mid-range transmitter and (b) model 180 spatial sensor are connected to the labeled sockets at the front of (c) driveBAY control unit. The system supports at most 4 sensors working simultaneously. The control unit is connected to the computer via a USB port. Users can control the system through computer software provided by the company. Figures were adopted from (Ascension Technology Corporation, 2016). 63

Figure 3-3 Schematic diagram of data transmission in the newly developed manual indentation system.....64

Figure 3-4 The user interface of the LabVIEW program for controlling the indentation system and data collection. This figure captures the display of the program during an indentation measurement along z-direction of the transmitter. 65

Figure 3-5 An illustration of coordinate systems between the probe and the magnetic field transmitter. Pivot calibration allowed the unknown transformation matrix from sensor to indenter ($^{C}T_{R}$) to be found with the locations of the other two points known. Location of indenter center to transmitter ($^{T}T_{C}$) during indentation was found later through matrix operation.....68

Figure 3-6 A plastic calibration stand designed for pivot calibration of the indentation probe. The stand can be fixed at different distances from the transmitter with plastic bolts. The indentation probe is connected to the cap with the free end of the load cell. Once connected, the probe can be moved to all orientations about the same point.....70

Figure 3-7 The typical force and deformation responses from tissue during indentation test after synchronization. The rising part of the indentation curve suggested that the indentation was moving into tissue. This part was used for Young's modulus calculation in this study.....73

Figure 3-8 The user interface of the data analysis program in MATLAB. After a data file is uploaded, user labels the start as "trough" and the end as "peak" of each cycle's indention phase by mouse clicking on the curves. The resulted force-deformation curves of all cycles

are shown in the space below. Initial tissue thickness of the measured object, indenter radius and range of indentation force for analysis are required to be filled in the respective textboxes for calculation using the Hayes' model. Results calculated for each cycle are shown in the table at lower right corner. 75

Figure 3-9 (a) Setup of the translation platform with the probe attached on. The platform was installed on a movable stage driven by a micrometer head. (b) An enlarged view of the movable stage controlled by the micrometer head. Figure b was adopted from (Mitutoyo, 2012). 77

Figure 3-10 The standard mechanical testing machine used in this study. A silicone phantom (black in color) was placed on the flat platform readied to be indented. A flat-ended steel rod with 9 mm diameter was used as the indentation probe and connected to the force actuator of the machine. 78

Figure 3-11 The setup of location dependency test. 80

Figure 3-12 The 3D ultrasound imaging system. Patients are required to stand on the anti-fatigue mat and face the patient monitor during scanning. 84

Figure 3-13 (a) A patient stood on the mat and four supporters were placed at his acromia and lateral anterior superior iliac spines. (b) The patient was being scanned. The spine from L5 up to C7 would be scanned. 85

Figure 3-14 (a) A typical 2-dimensional spine image in frontal view obtained from a scoliosis subject which is similar to a posterior-anterior radiograph. (b) The measurement of SPA to indicate spinal deformity on the spine image. A pair of lines were drawn on the shadow of spinous processes of the most tilted vertebrae along the curve. The angle was calculated automatically after the lines were drawn. If there are two curves, a third line could be drawn at the lower end vertebra of the second curve to calculate the second angle. 87

Figure 3-15 The 8 locations for measurements on normal subjects were labelled by dots. Measurements were taken at different separations from the spinous process of the same vertebral level for groups Normal_1.5cm and Normal_3cm. Picture was adopted and modified from (Department of Nursing and Orthopaedic Surgery, 2011). 88

Figure 3-16 An ultrasound image taken at L4 in transverse direction. The arrow indicated the spinous process. The up-down arrow indicated the initial tissue thickness 1.5 cm from spinous process at L4. 89

Figure 3-17 The 14 locations for measurements on scoliosis subjects were labelled by dots. Measurements were taken at different separations from the spinous process of the same vertebral level for groups Scoliosis_1.5cm and Scoliosis_3cm. Picture was adopted and modified from (Department of Nursing and Orthopaedic Surgery, 2011). 90

Figure 4-1 The correlation between displacement of the indenter reported by the calibrated system and displacement of the translation platform controlled by the micrometer. 93

Figure 4-2 Young's modulus of the phantoms measured by Instron and the manual indentation

system. The asterisk "*" signs marked the phantoms that were fabricated with chemicals from another brand. 94
Figure 4-3 The correlation between Young's moduli of the phantoms measured by Instron and the manual indentation system. 95
Figure 4-4 Young's modulus of the phantoms measured by the manual indentation system at three separations from the origin of the field transmitter along its positive x-axis. 96
Figure 4-5 The average Young's modulus of para-spinal muscles measured at 1.5 cm and 3 cm bilateral to the spinous processes at vertebral level T3, T7, T11 and L4 of normal subjects. 99
Figure 4-6 The average Young's modulus of para-spinal muscles measured at 1.5 cm and 3 cm bilateral to the spinous processes at vertebral level T3, T7, T11 and L4 of scoliosis subjects. 105
Figure 4-7 The average Young's modulus measured at different locations of scoliosis subjects. (a) Results of 1.5 cm group with lumbar curve. (b) Results of 1.5 cm group with thoracic curve. (c) Results of 3 cm group with lumbar curve. (d) Results of 3 cm group with thoracic curve. A pair with significant difference is marked by an asterisk "*" on top. 112
Figure 4-8 The apexes locations and the curves' direction of scoliosis subjects in this study. The apexes of lumbar curves were in between T11-L4 while the apexes of thoracic curves were mostly in between T7-T11. Lumbar curves mainly convexed to the left while thoracic curves mainly convexed to the right. 113
Figure 4-9 The average Young's modulus at different locations on the corresponding spinal regions between normal and scoliosis groups. (a) Comparison at lumbar at 1.5 cm. (b) Comparison at thoracic 1.5 cm. (c) Comparison at lumbar 3 cm. (d) Comparison at thoracic 3 cm. A pair with significant difference is marked by an asterisk "*". 116
Figure 5-1 the deformation relative to the intial thickness of each layer in a porcine tissue during indentation. Tissue deformation was monitored with ultrasound. Figure was adopted from (Zheng and Mak, 1996). 120
Figure 5-2 (a) An eccentric loading on a vertebral body caused asymmetric growth on the vertebrae. (b) The reaction froce applied to the superior and inferior normal vertebrae resulted in a force vector in the vertebrae with asymmetric growth and ld to deviation to one side. Figures were adopted from (Burwell, 2003). 122
Figure 5-3 (a) Mean rotation angle at each vertebral level from T2 to L5 of normal subjects without scoliosis. (b) Mean rotation angle at each vertebral level from T2 to L5 of subjects with situs inversus totalis and without scoliosis. Figure were adopted from (Kouwenhoven et al., 2007). 126
Figure 5-4 Muscle activity levels normalized to the baseline activity of some muscles groups in human in erect standing (in the middle of 3 columns). In this discussion, only the relationship between superficial lumbar multifidus (SLM) and thoracic erector spinae (TES)

was focused (in brackets). TES had a higher activity than SLM. Figure was adopted from (O'Sullivan et al., 2002). 132

Figure 5-5 The percentage change of skinfold thickness between the convex side and the concave side along the curvature. The greatest change was identified at the apex level. Figure was adopted from (Zoabli et al., 2007)..... 139

LIST OF TABLES

Table 4-1 Physical characteristics of normal subjects measured at 1.5 cm and 3 cm bilateral to the spinous processes. 97

Table 4-2 Physical characteristics of scoliosis subjects measured at 1.5 cm and 3 cm bilateral to the spinous processes. For apex location, T, TL and L stand for thoracic, thoracolumbar and lumbar respectively. 97

Table 4-3 Average Young's modulus of muscles measured on different vertebral levels and locations from the spine. Results of statistical comparisons between "side" are included. Bold P-value shows a significant difference between the Young's moduli of lateral sides at that vertebral level. 99

Table 4-4 P-values generated by statistical analyses on the Young's moduli of any two vertebral levels in Normal_1.5cm group. Bold P-value shows a significant difference between Young's moduli of the two levels. 101

Table 4-5 P-values generated by statistical analyses on the Young's moduli of any two vertebral levels in Normal_3cm group. Bold P-value shows a significant difference between Young's moduli of the two levels. 102

Table 4-6 Average Young's modulus of muscles measured on different lateral locations from the spinous process on the same side of a vertebral level in normal subjects. Results of statistical comparisons between locations are included. Bold P-value shows a significant difference between the Young's moduli of different locations at that vertebral level. 103

Table 4-7 Average Young's modulus of muscles measured on different vertebral levels and locations from the spine of scoliosis subjects. Results of statistical comparisons between "side" are included. Bold P-value shows significant difference between "side" at that vertebral level. 105

Table 4-8 P-values generated by statistical analyses on the Young's moduli of any two vertebral levels in Scoliosis_1.5cm group. Bold P-value shows a significant difference between Young's moduli of the two levels. 106

Table 4-9 P-values generated by statistical analyses on the Young's moduli of any two vertebral levels in Scoliosis_3cm group. Bold P-value shows a significant difference between Young's moduli of the two levels. 107

Table 4-10 Average Young's modulus of muscles measured on different lateral locations from the spinous process on the same side of a vertebral level in scoliosis subjects. Results of statistical comparisons between locations are included. Bold P-value shows a significant difference between the Young's moduli of different locations at that vertebral level. 108

Table 4-11 The average Young's modulus measured at different locations of subjects from group Scoliosis_1.5cm separated according to curve's apex location. Results of statistical comparisons between "side" at the 3 levels are included. Bold P-value shows significant

difference between "side" at that vertebral level. 111

Table 4-12 The average Young's modulus measured at different locations of subjects from group Scoliosis_3cm separated according to curve's apex location. Results of statistical comparisons between "side" at the 3 levels are included. Bold P-value shows significant difference between "side" at that vertebral level. 111

Table 4-13 The average Young's modulus on both sides at apex level of group Scoliosis_1.5cm and on the corresponding spinal region of group Normal_1.5cm. Results of statistical analysis between groups are included. Bold P-value shows significant difference between groups at that vertebral level. 115

Table 4-14 The average Young's modulus on both sides at apex level of group Scoliosis_3cm and on the corresponding spinal region of group Normal_3cm. Results of statistical analysis between groups are included. Bold P-value shows significant difference between groups at that vertebral level. 115

Table 5-1 Young's Modulus results for left handed normal subjects at 4 vertebral levels. 127

CHAPTER 1 Introduction

In the beginning of this dissertation, a brief introduction is presented to illustrate the initiative of current research direction and rationale of this study.

1.1. Background

Scoliosis is a pathological condition that there is a notable 3-dimensional spine deformity and frequently accompanied by asymmetries of trunk and extremities (Cheng et al., 2015). Around 80% of scoliosis affected population is idiopathic and deformity occurred with unknown cause (Luk et al., 2010, Schlösser et al., 2014). When the lateral curvature in frontal plane is larger than 10 degrees of Cobb angle, it is considered to have clinical significance (Weiss et al., 2006). The onset of idiopathic scoliosis (IS) is most prevalent during growth spurt at adolescence (Luk et al., 2010). There may be risk of progression in scoliosis depending on the patient's gender, age at first detection, bone maturity and location of scoliosis apex (Lonstein and Carlson, 1984).

Patients are regularly monitored for curve progression or referred to physiotherapy if necessary. Bracing or ultimate spinal fusion surgery would be recommended if curve progressed to a certain extent (Weiss et al., 2006). The efficacy for inhibiting curve progression by long period bracing and curve correction by surgery has been supported by previous studies (Asher and Burton, 2006, Weinstein et al., 2013). Nevertheless, a large proportion of patients are unwilling to simply receive observation or be put under aggressive treatments (Lantz and Chen, 2001).

At the same time, uneven rib cage resulted from scoliosis often affects cosmetic appearance of the patient. Scoliosis is sometimes accompanied by back pain

(Weinstein et al., 2008). Although the influence of scoliosis on patients' quality of life was inconclusive (Asher and Burton, 2006), it cannot be ruled out that some patients suffered from negative impacts (Tones et al., 2006). Being unsatisfied with common modes of scoliosis treatments and wishing to reverse scoliosis has therefore motivated patients to seek alternative therapy like manual therapy (MT).

MT is a diverse field with different disciplines such as chiropractors in Western society and Chinese bone setting in Chinese society, but in general, they share a common belief that the cause and development of IS is related to para-spinal muscle abnormality (Danbert, 1989, Li, 2001). When one side of spinal muscles experiences alternation which can be reflected by a change in muscle stiffness, the effect slowly leads to convexity of scoliosis. Different therapists reported the observations of para-spinal muscle stiffness imbalance across and along the curvature of IS patients. However, the distribution pattern of muscle stiffness due to the curvature is conflicting (Du et al., 2013, Muscolino, 2015). Judgements by manual therapists were not convincing as they were made based on subjective manual palpation. Objective measurement of para-spinal muscle stiffness is definitely required to investigate the possibility of stiffness imbalance in IS patients.

The notion of para-spinal muscle stiffness imbalance in IS patients has been mentioned for many years; however only one recent study was found to have measured para-spinal muscle stiffness on IS patients (Oliva-Pascual-Vaca et al., 2014). This study reported no significant difference in the stiffness between para-spinal muscles across the deformed spine at different vertebral levels in prone posture although stiffness appeared to be larger on the concavity. Subjects with mild curvature in prone posture with reduced physiological loading adopted for their measurements could be a reason for not showing statistical significance (Oliva-Pascual-Vaca et al.,

2014). There is a need for more related objective study on para-spinal muscle stiffness in scoliosis subjects with larger curvature and in different postures such as standing.

Any imbalance of para-spinal muscle stiffness that may exist in scoliosis subjects should not be certified without comparing with normal para-spinal muscle stiffness distribution. Limited past published results could be found for the quantification of para-spinal muscle stiffness value or evaluation of muscle stiffness symmetry across and along the normal straight spine (Waldorf et al., 1991). Information about the normal para-spinal muscle stiffness distribution across and along different spinal regions is essential as reference for the study of muscle stiffness in scoliosis and for the understanding of human spinal muscles functionality.

Meanwhile, para-spinal muscles are often associated with the etiology of scoliosis as it is a major structure to maintain the structure of human spine and an active system to bring about movement of the skeleton (Mannion et al., 1998). Therefore, a lot of past researches were dedicated to identify abnormal change in para-spinal muscles in IS patients from normal population. Previous studies focused on muscle electromyography (EMG) at different loading conditions, muscle histologic compositions and morphology (Avikainen et al., 1999, Mannion et al., 1998, Kennelly and Stokes, 1993). Most studies found abnormality and asymmetric behavior of para-spinal muscles across curvature despite the results being contradicting. In general, muscles on the convex side exhibited higher EMG signals (Machida, 1999), higher type I muscle fiber for tonic activity (Ford et al., 1984) and reduction in dimension (Kennelly and Stokes, 1993). Previous studies related to other para-spinal muscle properties have provided confidence to the existence of stiffness imbalance in IS patients. Since muscle stiffness relates to muscle activity and compositions, it is not surprising to find asymmetric para-spinal muscle stiffness in IS patients.

Therefore, we hypothesized that para-spinal muscle stiffness imbalance may exist and is significant in IS patients compared with normal subjects. The asymmetry might be related to the direction of spinal curvature or the region of deformity.

Limb muscle stiffness quantification and analysis at different physiological conditions have been widely published and discussed by different research groups. Most common ways of muscle stiffness measurement involve indentation and elastography. Indentation method simulates the action of manual palpation so it is more suitable for this study. Muscle stiffness is calculated by measuring the degree of muscle deformation under various force applied by the indentation probe. Different measurement tools either performed manually or mechanically have been developed and reported (Zheng and Mak, 1996, Fischer, 1987b, Leonard et al., 2003). However, different tools and stiffness calculation methods have various limitations such as poor reliability (Arokoski et al., 2005), analysis method omitted boundary condition (Koo et al., 2011) and chance of signal disconnection (Zheng and Mak, 1996) which are not favorable to be used in para-spinal muscle stiffness measurement. Therefore, we intended to develop another indentation tool for measurement.

Stiffness, which represents muscle functionality, can be measured more conveniently compared with other factors studied in para-spinal muscles. It requires less preparation work and operational skills than EMG recording and different clinical imaging. Also, unlike histologic studies performed previously, it can be measured repeatedly. If para-spinal muscle stiffness distribution in normal and scoliosis subjects can be successfully demonstrated, the muscle stiffness can serve as a potential indicator of muscular change under pathological conditions in clinical settings. Also it has the advantage of repeatable measurement for extensive research of para-spinal muscle change during the course of progression and treatment in scoliosis.

1.2. Objectives

The following objectives were aimed to be achieved through this study.

1. To develop a reliable, effective and non-invasive measurement system for *in vivo* para-spinal muscle stiffness;

2. To establish a baseline of para-spinal muscle stiffness distribution along and across the spine in normal subjects in standing posture;

3. To identify para-spinal muscle stiffness distribution along and across the deformed spine in scoliosis subjects in standing posture;

4. To compare the para-spinal stiffness between normal and scoliosis subjects in the same spinal region.

1.3. Dissertation outline

The main content of this dissertation is divided into following chapters.

Chapter 2 is a literature review on human spinal musculoskeletal anatomy, general knowledge about idiopathic scoliosis, MT and its theory on para-spinal muscle imbalance. A summary of previous studies on para-spinal muscles in scoliosis subjects and a comparison of objective measurement tools for muscle stiffness are also given.

Chapter 3 includes the development and verification of the manual indentation system. The protocol for the para-spinal muscle stiffness measurement in normal and scoliosis subjects and subsequent statistical analyses are also presented.

Chapter 4 presents the verification results of the manual indentation system and the findings on para-spinal muscle stiffness in both subject groups.

Chapter 5 discusses the performance of the manual indentation system and focuses mainly on explaining the para-spinal muscle stiffness distribution pattern observed in both subject groups. Limitations of this study and future research directions sprang up from this study are proposed at the end.

Chapter 6 summarizes and concludes the major findings on para-spinal muscle stiffness distribution in normal and scoliosis subjects and the potential reasons for such results.

CHAPTER 2 LITERATURE REVIEW

In this chapter, background knowledge for this study is elaborated. Basic anatomy of normal human spine and the supporting para-spinal muscle system are described. Basics of scoliosis and idiopathic scoliosis are also explained. Manual therapy and the field's understanding on initiation of idiopathic scoliosis are presented to point out the necessity of studying muscle stiffness. Previous studies investigating para-spinal muscles asymmetries in scoliosis are listed out and used to raise the possibility of muscle stiffness imbalance in the same condition. Related studies on para-spinal muscle stiffness in normal and scoliosis subjects are also reviewed to indicate the significance of our study in this research direction. Finally, a need for developing a new measurement system for this study is presented by evaluating a list of instrumentations used in reported muscle stiffness analysis.

2.1. Spine anatomy—Bones

Human spine is an important musculoskeletal structure that provides support and movement to our body (Figure 2-1). The spine contains 30 pieces of vertebrae and is divided into 5 regions down its length. The first 3 regions: cervical, thoracic and lumber descending from the top are comprised of 24 pieces of movable vertebrae. The remaining vertebrae in sacral and coccygeal regions are fused into one piece and cannot be distinguished. Each vertebra is joined on top of another to form a column. In upright posture, a normal human spine is curved when viewed in sagittal plane. The spine has natural curves for balancing where cervical and lumber spines are convex forward and thoracic and sacral spines are convex backward (Roussouly et al., 2005). However, the erect spine has a straight alignment when viewed in frontal plane.

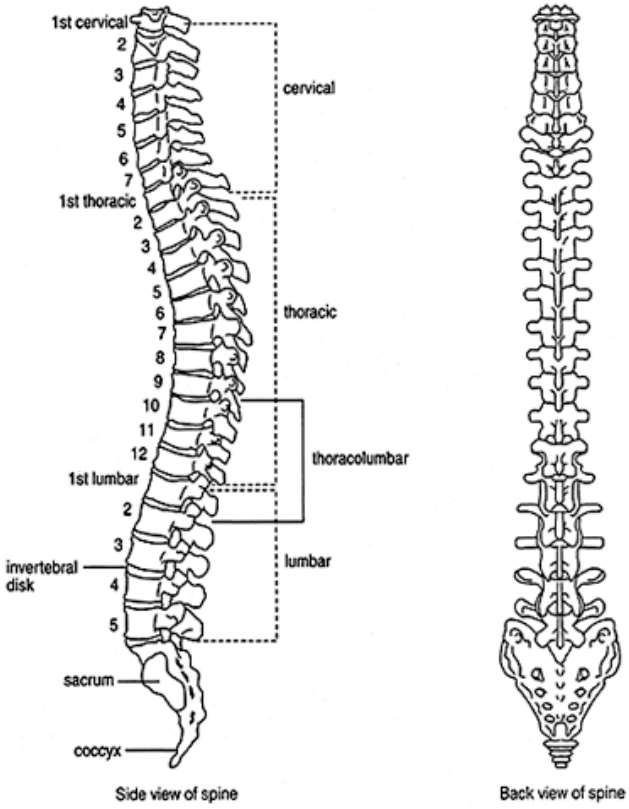

Figure 2-1 Normal human spine viewed from side in sagittal plane (left) and from posterior direction in frontal plane. Thirty vertebrae are interconnected to form the spine. Spinal alignment is curved in side view and straight in back view. Figure was adopted from (NIAMS, 2015).

Each movable vertebra has different size and shape but generally they all contain similar structures except the first two vertebrae in cervical spine. A normal vertebra has a round vertebral body in front (Figure 2-2). A pair of pedicles are extended to the back from vertebral body and connected by a flat sheet of bone called lamina. A space is formed in the middle allowing spinal cord to pass through. Lamina continues to grow backward and downward to form spinous process which can be felt as a bony prominence on the back. Transverse process is projected sideways from each pedicle. These bony extensions shape the major features of vertebral arch at the back of a vertebra. All vertebrae are linked by muscles and ligaments. The bony projections on the vertebral arch provide sites for ligaments and muscles attachments (Martini and Nath, 2009).

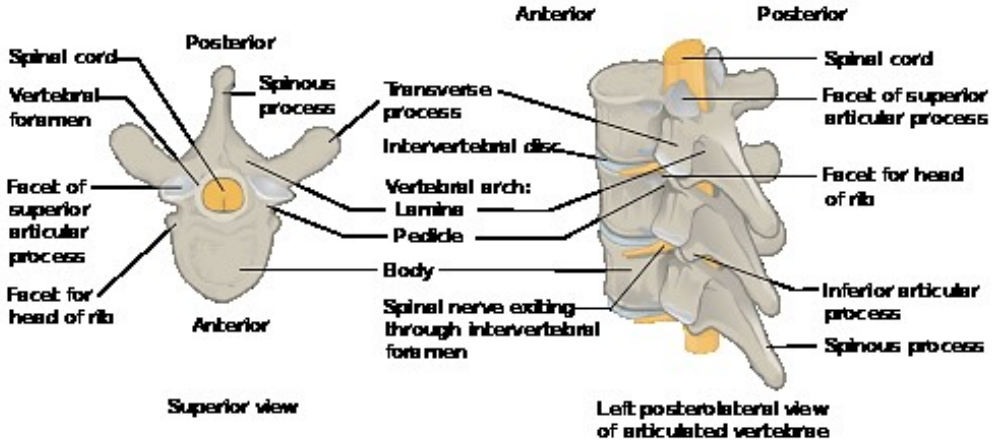

Figure 2-2 Outline of a vertebra from superior view (left). Vertebral arch is extended to the posterior side of vertebral body and connected by a pair of pedicles. The vertebrae are interconnected at the articular surfaces on the processes as shown in side view (right). Figure was adopted from ('Vertebral column', 2015).

2.2. Spine anatomy—Muscles

Human spine is capable of maintaining an upright posture and performing a range of movements. These functions are supported by layers of muscle groups attached on both anterior and posterior but dominating on the posterior side of spine. So "para-spinal muscles" or "back muscles" in this study only describes muscles at posterior of spine.

Back muscles can be separated into five layers. Both sides of the spine are covered by same layers of muscles symmetrically. The deepest layer (the first layer attached on the spine) is postural muscles which mainly contribute to maintaining erect posture. At the same time, this muscle layer facilitates active movement of spine in bending and rotation (Dimon, 2008).

Deep back muscle groups are comprised of small muscles that cover the entire length of spine (Figure 2-3). Muscles run between the bony projections of one vertebra and its superior vertebra or inferior rib. Some familiar muscle groups in this layer are multifidus and rotatores. Multifidus can be found almost in all spine regions. This muscle group spans from sacrum and links from one transverse process to the spinous process of the above vertebra (can be 3 to 6 levels up) (Maruyama, 1999, Bojadsen et al., 2000). The surfaces of laminae on both sides are filled with multifidus muscles. Rotatores, as the name suggests, assist in spinal rotation. This group of muscles inserts between transverse process of a vertebra and lamina of the next upper vertebra on the same side along thoracic spine.

Posture control and spine alignment are strengthened by the second layer of back extensor muscles on top of the deepest layer. This layer of muscles is known as erector spinae which is a board muscle sheet made up of three parallel columns of muscle bundles: iliocostalis, longissimus and spinalis from outside to innermost (Figure 2-3). Initiated from sacrum as masses of muscles, the muscles are divided into many ends and attach to above ribs or vertebral arch projections at different levels up to the head. Longissimus is in the middle and it is the longest column covering the whole length of spine. Its insertion ends are attached to transverse processes of thoracic and lumber spine and continue to go up to transverse processes of cervical vertebrae and finally arriving at the mastoid process of skull.

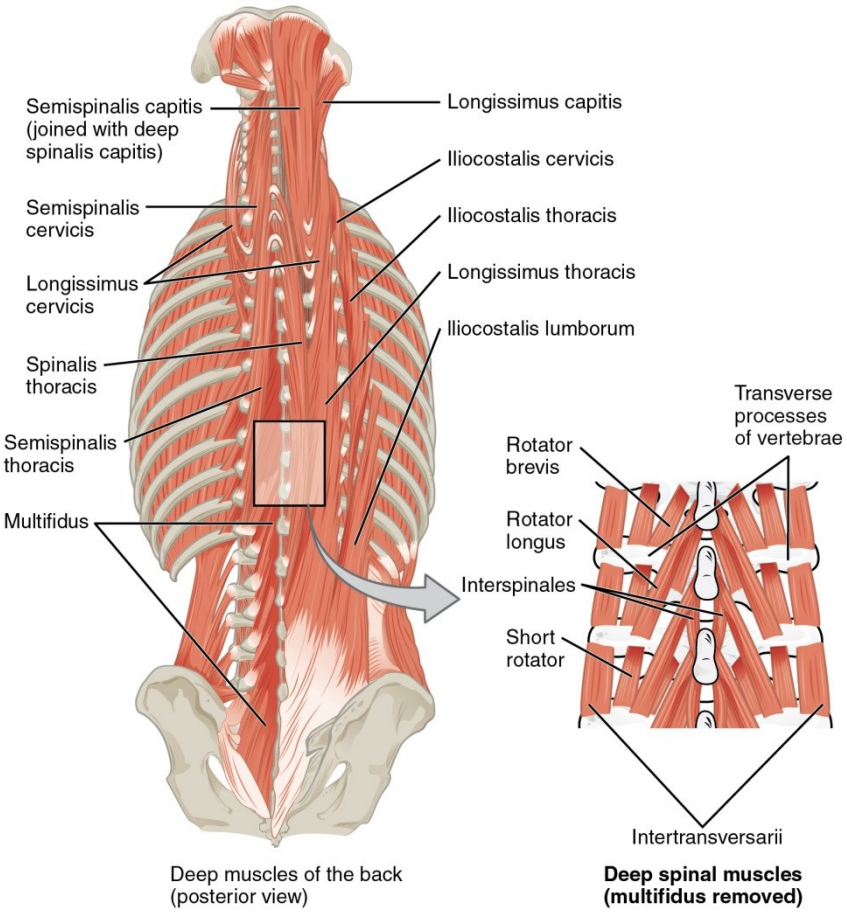

Figure 2-3 The first and second layers of normal human para-spinal musculature counting from the bottommost. Multifidus of the first layer is shown on the left hand side of the spine. A portion of rotatores muscles being covered by multifidus are shown in the enlarged figure on the right. Erector spinae is the second layer and it is drawn on the right of the spine. The number and connection of para-spinal muscles are symmetrical in human body. Figure was adopted from (Anatomy human body, 2016).

The middle and superficial layers are less involved in supporting erect posture. Muscles in the middle layers join between spinous processes of different vertebrae and ribs or scapulae for supporting these structures and widening the back. Meanwhile, the superficial layer (the final layer) consists of two broad muscles originated from spinous processes to shoulder and humerus which provide powerful movements of the upper limbs.

Keeping an erect posture relies heavily on the coordination of the two deep layers of extensor muscles. Different groups of muscles connecting to and along spine dominantly control the elongation of trunk as well as body movements. The term “para-spinal muscles” used in this study refers to the two deepest muscle layers. These two muscle layers combine to perform similar functions and run parallel to the spine on both sides.

2.3. Introduction of scoliosis

Human spine does not always follow the natural alignment and deformation can occur. Scoliosis is a three-dimensional (3D) spinal deformity and frequently accompanied by trunk and extremities asymmetries (Cheng et al., 2015). The spine has a structural lateral curvature in the frontal plane, change in sagittal alignment and axial rotation of vertebrae in the transverse plane simultaneously (Kotwicki, 2008). Rotation takes place as spinous process of vertebrae along the deviated spine segment rotates towards the concave side of curve and vertebral body to the convex direction (Stokes et al., 1987). A rib hump is often seen on the curve’s convex side due to asymmetric rib growth in the pathogenesis of scoliosis (Grivas et al., 2007).

Although a normal spine is generally straight in the frontal plane, a small degree of curvature is commonly observed in the human spine. The widely accepted method to determine spinal deviation is Cobb angle measurement on plane standing posterior-anterior radiograph (Weinstein et al., 2008, Negrini et al., 2012). Cobb angle is measured between two lines drawn on the endplates of the most tilted end vertebrae as shown in Figure 2-4d (Stokes, 1994). Only for curvatures with a deviation larger than 10 degrees from normal long axis of the spine should be considered as clinically significant and regarded as scoliosis (Weiss et al., 2006).

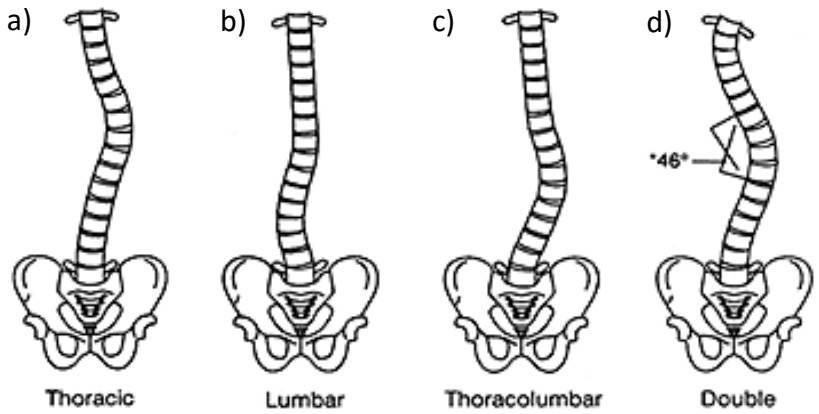

Figure 2-4 Different types of scoliosis curve: (a) right single thoracic curve, (b) left lumbar curve, (c) right thoracolumbar curve and (d) double thoracic curve. Measurement of Cobb angle to describe the degree of deformity is also shown in (d). Figures were adopted from (NIAMS, 2015).

Vertebral misalignment can be found in any region along the spine. Scoliosis pattern is classified by the spinal region where the apical vertebra locates in frontal plane (Figure 2-4a, b and c). The definition of apical region is set by the Scoliosis Research Society (Lenke et al., 2001). An apex can be skewed to either left or right hand side (Figure 2-4a and b). A deformed spine can have more than one apex on one deformed spine. Single curve, “C-shaped”, as shown in Figure 2-4a and double curves, “S-shaped”, in Figure 2-4d are predominant while triple curves is rarely observed in IS patients (Stokes et al., 1988). For double curve pattern, the curve with a larger Cobb angle measured is termed as major curve (Lenke et al., 2001).

The cause of scoliosis is multi-factorial (Hresko, 2013). Such spinal deformation can be brought about by neuromuscular dysfunctions and diseases (McCarthy, 1999), congenital spinal anatomical anomalies (Hedequist and Emans, 2007) or degeneration (Tribus, 2003). However, most cases of scoliosis have unrecognized cause and the occurrence is simply idiopathic (Burwell, 2003).

2.4. Introduction of idiopathic scoliosis

Idiopathic scoliosis (IS) is the most common form of scoliosis (Cassella and Hall, 1991) which accounts more than 80% (84-89%) of all scoliosis cases (Schlösser et al., 2014). Different possible causes of IS have been proposed. Hypotheses were made from concomitant abnormalities observed in IS patients. The etiology of scoliosis could be any intrinsic factor in spine such as asymmetrical loading in vertebrae during growth, posture equilibrium or alignment of the upright human spino-pelvic complex. It could also be due to extrinsic factors including neuromuscular, metabolic, chemical, and genetic abnormalities. There was no strong evidence to tight an abnormality to the onset of IS up to the present moment (Schlösser et al., 2014).

A lot of speculations and examinations have been devoted to IS but the exact etiology and natural history were still inconclusive (Wang et al., 2011). However, some factors originally proposed as etiological factors were believed to be secondary effect to scoliosis (Lowe et al., 2000). Scientists have meanwhile reached a general consensus that IS appears to have multiple etiological factors (Lowe, 2000, Wang et al., 2011) and such factors could be inter-correlated. Also, the same etiology and progression pathway might not be applied to all curve patterns (Machida, 1999).

IS can be further divided into three groups according to age of onset. From infantile (0-3 years) and juvenile (4-9 years) to adolescent (10-18 years), IS can develop or appear at any age (Yaman and Da Lbayrak, 2014). Adolescent idiopathic scoliosis (AIS) in which scoliosis develops between start of puberty and skeletal maturity has the highest prevalence among the 3 age groups.

Most literatures reported AIS ,when defined at above 10 degrees Cobb angle, affects 1-3% of the overall adolescent population on average (Weiss et al., 2006, Weinstein et al., 2008, Negrini et al., 2012), however in another study, it was reported to affect 9.2% of the adolescent population (Asher and Burton, 2006). In Hong Kong, about 2.5% to 3.5% of adolescent population by the age of 19 was diagnosed with scoliosis with curvature greater than 10 degrees Cobb angle through school scoliosis screening (Luk et al., 2010, Fong et al., 2015). The prevalence rate of AIS in Hong Kong was estimated by two large population based studies involving more than 150,000 (Luk et al., 2010) and 300,000 (Fong et al., 2015) local students. The students were monitored longitudinally from around aged 10 up to the age of 19.

Fong's study published in 2015 also found that the prevalence of AIS with curvature greater than 10 degrees showed a tendency of linear increase at 0.61% per year when comparing results among local students recruited in 1995/1996 academic years and the consecutive 5 academic years. With the sensitivity and specificity of the screening sustained above 90% during a period of data collection for at least 15 years, raise in participation and enhanced sensitivity of the screening program may lead to the increase of AIS prevalence in Hong Kong (Fong et al., 2015).

The prevalence rate of AIS is found to drop exponentially while the degree of curvature increases (Weiss et al., 2006). For the case in Hong Kong, incidence of curves greater than 20 degrees Cobb angle drops to 1.8% and further reduced to 0.2% for curves exceeding 40 degrees Cobb angle (Fong et al., 2015).

AIS affects females more than males with different severity of curvature and in a common ratio of 2:1 for curves greater than 10 degrees Cobb angle (Yaman and Da Lbayrak, 2014). Female to male ratio affected by AIS for curves greater than 10 degrees is about 2.2-2.7:1 in Hong Kong which matches with the general findings (Luk et al., 2010, Fong et al., 2015). Gender variation in AIS increases with a larger degree of deformity. The affected female to male ratio was reported to be up to 7:1 for curve angle greater than 30 degrees (Morais et al., 1985).

The spinal deformation may or may not progress after the initial detection depending on pattern and degree of deformity and age of onset. About 23% of deformed curves were observed to have progressed to a larger deformity until the end of skeletal growth (Lonstein and Carlson, 1984). About 45% of the AIS patients with initial curvature greater than 10 degrees progressed in which close to 15% of the cases had at least 5 degrees increase in curvature (Soucacos et al., 1998). For those patients with severe curve types, treatment may be required to control the deformity.

2.5. Current medical management for IS patients

Current medical management for AIS depends on degree of curvature, skeletal maturity and progressive rate (Weiss et al., 2006). Degree of curvature and skeletal maturity are graded by Cobb angle and ossification stage of the iliac apophysis with Risser sign (Hacquebord and Leopold, 2012). Progressiveness is defined as at least 5 degrees of Cobb angle increase between two consecutive check-ups within 6 months and at a rate of more than 12 degrees per year (Cheung et al., 2015, Luk et al., 2010).

Lonstein and Carlson (1984) formulated a mathematical function to predict risk of scoliosis progression based on Cobb angle, skeletal maturity and age. The guidelines from the International Scientific Society on Scoliosis Orthopaedic and Rehabilitation Treatment for conservative treatment of IS which is a consensus formed among international scoliosis experts also refer to the calculation from Lonstein and Carlson's formula to predict patients' progression risk (Weiss et al., 2006). The higher the value calculated of progression factor, the greater chance of progression for the patient (Figure 2-5). Thus, curve progression has a likeness to develop in younger IS patients with lower bone maturity level and/or with a greater curve magnitude at presentation and especially affecting female patients (Bettany-Saltikov et al., 2013).

About 0.25% of all adolescent population progressed to an extent that is referred to treatment (Asher and Burton, 2006). A slightly higher number of the adolescents (between 0.3% and 0.4%) in Hong Kong reach to a stage of deformity before maturity where conventional scoliosis treatment is required (Luk et al., 2010, Fong et al., 2015).

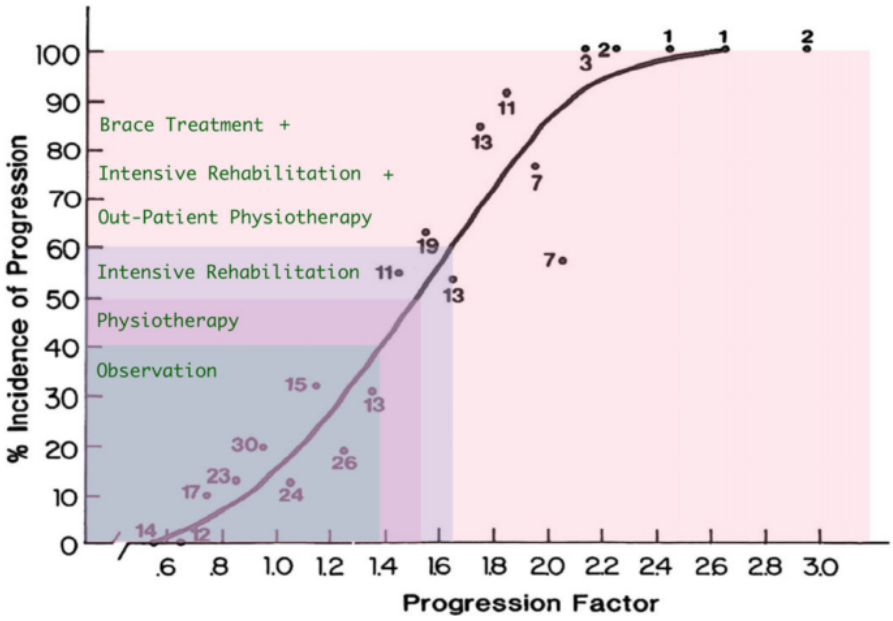

$$\frac{Cobb\ \ angle - 3\ \ \times Risser\ \ sign}{chronological\ \ age}$$

Figure 2-5 The chance of scoliosis progression with the progression factor was estimated by Lonstein and Carlson(1984). The progression factor was calculated using the formula listed under the graph. The numbers next to the data points indicated the number of cases it was based on. The form of treatment indicated to patients corresponding to the percentage of progrssion incidence was also labelled on the figure. Figure was adopted from (Weiss et al., 2006).

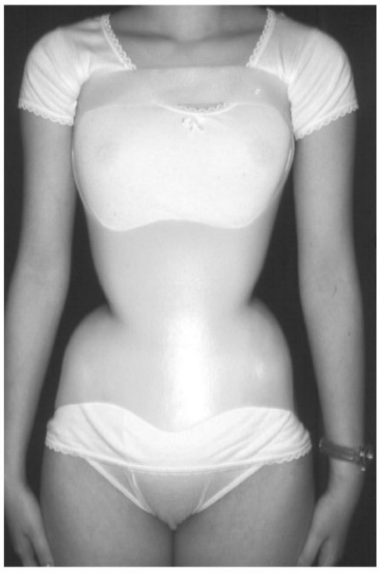

Figure 2-6 Front view of a patient wearing a custom-designed rigid orthosis around the body from axilla to sacral level. Figure was adopted from (Wong et al., 2008).

Figure 2-7 Front view of a patient wearing SpineCor, a kind of soft brace that puts harness on the body from multiple directions. Figure was adopted from (Wong et al., 2008).

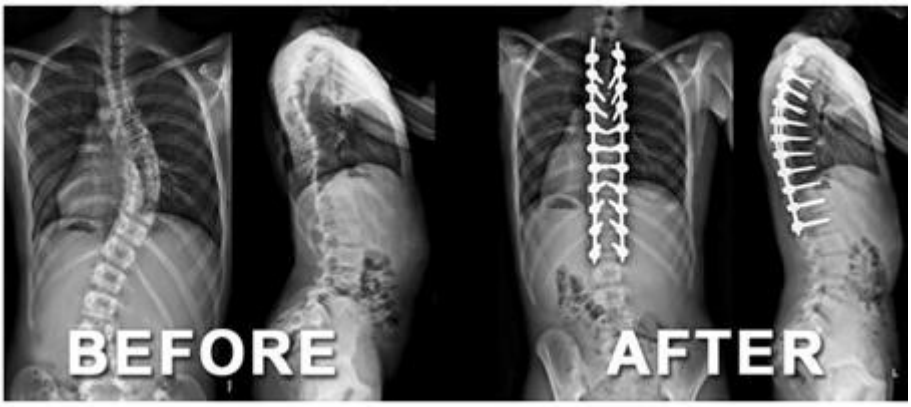

Figure 2-8 Radiographs in frontal and sagittal plane of a patients with severe IS before (left) and after surgical correction (right). Curvature is straightened by fusing the vertebrae together by implants which appears as the brightest rods in the post-surgical radiographs. Figure was adopted from (British Columbia Children's Hospital, 2016).

Deformity ceases literally until growth is completed (Hacquebord and Leopold, 2012). All patients until skeletal maturity are therefore monitored continuously for changes in spinal curvature and progression sign at every 6 to 12 months (Weiss et al., 2006). Patients with Cobb angle below 25 degrees at detection and low risk of progression are put under observation and sometimes prescribed with physical therapy. Bracing is recommended for patients with immature skeleton and having 20 to 25 degrees of Cobb angle at progression or larger than 25 to 45 degrees. Figure 2-6 and Figure 2-7 show two examples of bracings worn by IS patients in current clinical practice. For patients with severe deformity at above 50 degrees, spinal fusion surgery may be required to stop progression and correct the deformity (Andersen et al., 2006). A radiograph taken on a patient post-surgery is shown in Figure 2-8.

Most IS patients with mild or non-progressing deformity are not assigned to vigorous intervention under current treatment guideline (Weiss et al., 2006). Some patients and their families may not feel calm with only medical observations. They may express concerns for their prognosis and worry about risk of curve progression. For untreated IS patients, they often face typical long-term outcomes including back pain, poor cosmetic appearance and psychosocial concerns (Weinstein et al., 2008). There is also a chance that some patients regard themselves having compromised cardiopulmonary function because of a distorted trunk contour even though this is rare unless early-onset IS or with thoracic apex greater than 80 degrees Cobb angle (Lehnert-Schroth, 1992, Weinstein et al., 2003).

Conventional non-operative managements for scoliosis focus on slowing and stopping curve progression in order to avoid undergoing surgery. Common forms of bracing used nowadays include rigid thoracolumboscaral orthosis and soft bracings as shown in Figure 2-6 and Figure 2-7. Regular rigid brace treatment could stabilize and deter

curve progression in 20-40% of the cases but showed insignificant effect on reversing the curvature (Asher and Burton, 2006). Soft bracing has been compared with rigid bracing for its efficacy in IS treatment. The comparison results are variable as some pointed out that soft bracing had a lower successful rate in controlling curve progression (Wong et al., 2008) while others obtained equal results for treatments with rigid and soft braces (Gammon et al., 2010). Therefore, it cannot be concluded that one type of bracing is better than the other (Negrini et al., 2012).

However, it is certain that the successful rate of brace treatment increases with longer hours of wearing, so patients are usually instructed to put on the brace for 18 to 20 hours per day (Weinstein et al., 2013). Given that most patients are assigned with the hard brace in common clinical practice, patients do not readily accept this form of treatment because of the discomfort after long period of wearing (Wong et al., 2008). Meanwhile, operation as the ultimate treatment for scoliosis puts patients at usual risks of major surgery. Although surgical risks have decreased significantly from advanced surgical techniques, the chance of infection, pseudarthrosis, and neurological complications after surgery should not be omitted (Asher and Burton, 2006). Spine functional degeneration and increase in pain can occur in the long run and by then re-operation may be required (Asher and Burton, 2006).

2.6. Alternative treatment for IS

In fact, conventional management of "observation, orthosis and operation" tends not to be readily accepted by IS patients and their families. It has been reported that half of the patients prescribed with bracing or surgery refused to follow the arrangement (Lantz and Chen, 2001). Patients who hold concerns with conventional management show increasing interests in consulting alternative and complementary treatments such as manual therapy (MT) (Romano and Negrini, 2008). In the United States alone, there are approximate 2.7 million patients per year seeking treatments for scoliosis and related complaints from therapists practicing MT such as chiropractors (Rowe et al., 2006). Patients who consulted manual therapists were in hopes of stopping curve progression, reducing the curvature and preventing consequences of the deformity such as pain and surgery (Asher, 2006).

Manual therapy, also known as manipulative therapy, is a form of musculoskeletal treatment. It has been practiced by physiotherapist, chiropractor and osteopaths in Western medicine for over a century. Such treatment regime is targeted to relieve pain and illness in muscle, bone and joint so as to restore normal functions. Traditional Chinese medicine (TCM) also adopts general MT principles for treatment. TCM integrates unique meridian and acupuncture point theories with general MT techniques to form specific *tuina* (a term used in TCM to describe MT) for scoliosis.

In general, objectives of MT can be summarized as "application of an accurately determined and specifically directed manual force to the body, in order to improve mobility in areas that are restricted; in joints, in connective tissues or in skeletal muscles" (Korr, 1978). Many basic therapeutic techniques from Western and Chinese MT share similar principles but the execution method may be slightly different.

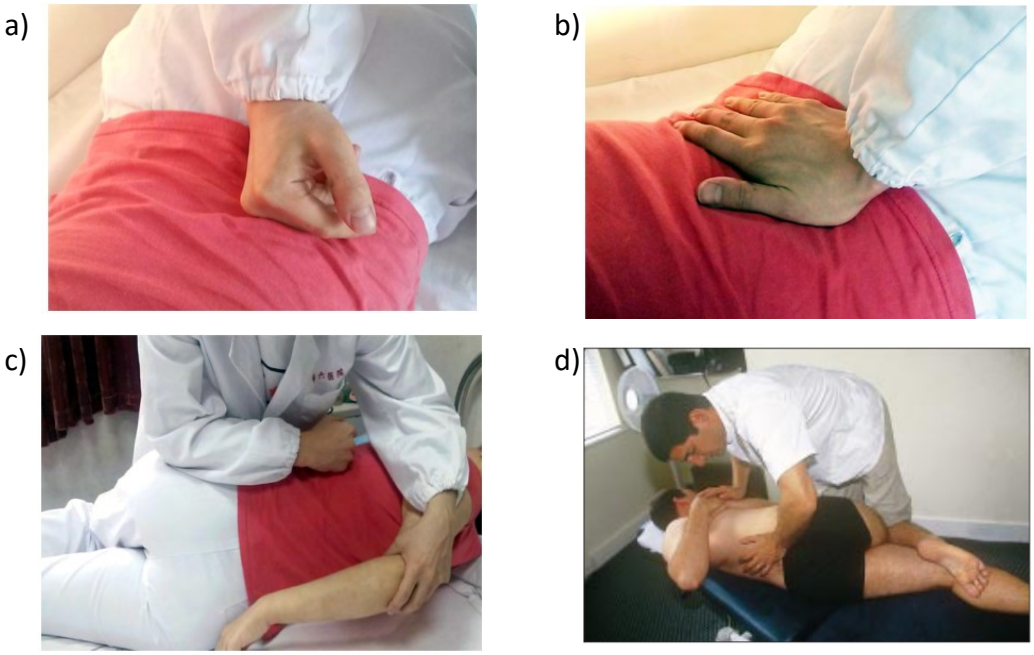

Figure 2-9 Examples of MT techniques used by Chinese and Western therapists. (a) Pressing-and-kneading technique and (b) rolling technique are two kinds of mobilization techniques delivered in slow velocity. (c) Pulling and (d) levered thrust are two kinds of manipulation techniques delivered in high velocity. Notice that the same treatment outcome is achieved by slightly different MT techniques by each MT branch as shown in (c) and (d). Figures a-c were adopted from (Fan and Wu, 2014). Figure d was adopted from (Vickers and Zollman, 1999).

MT treatment techniques can be separated into two directions: mobilization and manipulation (Vickers and Zollman, 1999). They are complementary and used together to a complete treatment. Mobilization is to apply localized repetitive motions on associated soft tissues of the restricted joint at a slow pace with increasing amplitude of force (Figure 2-9a and b). Therapists believe through moving the joint and associated soft tissues and muscles continuously, tension built in soft tissue can be reduced and normal joint function can be resumed. Manipulation focuses on restoring the gliding of restricted joints by guiding the joint to its maximum range of motion then thrust back in a quick but gentle manner (Figure 2-9c and d) (Vickers and Zollman, 1999).

2.7. Concept of IS development in manual therapy

These non-mainstream medicines may share similar treatment methods; however Western medical and TCM have their particular theories and background knowledge to interpret pathology of diseases. For example, chiropractic and TCM have specific explanation on cause and development of IS and thus build their own rationale for treatment. Coincidently, the concept of para-spinal muscle imbalance plays a role in scoliosis development and management in both fields (Li, 2001). A brief description of the role of muscle imbalance in MT using chiropractic and TCM as examples is presented as follows.

Chiropractors view scoliosis as a mechanical problem and attempt to correct scoliosis through mechanical methods targeting on the apex(es) (Danbert, 1989). According to Danbert (1989)'s explanation, the rationale for manipulative treatment in scoliosis is correlated with spinal flexibility. A curved spine with a lower lateral bending ability is said to have a decreased flexibility and it is an indication for treatment. Such a reduction in curve flexibility and surrounding soft tissue laxity can be a result of intervertebral motor unit dysfunction. Bone and intervertebral disc structure are altered which subsequently lowers the spine flexibility. Muscle groups on the convex side of the curve when under contraction are believed to help straighten the curve. Whenever a curve is formed, the weight of the curve poses a bending moment on itself away from the mid-line of body. Active muscle contractions on the convex side act as the corrective force to resist and reverse the curvature. Therefore the main goal of chiropractic treatment protocol is to increase flexibility of curve and trunk muscle contraction forces (Aspegren and Cox, 1987).

TCM views scoliosis as a pathological change in bones and joints due to para-spinal muscles' physiological imbalance (Shi et al., 2009). Para-spinal muscles create a "dynamic equilibrium" on the spine under normal conditions. As further elaborated by Wei (2006) in his book about traditional Chinese orthopedics theories on spine, a normal spine is regarded as a "tower erected by four wires" and muscles on the anterior and posterior of the spine are the four wires. These groups of muscles maintain an "external stability" to support spinal structure and provide movement to the spine. By coordinated contraction and relaxation of the antagonistic muscles, the spine is able to achieve flexion, extension, side bending and lateral rotations. So if a group of muscles loses tension, the spine will naturally incline away from its neutral axis.

Based on clinical observations gathered throughout the history of TCM, para-spinal muscle imbalance leading to subluxation of vertebrae is the major cause of scoliosis (Wei, 2006). A partial or incomplete dislocation on the vertebral joints can easily happen during voluntary trunk motions as a result of muscle strength imbalance. Imbalance muscle strength is interpreted as muscles on one side in relaxation while the lateral side in tension. Fatigue and prolonged activity on a unilateral side on the para-spinal muscles can cause muscle imbalance. Dislocation of vertebrae gradually resulted in scoliosis due to rearrangement of spine biomechanics. Emphasis is placed on proper restoration of muscle stiffness balance and joint subluxation through mobilization on para-spinal muscles and ligaments followed by spinal joint manipulation, otherwise deformed spinal alignment cannot be corrected (Yang and Zuo, 2015). The overall concept of scoliosis development in TCM is illustrated in Figure 2-10.

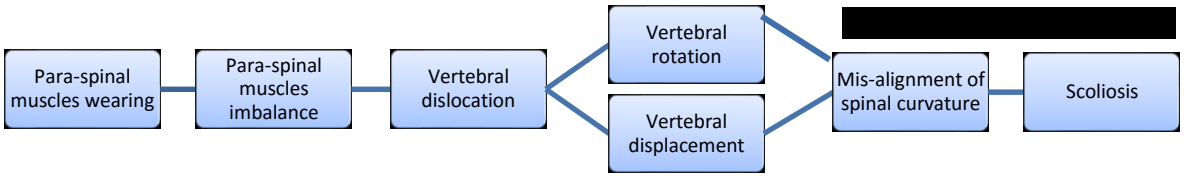

Figure 2-10 Theory of scoliosis development proposed in Traditional Chinese medicine summarized from Wei (2006).

The idea of "muscle imbalance" has been stressed in MT especially in TCM as a contributing factor to scoliosis. However, a general consensus is absent among manual therapists, even within the same field, on the mechanism of spinal deformation under para-spinal muscle imbalance as well as the presentation of imbalanced muscles across the deformed spine.

Previous research publications (mostly clinical studies) supporting the efficacy of MT treatment in reversing curvature have stated that the deformity starts with para-spinal muscles on the concave side of spine (Du et al., 2013, Polak, 2013, Lehnert-Schroth, 1992, Liang, 1991). Muscles along one side of the spine contract and bring the spine to its concavity under the "bowstring" effect (Du, 2013). Muscles under contracture are shortened which act as a string to pull the end vertebrae together while pushing the vertebrae in between away from natural linear alignment (Liang, 1991) (Figure 2-11). Para-spinal muscles on the lateral convex side of the spine are then overstretched (overstrained) and weaken (Lehnert-Schroth, 1992) (Figure 2-12).

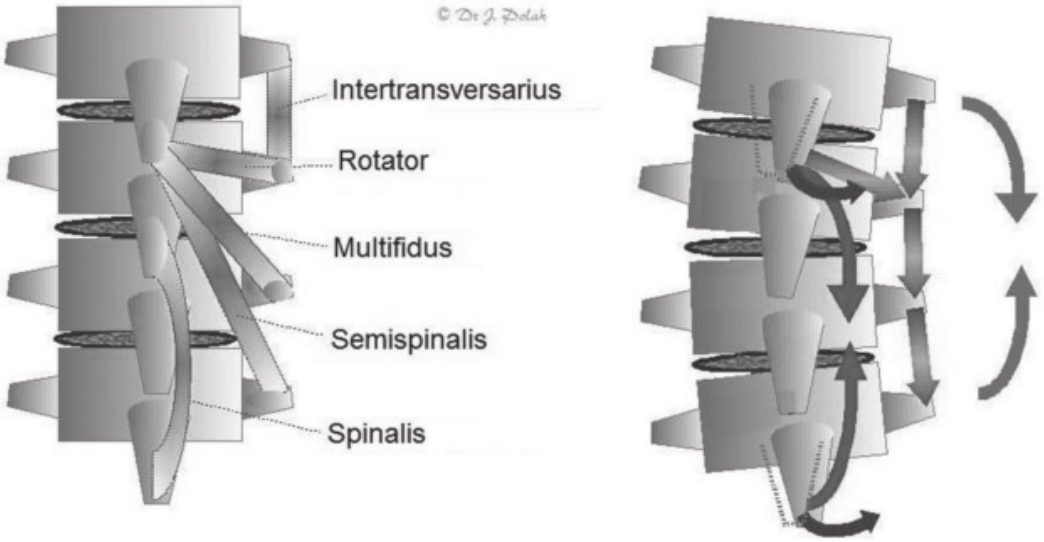

Figure 2-11 Co-contraction of deep para-spinal muscles on single side e.g. multifidus and rotators, results in the collapse of the adjacent vertebrae to the same side. Figure was adopted from (Polak, 2013).

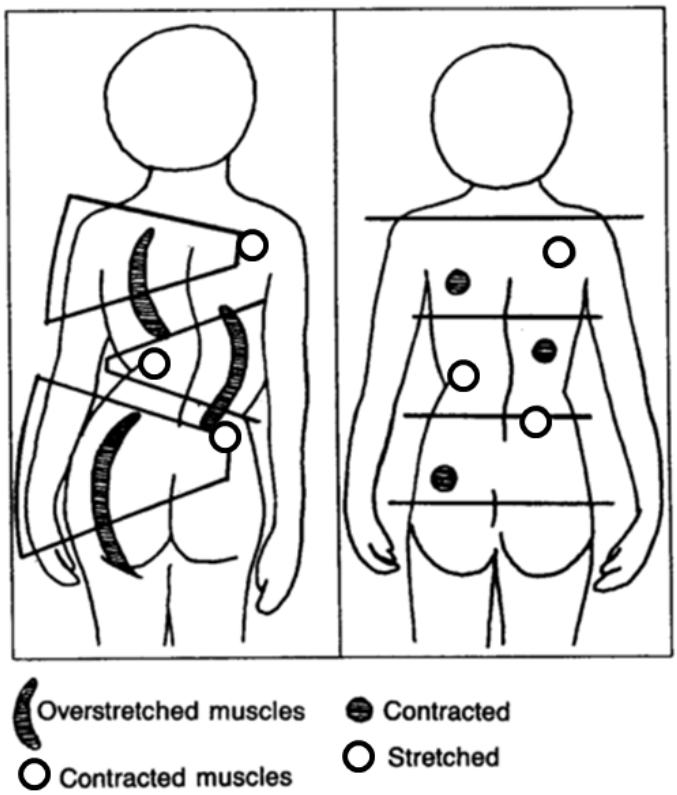

Figure 2-12 Muscles on the convex side of scoliosis curve are overstretched. By contracting the convex muscles and stretching the contracted muscles on the concave side using MT techniques, the curvature can be reversed and scoliosis is corrected. Figure was adopted from (Lehnert-Schroth, 1992).

On the contrary, some comments published online by other therapists and opinion from a practicing Chinese manual therapist that we consulted, suggested para-spinal muscles with increased contraction buckled the spine to form the convex side. Manual therapists supporting this argument often experience stiffer muscles on the convex side and softer muscles on the lateral side. Since stiffness of limb muscles increase during contraction (Arokoski et al., 2005), para-spinal muscles can also be in a contracted state when its stiffness increases. Thus, therapists generated their impressions that muscles on convex side contract harder than the lateral muscles and form scoliosis based on their clinical experiences.

There is also a third opinion suggesting that para-spinal muscles on both sides of a deformed spine are tight under different conditions. Muscles in the convex side appear stiffer as they are lengthened and stretched. Muscles in the concave side are shortened and stiff due to contraction. So, para-spinal muscles on both sides of the deformed spine should give a stiff feeling under manual palpation (Muscolino, 2015).

Despite an ambiguous relationship between “para-spinal muscle imbalance” and “scoliosis” in the field of MT, it is aware that muscle imbalance is likely to coexist with scoliosis. Muscle imbalance is greatly linked to different muscle activities on contralateral side from MT’s point of view. Muscles under various activity states show different levels of stiffness and sensation towards manual palpation. Therefore, clinical observations from MT provided an initiation for this study to investigate para-spinal muscle stiffness imbalance in scoliosis.

2.8. Previous studies on para-spinal muscle stiffness imbalance in scoliosis

The presumption of para-spinal muscle stiffness imbalance present in patients with scoliosis has been made based on clinical experiences through manual palpation. Manual palpation for differentiating differences such as stiffness and temperature between contralateral muscles for diagnosis has been a common clinical practice (Leonard et al., 2003). Manual palpation is a report of sensation and can only give a subjective conclusion (Arokoski et al., 2005). Therefore scientific study is needed to verify the presence of para-spinal muscle stiffness imbalance and its significance with scoliosis. And if such imbalance does exist, the correlations between stiffness and curve convexity and curve severity are important for further evaluation on MT's theories about scoliosis.

To our knowledge, only one study has directly measured and reported the para-spinal muscle stiffness imbalance in mild IS subjects (Oliva-Pascual-Vaca et al., 2014). In the same study, thirteen AIS patients aged between 9 and 18 with single curve apex, mostly in thoracolumbar region were included. Bilateral muscle stiffness was measured at 5 vertebral locations along the deformed spine in prone posture (i.e. upper limit, apex, lower limit and the two mid-points between the curve's limit and apex). Their results showed that para-spinal muscles on the concave side of scoliosis presented a higher resistance to the same pressure applied when compared with the muscles on the convex side at all locations, indicating a larger muscle stiffness on the concave side. However, no significant difference was found for the results between the convex and concave sides. The authors also reported a low (R^2 = 0.33) but significant negative correlation between Cobb angle and muscle stiffness at the mid-point between the apex and lower limit on the convex side.

The researchers further commented on their results and mentioned that para-spinal muscle imbalance in scoliosis subjects may be significant if the test is repeated on subjects with larger curve severity. Re-test on subjects in standing posture was also mentioned by the authors as bipedalism is correlated with etiology and development of IS (Oliva-Pascual-Vaca et al., 2014).

Significant effect of posture on para-spinal muscle stiffness has been demonstrated in a group of low back pain subjects (Chan et al., 2012). In that study, muscle stiffness was measured to compare stiffness of lumber multifidus at L4 level between healthy and low back pain subjects. Lumber multifidus stiffness measured in prone posture showed no significant difference between the two groups of subjects. However, muscle stiffness increased and was significantly higher in low back pain subjects under physiologic loading when subjects were in standing and different angles of stooping. Based on this finding, it is predicted that lateral para-spinal muscle stiffness in scoliosis in standing posture may also show larger discrepancy and yield a significant difference.

Due to a scarce number of evidence-based journal articles to demonstrate the presence of muscle stiffness imbalance in IS patients, more researches on para-spinal muscle stiffness should be performed to give supportive evidence.

2.9. Presence of para-spinal muscle asymmetry in scoliosis

Abnormality in para-spinal muscle is easily cohered with either cause or effect of spinal deformity including scoliosis as normal spine alignment and movement are maintained by muscles and ligaments (Zapata et al., 2015). The abnormality should also be asymmetrical in order to give a deformity shifted or rotated to one side. Therefore, muscle imbalance has been implicated as a possible cause or progressive factor of IS for a long time (Fidler and Jowett, 1976). MT treatments for scoliosis are devoted to deformity control by restoring para-spinal muscle stiffness balance but the expected effect on muscle is not monitored by any objective parameter (Kennelly and Stokes, 1993).

Though there is little research on para-spinal muscles stiffness distribution along and across the deformed spine, a lot of studies have revealed that para-spinal muscles in IS patients are different from normal subjects in terms of functional and morphological properties (Machida, 1999). The para-spinal muscles within IS patients between the convex and concave sides of the curvature are also asymmetric and correlated with scoliosis severity (Chan et al., 1999). Extensive research in the past has showed that lateral para-spinal muscles of IS patients have asymmetric electromyography (EMG) activation pattern (Avikainen et al., 1999, Cheung et al., 2005, de Oliveira et al., 2011), muscle histology (Mannion et al., 1998, Ford et al., 1984), and muscle dimension (Fidler and Jowett, 1976, Kennelly and Stokes, 1993).

2.9.1. Imbalance in electromyography in para-spinal muscles

EMG is a bio-potential signal generated by muscles which varies directly with voluntary contraction. Predominance of EMG on one side of the spine signals lateral para-spinal muscles are under asymmetric activities. Length and orientation between proximal and distal muscle endings may be influenced by muscle contraction and therefore affect the moment arm of muscle force. A potential outcome of asymmetric muscle activities can be imbalance muscle torque leading to vertebral joint rotation towards convex or concave side of the curvature (Chwala et al., 2014).

For people without scoliosis, no significant lateral EMG asymmetry is observed during trunk hyperextension in prone position (Zetterberg et al., 1984) but others claimed moderate asymmetric trunk EMG can be observed in normal girls during isometric task in standing (Schultz, 1984). In single curve IS patients, lateral resting EMG pattern is equal at the curve's apex in prone position (Chwala et al., 2014). A higher level of surface EMG has been observed on muscles on the convexity of curvature during standing and symmetrical loading (Machida, 1999, Schmid et al., 2010, Oliva-Pascual-Vaca et al., 2014). It is, however, believed that the lateral asymmetry is only significant when the curve angle is larger than 25 degrees (Schultz, 1984).

A comparison study between normal and IS subjects with right primary thoracic curve showed that EMG on the convex right side at 2.5cm from midline of the apex level was significantly higher than the concave left side (Zetterberg, 1984). The observed increase in muscle activity was due to a significant reduction of EMG at the concave left side compared with the left side of normal subjects while the convex right side was not significantly different from the right side of normal subjects. Asymmetric

EMG pattern could reverse, i.e. the concave side was more activated than the convex side, under a certain type of asymmetric loading exercises in IS patients (Schmid et al., 2010). Para-spinal muscle EMG imbalance at the apex level was found to correlate positively with Cobb angle but the authors did not specify which side had a higher EMG signal (Du et al., 2013). Such imbalance in para-spinal muscle activity in a group of IS patients was found to be diminished after spine fusion surgery but did not return to the same level as normal subjects during controlled activities (Lu et al., 2002).

Different from other studies which focused mainly on muscles at the apex level, Cheung and his colleagues (2005) conducted an EMG study on IS patients on multiple locations along the curvature at rest and under natural physiological loading in some controlled postures. EMG asymmetry was expressed in ratio form with convex over concave EMG. The authors found the ratio was constantly and significantly larger than one at the apex level but not at the end vertebrae for subjects with non-progressing IS. The ratio at the lower end vertebra was found to be significantly larger than one in patients with progressing IS at all scenarios compared with non-progressing subjects. Enhanced EMG imbalance at the curve's lower end vertebra might have suggested the incident of curve progression (Cheung et al., 2005).

However, de Oliveira et al. (2011) pointed out that some previous studies which concluded EMG increased at the convex side muscles were performed without defining the EMG collection method properly. The signal recording and analyzing reported among those studies were not consistent. The authors therefore performed another EMG study on erector spinae muscles at both the major and minor apexes in a group of matched double curves scoliosis subjects in attempt to provide a standardized protocol. Their results did not show significant difference in EMG

magnitude between lateral muscles with different degrees of voluntary isometric contractions during trunk extension. Also when comparing EMG signals between the affected subjects and normal subjects, there was no significant difference in signal amplitude measured on muscles attached on the homologues spinal regions (de Oliveira et al., 2011). The authors suggested that the use of subjects with mild curve up to 20 degrees (60% of subjects recruited) could be a reason for not obtaining similar results with previous studies.

2.9.2. Imbalance in histologic compositions in para-spinal muscles

Alternation of para-spinal muscle fiber characteristics with scoliosis had been demonstrated in past histologic studies. Two main types of muscle fibers can be found in skeletal muscles (Fidler and Jowett, 1976). Type I (or slow twitch fiber) is used during sustained tonic activity and fatigues slowly. Type II (or fast twitch fiber) is used in short term phasic activity and fatigues rapidly. Type I muscle fiber was found dominant in para-spinal erector spinae muscles and the overall muscle fiber distribution in normal asymptomatic subjects was not significantly different between left and right sides (Gonyea et al., 1985). The fiber type distribution was similar at different regions along spine and between genders as well (Mannion et al., 1997).

Histologic studies in IS patients focused on the fiber distribution between sides mainly at the apex level. A higher proportion of Type I fibers was generally found in para-spinal muscles on the convex side of curvature (Fidler and Jowett, 1976). Yarom and Robin (1979) found an atrophy of Type I fiber in para-spinal muscles on the concave side of the apex. Percentage of Type I fiber in superficial multifidus on the convex side of the apex as well as muscles above and below the apex increased significantly (Ford et al., 1984). A significantly lower percentage of Type I fiber was

found in the concave side of IS patients while there was no difference in the convex side when compared with control samples from healthy subjects (Mannion et al., 1998). Also Type II fiber composition increased on both sides but the change was only significant on concave side (Mannion et al., 1998). It should be noted that muscle samples were taken from superficial multifidus of scoliosis subjects and erector spinae of normal subjects in the study reported by Mannion et al. (1998). Similarity and difference between the two muscle groups were inconclusive as no relevant data was reported in journal articles that we have reviewed up to this moment.

It should be careful when comparing results from reported histologic studies as the para-spinal muscle samples taken for analyses were not always from the same muscle group. Samples could be taken from either superficial or deep layer of multifidus (Meier et al., 1997, Mannion et al., 1998), erector spinae (Mannion et al., 1997) or even a mixture of different groups of muscles (Yarom and Robin, 1979). Although samples came from para-spinal muscle groups which provide similar functions, the muscle fiber compositions may not be exactly identical.

Most studies obtained the tissues samples from IS subjects during spinal fusion surgery which indicated the spinal curvature of the subjects at the time of sample harvest was at above 50 degrees. Those subjects were most likely treated with bracing for a long period of time before surgery according to current conservative treatment guidelines. However, subjects' conditions before surgery were not reported in articles related to histologic studies. The effect of bracing on the alternation of muscle fiber compositions in para-spinal muscle was uncertain. Meier et al. (1997) carried out a study to compare multifidus muscles of IS subjects with and without brace treatment. It was found that Type I fiber on the concave side was lower than on the convex side of patients without brace treatment as Type I fiber was transited to Type II fiber.

Bracing could have started a fiber transformation at different locations along the spine as indicated by a significant increase in transitional fiber content. The direction of transition was not confirmed as the number of braced subjects in that study was inadequate. There could be a chance that Type I fiber further reduced in the concave side and led to a significant difference as found in most studies. The results reported in the past histologic studies might not represent the true muscle fiber compositions in IS subjects.

2.9.3. Imbalance in morphology in para-spinal muscles

Change in muscle dimensions is often used to indicate contractile function. Increase in cross sectional area, thickness and shortening of length are often observed during muscle contraction (Wallwork et al., 2007). The normal para-spinal muscle dimensions at resting prone posture were studied using lumbar multifidus with B-mode ultrasound in a group of normal young adults and no significant difference was found (Hides et al., 1992). However, any difference less than 10% between lateral cross sectional area of lumber multifidus is still considered normal in healthy individuals (Stokes et al., 2007).

The morphology of para-spinal muscles was also analyzed in IS patients in resting posture. Different patterns of cross sectional area asymmetry were found in L4 para-spinal lumbar multifidus of various curve types but the results from IS subjects were not compared with normal subjects (Kennelly and Stokes, 1993). Muscles with smaller cross sectional area were found in the convex side of lumbar and thoracolumbar curve and opposite to the convex of primary thoracic curve (Kennelly and Stokes, 1993).

Zoabli et al. (2007) divided the scoliotic spine into three equal portions: above, around and below the curve's apex and measured the bilateral erector spinae volume in each portion using magnetic resonance imaging. The muscle volume was found to be larger on the concave side and the lateral imbalance was more obvious at the apex region. Para-spinal muscle thickness was also found to be significantly larger on the concave side of the curve when compared with the convex side as well as with the dominate hand side of healthy controls in prone position (Zapata et al., 2015).

Length of multifidus on the convex side was found shorter than the opposite side in an IS cadaver examination (Fidler and Jowett, 1976). Lateral muscle length imbalance was the most obvious in the apex region and gradually became equalized when closer to the ends. Results from cadaver examination were later confirmed in two IS cases during spinal fusion. The authors concluded the findings were reasonable as the prolonged tonic muscle activity on the convex side resulted in a shorter muscle length. The explanation was illustrated with a spinal model with spinous process rotated to the convexity. However, the model did not seem to correlate with the fact that spinous process rotates to concavity in the presence of IS. Maruyama (1999) had an opposite finding to the previous one where the length of multifidus was demonstrated to be significantly longer on the convex side of severe IS patients using computer tomographic imaging. The asymmetry of muscle length was also found to correlate with the deformity in frontal plane.

2.9.4. Summary on studies in para-spinal muscle imbalance

Para-spinal muscle imbalance is one of the major directions in the study of IS etiology and progression. Up to now, majority of researchers tend to believe that the cause of para-spinal muscular changes in IS patients mentioned in previous sub-sections as a secondary effect and may lead to pathogenesis of IS (Meier et al., 1997, Maruyama, 1999, Machida, 1999, Lowe et al., 2000). Through this speculation, scoliosis progression and treatment evaluation may be able to trace by monitoring changes of para-spinal muscle symmetry (Du et al., 2013).

Common factors investigated by previous studies may not be efficient and feasible to perform in routine clinical setting. The use of surface EMG to monitor MT treatment effect was reported (Du et al., 2013). However, surface EMG measurement can be affected by muscle cross talk and skin conditions. Deep muscle EMG measurement can solve the issue but requires insertion of needle electrode. Other asymmetrical factors found in IS patients might neither be suitable for clinical evaluation. Histologic study involves taking out tissue samples. They are invasive and not ideal for clinical continuous examination *in vivo*. Morphological change of muscles in scoliosis can be viewed with clinical ultrasound scanning. But because of the natural anatomy of para-spinal muscles, not all locations along the spine can be visualized with common imaging diagnostic tools like real-time ultrasound (Kennelly and Stokes, 1993). Also cross-sectional change may be similar as observed in relax and stooping posture (Chan et al., 2012).

As muscle stiffness increases with muscle activity (Zheng and Mak, 1999) and may vary with different fiber composition. Muscle stiffness and symmetry in scoliosis can be a new factor for investigation. Thus, para-spinal muscle stiffness is proposed as a

potential parameter for investigation. In this study, we attempted to demonstrate the presence of para-spinal muscle stiffness imbalance in IS subjects. But first, we should have a better understanding on para-spinal muscle stiffness in normal population without scoliosis.

2.10. Para-spinal muscle stiffness distribution in normal population

Any para-spinal muscle stiffness pattern resulting from a disorder should be compared with a normal asymptomatic muscle stiffness pattern in order to confirm such a pattern is abnormal.

Fischer (1987b) claimed that abnormality of para-spinal muscles could be diagnosed when a difference of 2 mm displacement under the same loading existed in the affected muscle from the contralateral muscle. Conversely, muscle displacement should not have more than 2 mm difference under the same compression force between lateral normal asymptomatic muscles. The tissue displacement under a force was documented by tissue compliance meter (tCM) developed by Fischer (Fischer, 1987b) and details will be elaborated later in section 2.12.1. This claim was made based on the author's clinical experience and lacked systemic controlled study to support. Based on this 2 mm clinical threshold, abnormal lateral tissue consistency was found in normal asymptomatic population with an unreasonable variance in different studies (Jansen et al., 1990, Sanders and Lawson, 1992). Moreover, the accuracy and reliability of the tCM were questionable (Kawchuk and Herzog, 1995).

Waldorf et al. (1991) first reported the segmental (C7-L5) para-spinal muscle stiffness of asymptomatic female and male subjects in prone and standing positions. The measurement locations were 3cm bilateral to spinous process which corresponded to

the erector spinae muscles. The tissue penetration depth under the same loading was measured by tCM. Tissue with lower stiffness gave a larger penetration depth (mm) under a preselected compression force level (kg). In that study, penetration depth was consistently lower at mid thoracic levels for both genders in both postures (Figure 2-13). The overall trend remained the same but shifted downwards when posture was changed from prone to standing. Females had lower penetration depth at most vertebral levels compared with males. So tissue stiffness was expected to be larger in mid thoracic than upper thoracic or lumbar levels. Males also seemed to have lower para-spinal muscle stiffness than females at the same spinal regions.

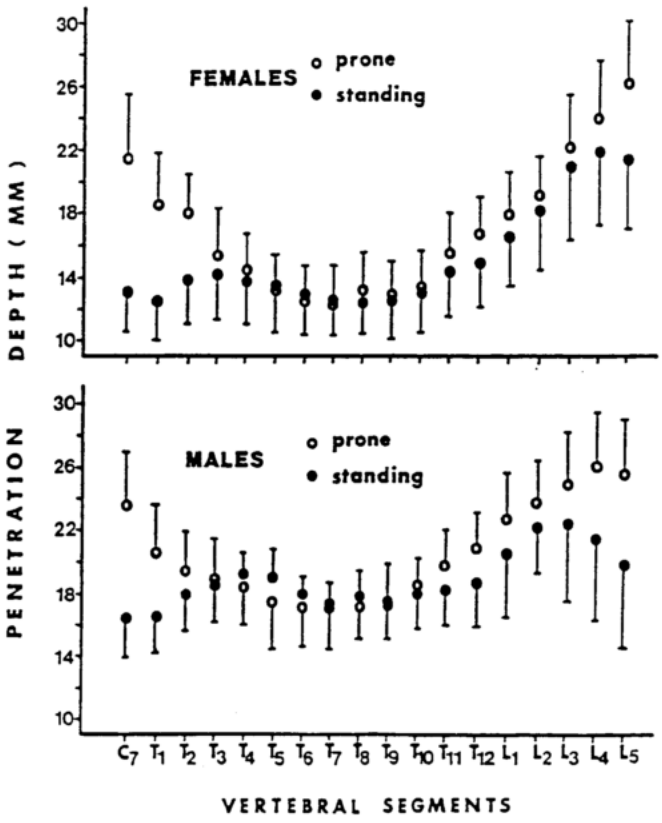

Figure 2-13 Average penetration depths of lateral para-spinal muscles induced by tissue compliance meter under the same indentation force. Both male and female healthy subjects were measured at two postures. Lower penetration depth indicated higher muscle stiffness at that location. Figure was adopted from (Waldorf et al., 1991).

Unfortunately, the data presented in that study failed to show if there existed para-spinal stiffness asymmetry in normal subjects. “Penetration depth” at each level reported in the study was an average of bilateral penetration depths. The study only gave an insight of the para-spinal muscle stiffness distribution along the spine but not lateral stiffness symmetry. Williams II et al. (2007) also demonstrated another stiffness measurement on lateral para-spinal muscles using a mechanical indentation system they developed. Although the test was performed only on a single subject in prone posture, they also recorded lower muscle stiffness in lumbar region than thoracic region (Figure 2-14).

Data from previous studies was insufficient to describe the distribution of para-spinal muscle stiffness in normal population. More information regarding the normal para-spinal muscle stiffness distribution along the spine and across a vertebral level is required to serve as a baseline for identifying any change in muscle stiffness in IS patients.

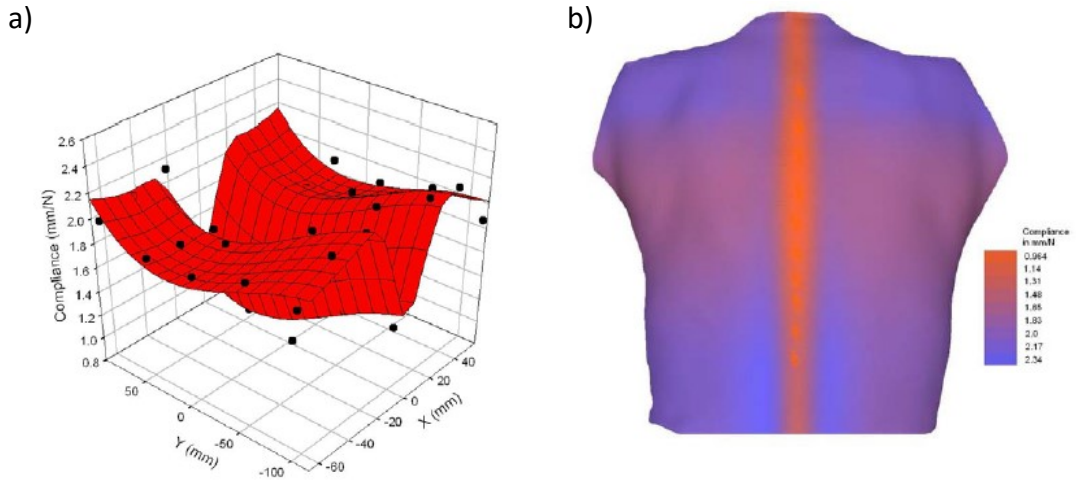

Figure 2-14 (a) Para-spinal muscle stiffness at different points as represented by penetration depths was plotted onto a best-fit surface according to the point’s location in an x-y plane defined on the back surface. (b) The projected para-spinal muscle stiffness across the back in form of color map. Brighter color (closer to red) indicates higher muscle compliance. Figures were adopted from (Williams II et al., 2007) .

2.11. Significance of para-spinal muscle stiffness measurement

“Para-spinal muscle stiffness” is an important concept in MT. It is the ground for assessment, defining treatment protocol and evaluation of treatment outcome in MT (Everaert et al., 1997). Muscle stiffness is normally examined by manual palpation (Fischer, 1987b). Although manual palpation is common in daily clinical practice, it is only a subjective evaluation. The technique is generally considered as unreliable for soft tissue examination (Seffinger et al., 2004) with poor inter- and intra- rater reliability (Koo et al., 2012, Haneline and Young, 2009).

A small change in muscle stiffness may be unable to differentiate manually (Koo et al., 2011). Furthermore, subjective manual palpation results provided by therapists are not repeatable and comparable. Feedbacks from therapists are usually expressed in terms of descriptive terminologies (Everaert et al., 1997). There is a lack of objective methods such as a grading scale or a definite value for documenting muscle stiffness in the field of MT.

If para-spinal muscle stiffness evaluation is objective, the result can provide an additional pathway for researchers to understand relationships between muscles and IS. Also the rationale of scoliosis treatment in MT can be verified by documenting the muscle stiffness change during course of treatment. A reliable measurement tool is therefore important for para-spinal muscle stiffness measurement in MT. There is also a need for a quantitative value representing “muscle stiffness” for comparisons in diagnosis, between treatments and among therapists.

2.12. Objective evaluation methods for muscle stiffness

Different methods have been developed to study the biomechanics of human soft tissue *in vivo* in the past decades. The intrinsic mechanical properties of muscles or other soft tissues were carried out by documenting its response to a given mechanical loading. Measurement techniques widely used in quantifying muscle mechanical properties included indentation (Fischer, 1987b) and elastography (Céspedes et al., 1993). Due to inconsistent results of the same mechanical property reported by various measurement techniques (McKee et al., 2011), it is the best to select a measurement technique that could reproduce the process of manual palpation.

Manual palpation on soft tissue can be simulated by a single-point measurement using mechanical or manual indentation. It is a simple and non-invasive way to determine tissue mechanical properties including stiffness *in vivo* (Zheng et al., 1999). Therefore in the following sub-sections, instrumentations used in indentation measurement reported by various studies and their results will be discussed with the aim to find an optimal solution to measure para-spinal muscle stiffness. As supplementary information, various modes of elastography imaging techniques used in muscle stiffness analyses are also introduced in this chapter.

2.12.1. Tissue compliance meter

Fischer (1987a) developed the first hand held indentation device for tissue stiffness measurement (Figure 2-15). Tissue compliance meter (tCM) comprises of a force gauge and a millimeter scale marked on the shaft of the force gauge. The shaft is pushed down manually to deform underneath tissue. The penetration depth is marked by the displacement of a platform ring slid along the shaft. tCM quantified soft tissue stiffness by reading the displacement of the platform ring under a known pressure measured by force gauge (Fischer, 1987b). Lower stiffness, or higher compliance as described in the reported article, was identified by a larger penetration under the same force applied.

Figure 2-15 Tissue compliance meter for measuring tissue stiffness. Force is applied onto the tissue by compressing the device perpendicularly. Level of applied force can be read from the force gauge on top while the displacement can be read from markings on the shaft. Figure was adopted from (Fischer, 1987a).

The reliability of tCM measurement on human para-spinal muscles was evaluated by Sanders and Lawson (1992). Their study concluded tCM measurements were repeatable on the same measurement site at 30 seconds intervals for 10 minutes. The conclusion was based on comparisons between the average coefficients of variation of tissue displacement from all measurements made by 5 examiners. However, the measurements made by each examiner were conducted on a different subject which is not a customary way to check inter-operator reliability.

More studies criticized the accuracy of tCM. Jansen et al. (1990) reported a significant change in para-spinal muscle displacement with the same degree of force applied was obtained by tCM in a group of normal subjects after a 10 minutes interval. The authors claimed their subjects remained stationary between the first and second tests. Arokoski et al. (2005) commented the design of tCM with a reference plate is difficult to achieve a perfect contact with skin surface in some measurement locations with curved surface contours and thus leading to low accuracy. The reliability and accuracy of the tCM were also poor even for measurement on non-biological test surfaces. The instrument produced displacement readings up to 2 mm on test surfaces that were supposed to be incompressible (Kawchuk and Herzog, 1995). Given that the platform ring can travel downward together with the shaft during indentation, the reading on the shaft cannot reflect actual displacement of the shaft. Sensitivity of measurement using tCM was also low for the narrower range of displacement reported (Ylinen et al., 2006).

Stiffness measurement with tCM requires identifying a displacement value on the shaft at a pre-determined force level which is highly affected by human visual error. Also non-perpendicular placement of the tCM can induce a significant false reading. Due to the instrument design and operation management, cautions should be made

when interpreting stiffness measurements obtained with tCM. Regardless of the device's reliability, manual reading from scales made tCM not the most sophisticated tool for this study.

2.12.2. Myotonometer®

Myotonometer (MMT) is improved from tCM to replace manual data recording by computer data logging (Leonard et al., 2003). MMT (patented by Neurogenic Technologies, Inc., Montana, USA) is a cylindrical case which houses a movable indenter (Figure 2-16a). The outer case is placed on skin level and held stationary during indentation. Only the inner indenter is pushed down perpendicularly onto the measurement site and deforms underlying tissue. Tissue displacement is taken as the distance between the end of inner indenter and the reference ring around the outer case which rests on skin level (Figure 2-16b). The force applied to compress the tissue is recorded by a force transducer connected to the inner indenter. Three maximum force ranges (0.25- 1, 1.5 or 2 kg) are available by the measurement system and each force range is divided into 8 increments. Tissue displacement in millimeter scale is saved automatically by the software provided at each increment up to the pre-set maximum force level during indentation (Gubler-Hanna et al., 2007). The probe can be released and the indenter retracts when maximum force detection level is reached. The whole data collection process is about 0.5-0.75s (Jarocka et al., 2012). Force-displacement curve is generated and stiffness of different tissue is represented in terms of area under curve (AUC) of the respective force-displacement curve. Tissue with lower stiffness exhibits a larger tissue deformation per unit force during indentation. Tissue with lower stiffness is said to have stored more energy and thus results in a larger AUC (Gubler-Hanna et al., 2007).

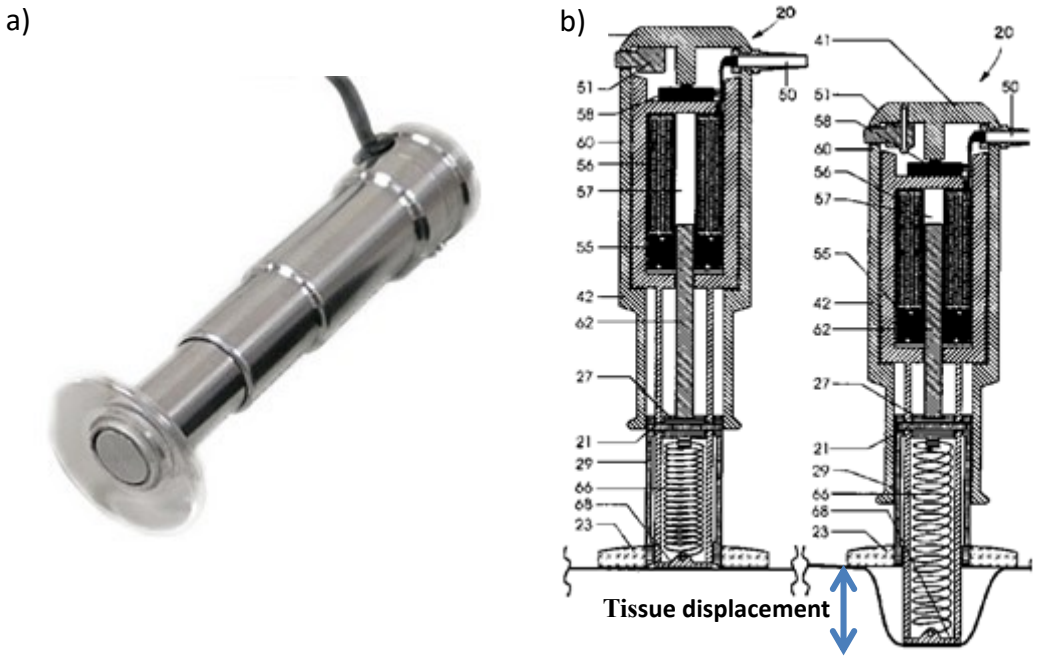

Figure 2-16 (a) Outlook of Myotonometer for indentation measurement. The cable on the top is connected to computer for data recording. (b) The internal structure and working principle of the probe. When the probe is pushed onto soft tissue, the reference ring remains stationary while the inner indenter extends to compress the tissue. Figure a was adopted from (Performance Analysis Laboratory, 2015). Figure b was adopted from (Leonard and Mikhailenok, 2000).

High to very high intra- and inter-examiners' reliability of MMT at above 0.25 kg exertion force was demonstrated by lateral gastrocnemius and branchii muscles stiffness studies on healthy adults (Leonard et al., 2003). Test-retest reliability of MMT was found to be above average to excellent by comparing AUC values measured on branchioradialis muscles of healthy young adults at rest and at different levels of maximal voluntary contraction in standardized positions (Jarocka et al., 2012).

Application of MMT in muscle stiffness measurement has been shown valid in different studies involving human subjects. MMT has successfully been used to demonstrate the positive correlation between muscle stiffness and surface EMG as well as joint force (Gubler-Hanna et al., 2007). The influence of age on muscle stiffness in resting and contraction states (Ikezoe et al., 2012) and lateral para-spinal muscle stiffness difference in IS (Oliva-Pascual-Vaca et al., 2014) were also investigated using MMT. Comparison of AUC values measured pre- and post-treatment in relaxed pathological muscles by MMT provided support to the positive treatment effect of *tuina* in patients suffering from acute lumbar sprain (Fan and Wu, 2014). MMT also gave an indication to muscle damage after maximal eccentric contraction exercise in upper limb of healthy male subjects by showing reduction of muscle stiffness (Chen et al., 2014).

MMT seems promising to the measurement of muscle stiffness as reported in related studies. However, this system was questioned for its ability to detect deep muscles compliance and performance on muscles that are not flat (Horikawa, 2001). Meanwhile as soft tissue and muscles are viscoelastic in nature, indentation force and subsequent deformation are in nonlinear relationship. Calculation of nonlinear viscoelasticity based on discrete measurements at the preselected force levels was inaccurate (Koo et al., 2011). Force-deformation response of the material that is measured continuously should be used for calculation. Neither tCM nor MMT can cannot provide continuous measurements. The accuracy of comparing measured results given by these systems with other continuous measuring systems should be aware.

2.12.3. Indentation instrumentation for research purposes

As an extension of tCM and MMT, a lot of indentation systems were developed to record force-deformation signals in soft tissues continuously (Horikawa, 2001, Keisaku et al., 2007). Those systems reported in journal articles also measure stiffness in terms of force-deformation correlation but only record up to a level of maximum force or displacement (Arokoski et al., 2005, Iivarinen et al., 2011). The major difference among the new systems is the application of force to soft tissues in forms of manual or mechanical mechanism (Ylinen et al., 2006, Koo et al., 2011, Koo et al., 2012). Those reported systems were mainly developed for research purposes and the repeatability has only been demonstrated on limited measurement locations. Also their reliability of performance, although in general good to excellent, was only discussed by their respective authors.

All these indentation systems mentioned so far in this chapter still hold limitations to the analysis of soft tissue and muscle stiffness. Soft tissue stiffness depends on tissue intrinsic parameters including tissue initial thickness, geometry and size of indenter (Ylinen et al., 2006, Iivarinen et al., 2013). Stiffness analysis applied by most of the previous studies did not consider these boundary conditions that control force-deformation responses. Thus it is not so suitable to directly compare soft tissue or muscle stiffness between locations, subjects and different measurement systems using the data reported in previous studies (Koo et al., 2011).

2.12.4. Tissue ultrasound palpation system (TUPS)

Zheng and Mak (1996) reported the development of another indentation system named Tissue ultrasound palpation system (TUPS), which utilizes a more rigorous mathematical model to estimate tissue stiffness. It is another improvement from previous analysis methods for soft tissue stiffness measurement.

The mathematical model was proposed by Hayes et al. (1972) to represent tissue stiffness by Young's modulus with boundary conditions taken into account. Soft tissue is assumed to be a thin, linearly elastic and homogenous layer bounded to a rigid-half space. The full equation is expressed as equation 2-1.

$$\mathrm{E} = \frac{1-v^2}{2a\kappa(v,a/h)} \cdot \frac{f}{d} \qquad (2\text{-}1)$$

where *E* is Young's modulus, ν is Poisson's ratio which is assumed to be 0.45 for soft tissue, *a* is indenter radius, *h* is initial tissue thickness, κ(*v, a/h*) is a scaling factor which is adjusted according to material's Poisson's ratio and ratio of indenter radius-to-tissue thickness. Values of κ in different combinations of the two variable were provided in previous papers (Hayes et al., 1972). Finally '*f/d*' is the linear slope of force applied over deformation. When applying the Hayes' model, soft tissue is assumed to be indented perpendicularly using a rigid indenter with a frictionless cylindrical end-plane.

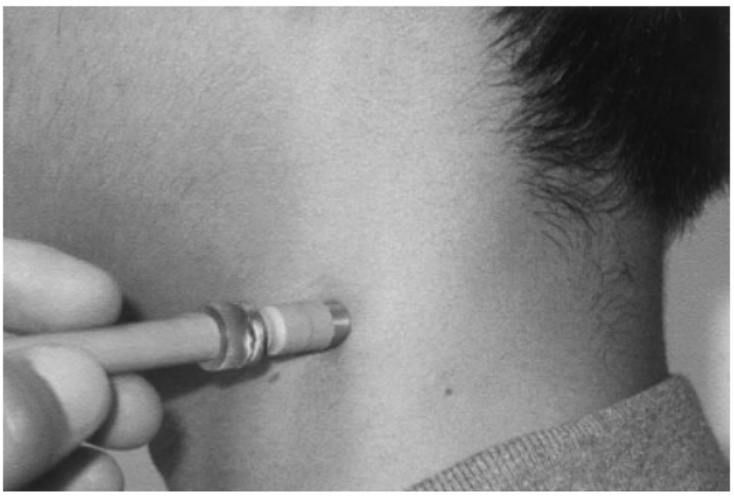

Figure 2-17 Tissue ultrasound palpation system measuring soft tissue stiffness on neck. The part that was touching the skin surface is the ultrasound transducer. The load cell was inserted in between the indenter and the pen-size holder. Figure was adopted from (Leung et al., 2002).

TUPS as shown in Figure 2-7 is an improvement from other indention systems mentioned above as it enables continuous force-deformation and tissue thickness measurements. This hand-held indentation system contains an A-mode ultrasound transducer at the end to serve as tissue deformation tracker and as the rigid indenter required by Hayes' mathematical model. The transducer constantly sends out ultrasound pulses and tissue thickness before and during indentation can be calculated from the travelling time of echoes between skin surface and underlying ultrasound reflective structure. Tissue deformation during loading and unloading can be measured instantaneously by the change of tissue thickness in a time interval. Force applied on the tissue is tracked by a load cell connected axially to the ultrasound transducer.

TUPS is a handy device which favors quick and easy soft tissue stiffness measurement. *In vivo* soft tissue stiffness has been conducted successfully with TUPS and reported in many articles. The accuracy and repeatability of TUPS measurement are validated (Zheng and Mak, 1996). This novel system has provided objective values of soft tissue stiffness in various scenarios including healthy lower limb muscles (Zheng and Mak, 1999), normal transverse carpel ligament (Zheng et al., 2006), plantar soft tissue stiffness change in elderly (Kwan et al., 2010) as well as soft tissue and muscle change in pathological conditions such as post radiotherapy neck tissue fibrosis (Zheng et al., 2000b, Leung et al., 2002), denervated soft tissues of spinal cord injured individuals (Makhsous et al., 2008), plantar soft tissue of diabetic patients (Zheng et al., 2000a) and low back pain (Chan et al., 2012).

The use of ultrasound allows TUPS to detect soft tissue thickness during indentation. A sizable and flat surface, usually bone, is required for reflecting the ultrasound signal transmitted into soft tissue back to the transducer. It is not guaranteed that a constant reflection of ultrasound signal can be maintained during a manually controlled indentation. When the indentation probe misaligns to a certain degree from the bone surface (i.e. 15 degrees), the returning ultrasound signal can be reflected away from the transducer and lost (Zheng et al., 1999). Ultrasound signal can also be attenuated in very thick fatty soft tissue and the reflected signal will be too weak to be detected. Also, a sizable bone structure is not always present underneath the soft tissue intended to be measured. Without a place to reflect ultrasound, TUPS cannot perform its function.

Since human back consists of several layers of muscles and the vertebral structures under para-spinal muscles are uneven and relatively small, constant detection of

ultrasound signal reflection may not be favorable. Owning to the intrinsic requirements for ultrasound signal detection, TUPS may not be suitable for the application on para-spinal stiffness measurement. Ultrasound detection method should be replaced by another displacement transducer to measure deformation change in muscles during indentation. Therefore in this study, an indentation system for the objective quantification of para-spinal muscle stiffness *in vivo* is required before proceeding to muscle stiffness measurement.

2.12.5. Ultrasound elastography

Besides indentation method, muscle stiffness can also be measured by ultrasound elastography (EUS) non-invasively. A disturbance is applied externally, normally through an ultrasound probe, to induce stress in a selected region of interest (ROI). Physiological displacements such as pulse and respiration are occasionally used as an excitation source to monitor tissue strain (Li and Snedeker, 2011). Subsequent tissue deformation is imaged by ultrasound imaging to visualize the distribution of tissue strain which is related to tissue stiffness (Drakonaki et al., 2012). Several EUS techniques have been developed in the past 30 years but not all techniques are commonly applied in the study of skeletal muscle stiffness. Compression elastography, shear wave elastography and vibro-ultrasound are some of the techniques employed in published muscle stiffness studies.

Compression elastography provides qualitative or at most semi-quantitative stiffness analysis. A B-mode ultrasound probe is used to compress the entire tissue structure in ROI quasi-statically and result in different levels of strain based on stiffness (Figure 2-18). The same ultrasound probe is used to collect images of the ROI continuously to measure the distribution of tissue displacement after compression along the direction

of ultrasound beam. By estimating the time shift of ultrasound echoes with constant

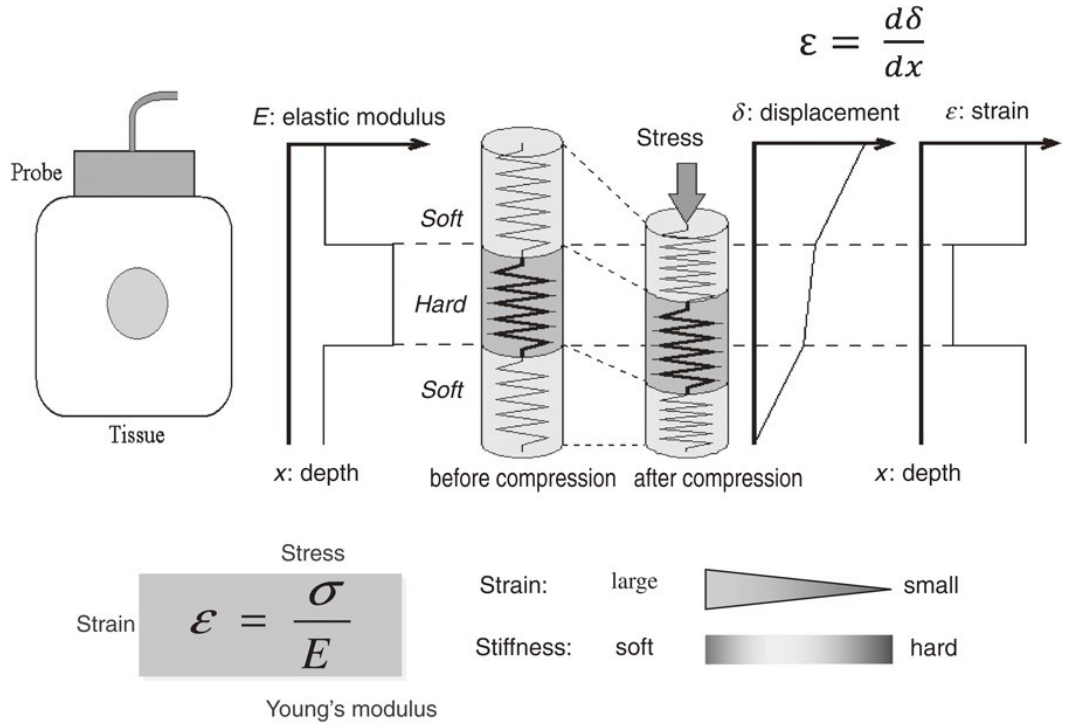

Figure 2-18 Summary of the operation principle and calculation method for compression elastography. When the tissue is compressed, stiffer structure deforms less and shows lower strain. Strain is calculated by the degree of deformation and represented in grey or color scale relative to the remaining structures. Figure was adopted from (Shiina, 2014).

travelling velocity (1540 m/s) assumed, tissue displacement can be calculated (Céspedes et al., 1993).

Stiffness by compression elastography expressed in terms of tissue strain instead of absolute value of Young's modulus as the measurement of internal stress distribution in tissue is impossible. The internal stress experienced by all points in ROI when compressed is assumed to be uniform so that strain is proportional to Young's modulus (Céspedes et al., 1993). Different levels of strain at each point are represented by grey or color code elastogram for direct qualitative visualization (Li and Snedeker, 2011). In another way, the strain of the ROI can be normalized to strain of surrounding tissue (usually fat) to provide a strain ratio for semi-quantitative

measurement (Drakonaki et al., 2012).

Versatile applications of compression elastography have been demonstrated by a number of muscle stiffness analyses in normal, pathological and post-treatment conditions. Compression elastography successfully showed variations of muscle stiffness immediately-after and post- exercise with the results comparable with muscle hardness meter availble in market (Yanagisawa et al., 2011). Higher stiffness was identified in a larger area of sternocleidomastoid muscle for more severe cases of congenital muscular torticollis and reduction of high stiffness area was observed after manual stretching treatment using compression elastography (Kwon and Park, 2012). Compression elastography was also found useful in characterizing structural alterations within a spastic muscle affected by cerebral palsy and the elastogram could serve as image guidance for muscle spasticity reduction injection treatment (Park and Kwon, 2012). Additional studies using compression elastography on different muscle groups under various conditions were reviewed by Drakonaki et al. (2012). Despite an apparent popularity in using compression elastography for muscle stiffness studies, Drakonaki and his colleagues commented that literatures available related to the feasibility and reliability of compression elastography in the study of either normal or pathologic muscles are still limited.

Compression elastography utilizes conventional ultrasound imaging for the visualization of tissue stiffness and naturally inherits the limitations of ultrasound imaging such as operator dependency. The resultant tissue strain is governed by the level of force applied to it (Céspedes et al., 1993). A larger force can easily result in a higher strain if nonlinearity of tissue is considered. The muscle strains measured by compression elastography within or between subjects cannot be compared directly as consistent compression force applied on each measurement or by each operator

cannot be guaranteed. The effect of stress on a particular tissue strain is expected to be canceled out by taking ratio with another soft tissue type in the same ROI assuming the stress distribution within tissue is uniform. However, it is difficult to assume the tissue type selected has the same nonlinearity and repeatedly select the same soft tissue type in each measurement.

Most commercially available ultrasound scanners with compression elastography function only provide an elastogram overlapped with real time B-mode image. This increases the difficulty to identify anatomical features in the captured screen of a "color wash" image. Also interpretation of strain on elastogram requires qualitative visual comparison of colors, operators with different visual sensitivity may generate inconsistent results (Wells and Liang, 2011).

In addition to the above limitations, Drakonaki et al. (2012) further raised issues about the technical considerations of compression elastography. Anisotropic structure in skeletal muscle can cause artefacts in B-mode images when ultrasound probe is not held perpendicular to the muscle during scanning. Elatogram result of compression elastography is therefore strongly affected by B-mode image quality.

Although the stress experienced by tissue is assumed to be uniform in compression elastography calculaton, in fact boudary conditions within the environment of scan plane can affect tissue stress distribution. When the ROI is adjancent to a prominent bone structure or the tissue in ROI has an uneven structure, homogenity of stress distribution inside the tissue can be affected. At the same time, the appearance of elatogram changes when the size of the selected ROI or scan plane varies. Color assigned to represent strain or stiffness of each tissue is relative to the stiffness of overall tissue contents within the image. For compression elastography images of

muslculoskeletal structures, more different tissue categories with a wide range of stiffness are included in the scan plane and the stiffness value of muscle acquired may shift along the color bar. Considering our target muscles are close to the vertebral arch, compression elastography may not be favourable for the purpose of para-spinal muscles stiffness analysis.

Shear wave elastography is another elastographic technique which provides quantitative analysis for muscle stiffness. With the guidance of B-mode ultrasound, an ultrasonic "pushing" beam is focused at different depths in an ROI (Bercoff et al., 2004). A shear wave is induced within the soft tissues by the excitation. The shear waves initiated from different depths travel in transverse directions and interfere along the mach cone (Figure 2-19). Propagation velocity of the travelling wave fronts between each push is tracked by the same ultrasound probe with an ultra-fast frame rate (i.e. normally over 5000 frames per second).

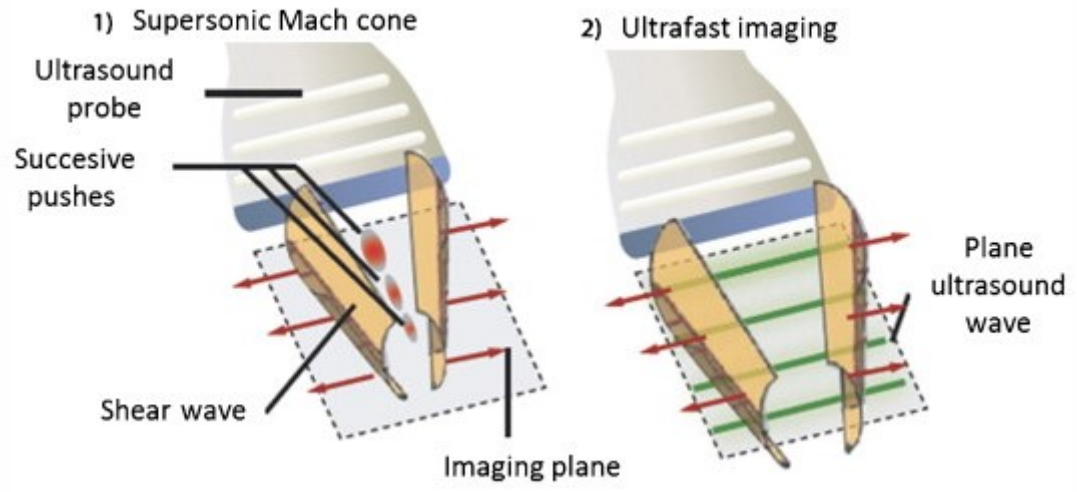

Figure 2-19 The working principle of shear wave elastography in two steps. Successive ultrasonic pulses excite multiple focused areas in muscle and induce two plane shear waves in transverse directions. The propagation velocity of the travelling waves is then monitored by ultrafast imaging. Figure was adopted from (Gennisson et al., 2013).

Tissue's Young's Modulus can be calculated with the wave's propagation velocity following the relationship of equation 2-2. The Young's modulus at all points generated is also displayed in color map at few milliseconds interval.

$$E = 3\rho V^2 \quad (2\text{-}2)$$

where E is Young's Modulus in kPa, ρ is material density and V is shear wave velocity in cms^{-1}.

Most muscle stiffness studies using shear wave elastography focused only on human's normal limb muscles at relax or at different voluntary activation stages (Arda et al., 2011, Gennisson et al., 2010, Shinohara et al., 2010, Leong et al., 2013, Eby et al., 2015). Some studies identified a transient decrease of the resting muscle stiffness after static stretching exercise for a greater joint flexibility (Taniguchi et al., 2013) and after massage therapy with shear wave elastography (Eriksson Crommert et al., 2015). Few examples in pathological muscle stiffness analysis have been found with shear wave elastography. Only one study was identified to have focused in hemiplegic cerebral palsy patients and found a higher shear wave velocity in muscles of the affected limb (Lee et al., 2016). Another study was performed on rabbits to demonstrate the muscle stiffness change in crush injury (Lv et al., 2012).

Shear wave elastography measures muscle stiffness value in a totally different mechanism from compression elastography. However, both techniques are based on ultrasound imaging. Therefore, shear wave elastography also shares some limitations mentioned in compression elastography such as tissue's boundary conditions, probe alignment and pre-compression force level (Kot et al., 2012). EUS can provide a seemingly faster non-invasive muscle stiffness measurement compared with

indentation methods. The intra-and inter-operator reliability of measurement using both EUS techniques was proven to be high (Chino et al., 2012, Cortez et al., 2016). Despite the growing clinical availability and popularity, the operation protocol of EUS should be standardized for a systemic comparison between measurements. Also the feasibility of muscle stiffness measurement with EUS should be explored in more regions, for example in para-spinal muscles which has not been mentioned in any EUS study so far.

Common EUS modalities are unable to detect muscle stiffness at a high level of voluntary contraction where the muscle stiffness is expected to be large. A modified vibro-ultrasound system was developed aiming to provide a larger stiffness measurement range (Wang et al., 2012). Muscle stiffness is assessed by detecting the propagation shear wave velocity along the muscle fiber direction after a short external mechanical vibration. An independent ultrasound probe is used to record the travelling time of the wave across a two fixed scan lines (Figure 2-20). The estimated propagation velocity is then converted to Young's modulus through equation 2-2.

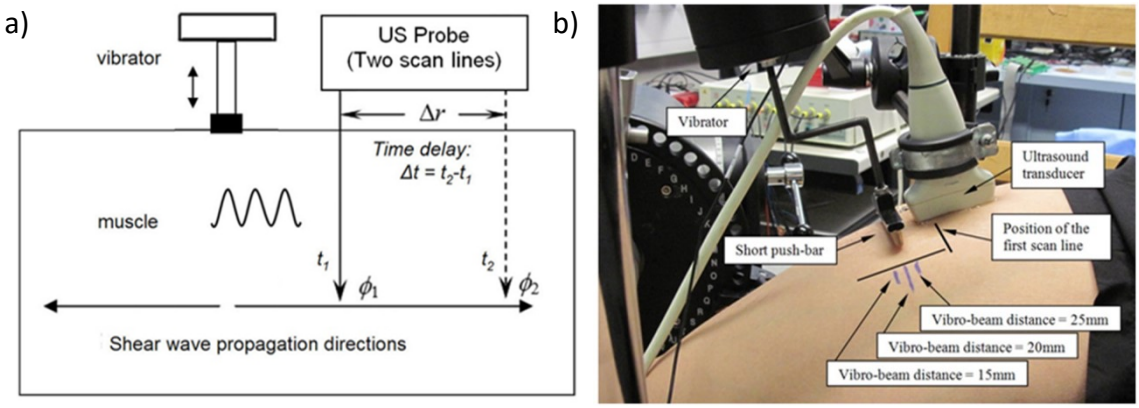

Figure 2-20 (a) A diagram depicting the vibro-ultrasound system. Shear wave is induced in muscle by a mechanical vibrator and the propagation velocity of the shear wave is monitored by an ultrasound probe connected next to the vibrator. (b) The setup for measuring thigh muscle stiffness during a series of voluntary contractions. Figures were adopted from (Wang et al., 2014).

Using this technique, the positive correlation between muscle stiffness and various levels of voluntary isometric contraction level from rest to maximal was demonstrated (Wang et al., 2012). Also, thigh muscle stiffness was identified to be larger in normal male subjects than female and in younger subjects during increasing isometric contraction but without significant difference in resting state (Wang et al., 2012, Wang et al., 2014). The level of para-spinal muscle stiffness in IS subjects compared with normal subjects is still unknown. If the magnitude of para-spinal muscle stiffness is too high and out of the detection range of common EUS systems, vibro-ultrasound may be applicable for measurement. However, the operation of vibro-ultrasound has only been demonstrated in relatively large and flat muscle. It is uncertain if the technique can still be applied in para-spinal muscle muscles whose boundary conditions are dissimilar. In addition, the current setup may not support measurements in different subject postures (e.g. standing or stooping) other than posture in a relatively horizontal level with the system.

CHAPTER 3 METHODS

This study was comprised of two parts. An instrument for soft tissue stiffness measurement was first developed, then validated using phantoms and finally be applied to para-spinal muscle stiffness measurement on human subjects. In this chapter, the design of the manual indentation system for stiffness measurement is elaborated, followed by details of system verification tests. The methods of para-spinal muscle stiffness measurement on normal subjects as well as on IS subjects are presented. Statistical analysis on stiffness measurement results is also explained.

3.1. Manual indentation system for stiffness measurement

The manual indentation system consisted of an indentation probe and a computer program to control the data acquisition during an indentation process. Components of the indentation probe and the required calibration works are described in following subsections. The layout of the data acquisition program is included as well.

3.1.1. Hardware — Indentation probe

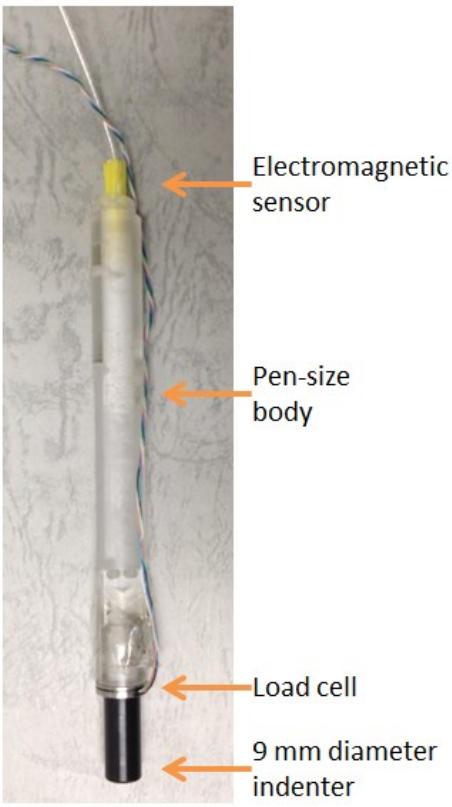

Figure 3-1 The hand-held indentation probe for stiffness measurement. The electromagnetic spatial sensor was put inside a plastic plug and inserted in the top of the probe.

The indentation probe was designed to be in pen-size and suitable for hand-held. It was capable of recording force applied on tissue and tissue displacement simultaneously during indentation. Two sensors were embedded in the two ends of a pen-size plastic holder including a 6 degree-of-freedom electromagnetic spatial sensor (Model 180, Ascension Technology Corporation, Burlington, VT, US) on the top and a 10 N load cell (ELFS-T3M, Entran Devices, Inc., Fairfield NJ, US) at the bottom. The load cell had another end which was capped by a 9 mm diameter flat end-surface plastic indenter. The indenter was in direct contact with the testing object during indentation (Figure 3-1).

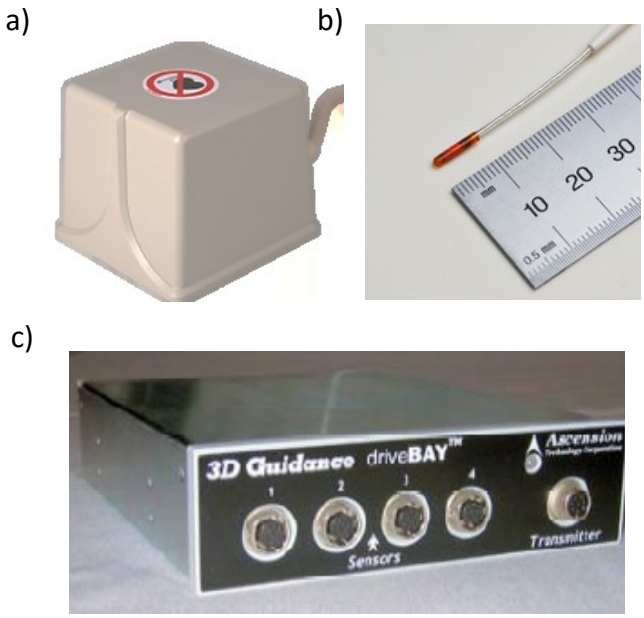

Figure 3-2 Key components of the Ascension electromagnetic spatial sensing system. (a) Mid-range transmitter and (b) model 180 spatial sensor are connected to the labeled sockets at the front of (c) driveBAY control unit. The system supports at most 4 sensors working simultaneously. The control unit is connected to the computer via a USB port. Users can control the system through computer software provided by the company. Figures were adopted from (Ascension Technology Corporation, 2016).

The electromagnetic spatial sensor placed in the probe was part of an electromagnetic spatial sensing system. The control unit of the spatial sensing system (3D Guidance driveBAY, Ascension Technology Corporation, Burlington, VT, US) commanded the transmitter (mid-range transmitter, Ascension Technology Corporation, Burlington, VT, US) to emit a continuous magnetic field. The sensor reported its current position inside the magnetic field relative to the 3D coordinate system (x, y, z) of the transmitter back to the control unit in real time. The current orientation of the sensor (Rotation, Elevation and Azimuth) to its own coordinate system was also returned to the control unit and passed to a computer. The key components of the electromagnetic spatial sensing system are shown in Figure 3-2.

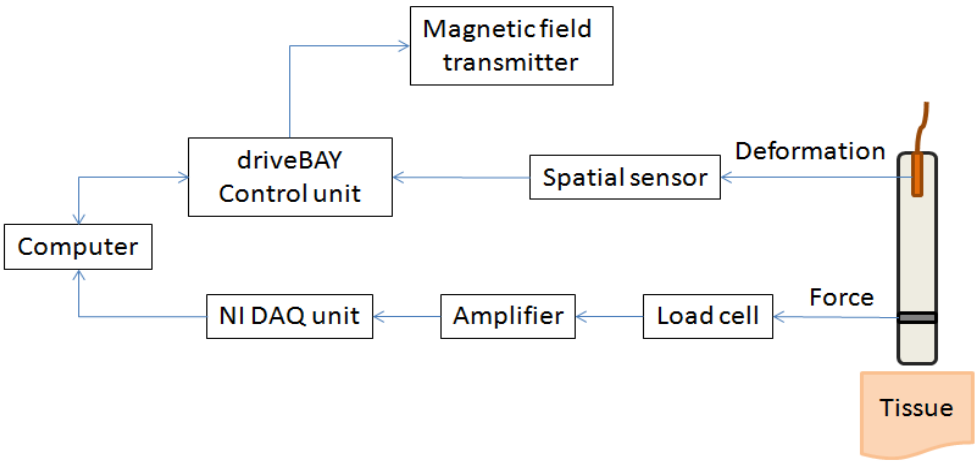

Figure 3-3 Schematic diagram of data transmission in the newly developed manual indentation system.

In parallel, voltage output from the load cell was amplified before transmitted to computer. Amplified voltage signal from the load cell was passed to a data acquisition box (NI USB-6211, National Instruments, Austin, TX, US) and imported to the computer via another USB port. Figure 3-3 outlines the connection and flow of data transmission of the manual indentation system. The control of data collection by the computer software is presented in the next subsection.

3.1.2. Software — Data acquisition

A LabVIEW program (Version 11.0, National Instruments, Austin, TX, US) was written to control the operation of the two sensors and to collect signal transmitted to the computer from both sensors. The user interface of the LabVIEW program is shown in Figure 3-4.

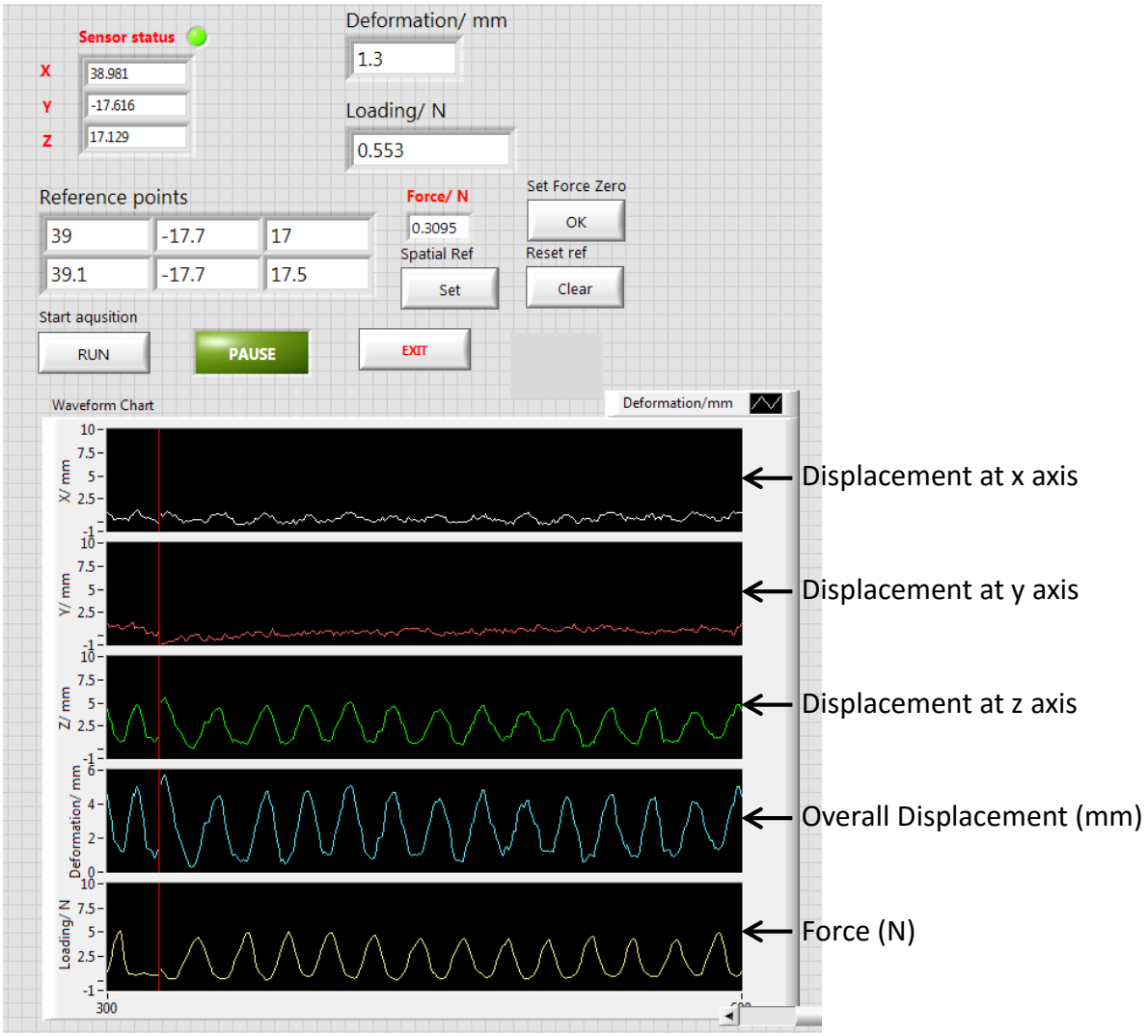

Figure 3-4 The user interface of the LabVIEW program for controlling the indentation system and data collection. This figure captures the display of the program during an indentation measurement along z-direction of the transmitter.

The program commanded data transmission from the electromagnetic spatial sensing control unit to the computer. Data containing spatial information of the spatial sensor which was passed from the control unit was decoded in the same program. Communication between computer and control unit was achieved by a list of company-defined commands (Ascension Technology Corporation 2008) and a Dynamic Link Library provided by the manufacturer. The program received the amplified voltage signal from DAQ unit at the same time. The program captured data point from each sensor at a time interval of 0.1 second.

The position of the indenter and the force applied on tissue were related to the position of the spatial sensor and the amplified voltage signal. The position of the indenter and the force applied on tissue were converted from position of the spatial sensor and the amplified voltage signal through respective calibration relationships in the same LabVIEW program before displaying on the user interface at real time. Calibration procedures for data conversion of both sensors are explained in the following parts.

To start the data collection, the positions of the indenter on the measurement surface and after a slight push onto the surface were recorded as reference points to indicate the indentation direction. Once the “Start” button was clicked, the displacement of indenter on each axis (x, y, z), the overall displacement (i.e. vector sum of all axes) as well as the force applied by the indenter would be plotted on the chart instantly. Force and displacement were offset from the initial loading and position of the indenter at the moment when “Run” button was clicked. Data collection was terminated and the recorded data was automatically saved after clicking the “Exit” button.

3.2. Calibration of indentation system — Loading on tissue

The load cell generated voltage signal that varied with the force applied on the tissue during indentation. Calibration of the load cell was performed by placing a range of standard masses (from 0g to 1000g) on top of the load cell and measured the voltage output with a multimeter. A correlation curve was drawn between varying weights on the load cell (unit: N) and the reported voltage values (unit: mV). The resulted correlation equation was used in the LabVIEW program for numeric conversion between voltage and force during data acquisition.

3.3. Calibration of indentation system — Deformation of tissue

Displacement of electromagnetic spatial sensor was often perceived as the magnitude of tissue deformation during indentation, despite that a fixed separation existed between the spatial sensor and the indenter surface. Such representation of tissue deformation was correct if and only if the probe always followed the same alignment during the whole indentation process. However, as the indentation was driven manually, it was challenging to maintain the probe at a fixed alignment throughout the whole process. When the probe was held on skin surface vertically by hand, the probe could be orientated to all directions at the same pivot (i.e. the contact of flat-end indenter surface and the skin). In this case, the spatial sensor could have a displacement recorded while the intender remained on the same location. Thus, this displacement would be a false information to represent tissue deformation.

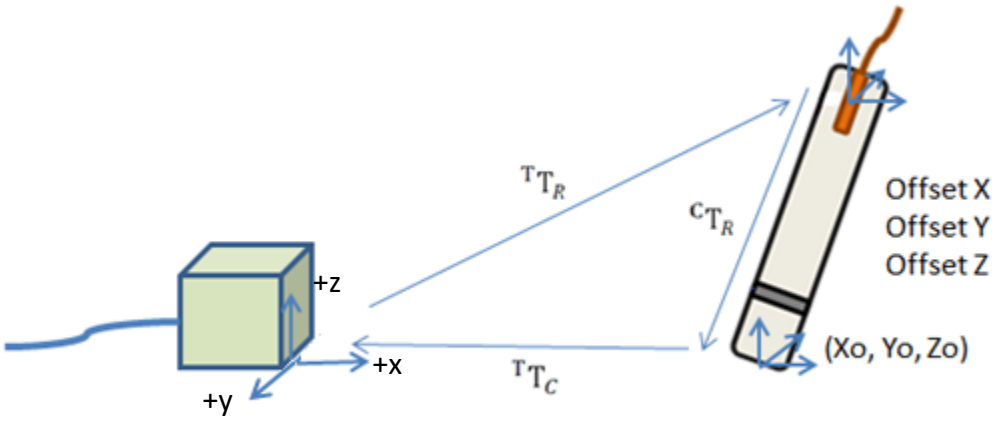

Figure 3-5 An illustration of coordinate systems between the probe and the magnetic field transmitter. Pivot calibration allowed the unknown transformation matrix from sensor to indenter ($^{C}T_{R}$) to be found with the locations of the other two points known. Location of indenter center to transmitter ($^{T}T_{C}$) during indentation was found later through matrix operation.

The true tissue deformation should therefore be set as the displacement of indenter's flat-end surface instead. A new coordinate system (^{T}Tc) was assigned to the center of flat-end surface with respect to the coordinate system of the magnetic field transmitter (0,0,0). Tissue deformation was represented by the displacement of the center point (Xo, Yo, Zo). The position of the center point could be found by matrix operation on the transformation matrixes of spatial sensor to transmitter ($^{T}T_{R}$) and spatial sensor to center point ($^{C}T_{R}$) using Singular Value Decomposition algorithm. However, the transformation matrix of $^{C}T_{R}$ could not be obtained without additional calibration steps. The relationships between the coordinate systems are shown in Figure 3-5.

3.3.1. Calibration for orientation matrix — Pivot calibration method

Pivot calibration method (Boctor et al., 2003) was adopted to define the transformation relationship ${}^{C}T_{R}$ between coordinate systems of spatial sensor and the indenter's surface center. Matrix ${}^{C}T_{R}$ was expressed in terms of the translational differences (Offset x, Offset y, Offset z) and rotation angles (α,β,γ) between the sensor's origin and the new coordinate system (Xo, Yo, Zo) and written as equation 3-1.

$$ {}^{C}T_{R} = \begin{pmatrix} C\gamma C\beta & C\gamma S\beta S\alpha - S\gamma C\alpha & C\gamma S\beta C\alpha + S\gamma S\alpha & Offset\ x \\ S\gamma C\beta & S\gamma S\beta S\alpha + C\gamma C\alpha & S\gamma S\beta C\alpha - C\gamma S\alpha & Offset\ y \\ -\mathrm{S}\beta & C\beta S\alpha & C\beta C\alpha & Offset\ z \\ 0 & 0 & 0 & 1 \end{pmatrix} \quad (3\text{-}1) $$

where C is cosine function and S is sine function.

This calibration method was originally adopted in locating the spatial position of the tip points of tapered surgical instruments used in 3D image guided surgeries. Standard calibration protocol required the instrument to be moved at different directions randomly while the tip point remained at a fixed point in the magnetic field during data capturing. Since the end of the indenter was not sharp, a special tool was designed to facilitate this calibration.

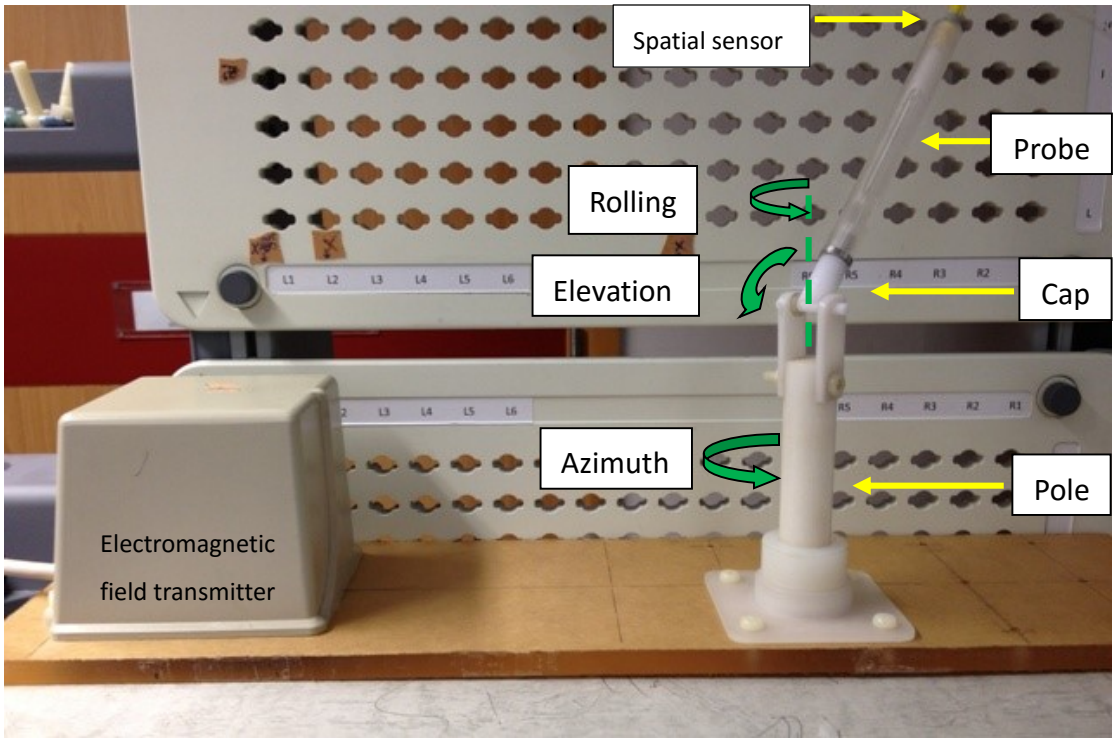

Figure 3-6 A plastic calibration stand designed for pivot calibration of the indentation probe. The stand can be fixed at different distances from the transmitter with plastic bolts. The indentation probe is connected to the cap with the free end of the load cell. Once connected, the probe can be moved to all orientations about the same point.

The calibration stand shown in Figure 3-6 was made of plastic to avoid interference in the electromagnetic field. The indenter was detached from the probe for calibration. The free end of the load cell was then connected to the cap on the pole. Once connected, the probe could be rotated in 3 ways: elevation, azimuth and rolling about a fixed pivot on the cap. The intersection point between the cap's vertical axis and rotational axis marked that fixed pivot point. The fixed point also coincided with the center point on the indenter surface. The coordinates of the fixed point during calibration was assigned as matrix ${}^{T}T_{C}$ and written as Equation 3-2.

$$ {}^{T}T_{C} = \begin{pmatrix} 1 & 0 & 0 & Xo \\ 0 & 1 & 0 & Yo \\ 0 & 0 & 1 & Zo \\ 0 & 0 & 0 & 1 \end{pmatrix} \tag{3-2} $$

The probe was oriented to 32 directions for each calibration (Leotta et al., 1995). Orientation matrix ${}^{T}T_{R}$ containing current positions (t_x, t_y, t_z) and rotation angles of the spatial sensor to the field transmitter at each turn was acquired from the control unit. Matrix ${}^{T}T_{R}$ was broken down and input to Equation 3-3 to find Offset x, Offset y and Offset z.

$$ \begin{pmatrix} ax & sx & nx & -1 & 0 & 0 \\ ay & sy & ny & 0 & -1 & 0 \\ az & sz & nz & 0 & 0 & -1 \end{pmatrix}_{3m \times 6} \times \begin{pmatrix} Offset\ x \\ Offset\ y \\ Offset\ z \\ Xo \\ Yo \\ Zo \end{pmatrix}_{6 \times 1} $$

$$ = \begin{pmatrix} -tx \\ -\mathrm{ty} \\ -tz \end{pmatrix}_{3m \times 1} \tag{3-3} $$

The rotational angles between sensor's origin and the indenter's surface center could be found by solving matrix ${}^{C}T_{R}$ in Equation 3-4. Equation 3-5 is a detailed matrix re-written from Equation 3-4. Matrix ${}^{C}T_{R}$ which contained the rotation angle values was the solution after solving the system of equations in Equation 3-5.

$$ {}^{T}T_{R} \times {}^{C}T_{R} = {}^{T}T_{C} \tag{3-4} $$

$$\begin{pmatrix} 1 & 0 & 0 & Xo \\ 0 & 1 & 0 & Yo \\ 0 & 0 & 1 & Zo \\ 0 & 0 & 0 & 1 \end{pmatrix}_{4m \times 4} \times \begin{pmatrix} ux & vx & wx & offset\ x \\ uy & vy & wy & offest\ y \\ uz & vz & wz & offset\ z \end{pmatrix}_{4 \times 4}$$

$$= \begin{pmatrix} ax & sx & nx & tx \\ ay & sy & ny & ty \\ az & sz & nz & tz \end{pmatrix}_{4m \times 4} \quad (3\text{-}5)$$

where $\beta = -\sin^{-1} uz$, $\alpha = \sin^{-1} v(z/\cos\beta)$ and $\gamma = \sin^{-1}(uy/\cos B)$. Each rotational angle could be found from the respective elements in matrix ${}^{C}T_{R}$.

By replacing the stand at different distances to the field transmitter, the process was repeated at three different pivot points for an average of Offset x, Offset y, Offset z, α, β and γ (Leotta et al., 1995).

The 6 translational and rotational values obtained from the calculations were substituted into the transformation matrix ${}^{C}T_{R}$ in Equation 3-1. Real time position and orientation of the center of the indenter surface ${}^{T}T_{C}$ can be calculated in the LabVIEW program following Equation 3-4.

3.4. Data collection and analysis

The calibrated probe was used to measure material stiffness in a manually controlled indentation. Multiple cycles of hand-driven indentations and retrievals of the probe are described as “indentation” in this study (Figure 3-7). The preload was maintained to be less than 0.5 N while maximum force applied on the measurement surface was limited to 10N. Indentation depth was controlled to be not more than 20% of initial thickness of the testing object (Zheng et al., 1999). For testing on silicone phantoms, the initial thickness was measured with a caliper. For testing on human muscles, the initial tissue thickness was measured on a B-mode ultrasound image of the measurement site with free image processing software ImageJ (National Institutes of Health, US). The distance between skin and the underlying bone surface was taken as tissue thickness. The initial thickness measured was used again as a parameter in the calculation of stiffness.

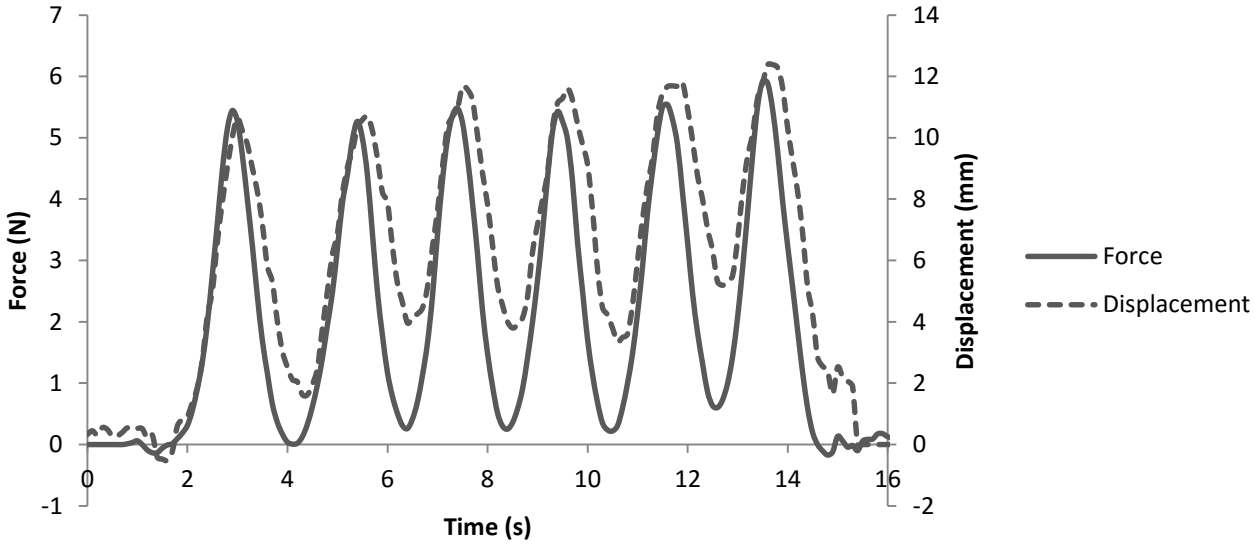

Figure 3-7 The typical force and deformation responses from tissue during indentation test after synchronization. The rising part of the indentation curve suggested that the indentation was moving into tissue. This part was used for Young’s modulus calculation in this study.

Soft tissues and muscles are viscoelastic in nature and their mechanical properties vary with the indentation rate. Constant indentation rate is difficult to be controlled in manual indentation, however soft tissue stiffness has been demonstrated as insensitive to indentation rate within a certain range (Lu et al., 2009). Indentation rate was therefore kept at about 2.5-6 mm/s in this study which was manageable by human operation. The probe was placed perpendicular to the measurement surface based on visual alignment before the indentation measurement began.

The number of cycles for each indentation measurement was not restricted in previous studies using indentation method. In reality, subjects may feel tired and have unwanted movement if the indentation measurement is too long. Also, the chance of probe misalignment increases at later indentation cycles when the total number of cycles is more. Therefore, the duration for each indentation measurement was controlled within one minute and the number of indentation cycle was set as 6 cycles in this study.

Force and deformation data during the indentation measurement were saved in text file and analyzed offline. An analysis program was created using MATLAB (Version R2012a, MathWorks, Natick, MA, US). The user interface of the MATLAB program is shown in Figure 3-8. Due to asynchronous data transmission from the electromagnetic spatial sensing system and the load cell sensing module to the computer, a time shift existed between the force and deformation information. Temporal calibration was performed in the analysis program to adjust the offset between two data channels when the file was called. The adjusted data were plotted and displayed on the upper right corner. The beginning and maximal indentation of all cycles were then labelled manually on the adjusted force and deformation curve displayed on the user interface.

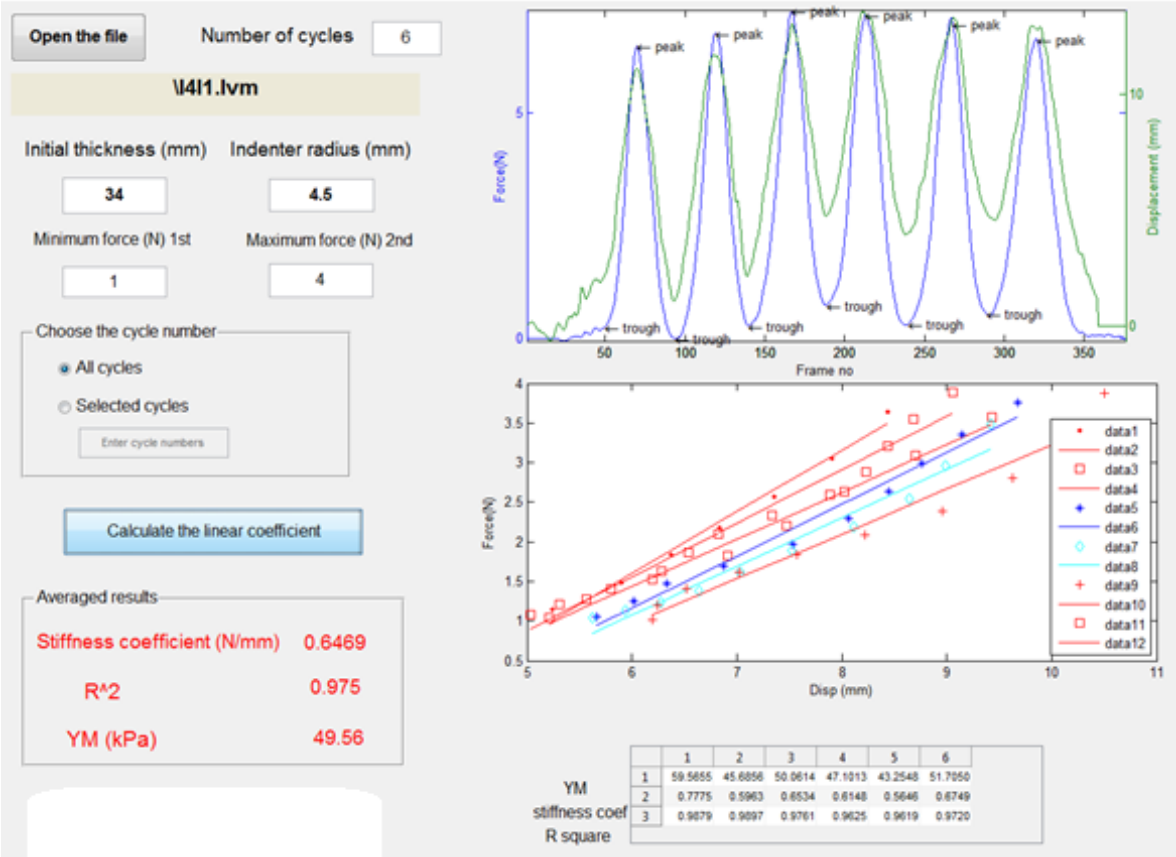

Figure 3-8 The user interface of the data analysis program in MATLAB. After a data file is uploaded, user labels the start as “trough” and the end as “peak” of each cycle’s indention phase by mouse clicking on the curves. The resulted force-deformation curves of all cycles are shown in the space below. Initial tissue thickness of the measured object, indenter radius and range of indentation force for analysis are required to be filled in the respective textboxes for calculation using the Hayes’ model. Results calculated for each cycle are shown in the table at lower right corner.

Young’s Modulus was calculated from all force-deformation curves at indentation phase following the Hayes’ model mentioned in Section 2.12.4. Parameters such as initial tissue thickness and indenter radius in the model were required to be keyed in on the user interface as well. Since soft tissue is nonlinear viscoelastic in nature, the force-deformation curve is not completely linear. The slope calculated varies depending on the force or deformation interval selected. Indentation rate has been

observed to be relatively consistent while force applied was between 0.5 N and 75% of the peak force (Zheng and Mak, 1996, Zheng and Mak, 1999). Force range from 1N to 4 N was selected to standardize the Young's Modulus calculation in all analyses for this study. User could define another tissue loading criterion for Young's Modulus calculation in the program. Young's Modulus of a testing object presented in this study was the average value of a number of indentation cycles. The first cycle was discarded in the calculation due to stress relaxation response in muscle to cyclic indentation (Koo, 2012). Any cycle with extreme value or poor force-deformation correlation was also rejected when calculating the average stiffness.

3.5. Validation tests of manual indentation system performance

The performance of the indentation system was evaluated through several tests. Displacement reported by the new coordinate system ${}^{C}T_{R}$ was validated. Young's modulus measurement using the manual indentation system was compared with a standard mechanical testing machine. Relationships between measurement results and measurement locations in the electromagnetic field as well as operator dependency were also looked into.

3.5.1. Validation of probe displacement measurement

To validate the displacement reported by the indentation probe after calibration, the probe was assembled onto a one dimensional translation platform driven by a micrometer head (Mitutoyo Corporation, Kawasaki, Japan) as shown in Figure 3-9 a. The platform was extended to different lengths by turning the micrometer (Figure 3-9 b) intermittently. Both readings of the micrometer and the reported ${}^{C}T_{R}$ position at each stop were marked to calculate the displacement. The displacement calculated from reported readings should be the same as displacement of the platform if calibration was correct.

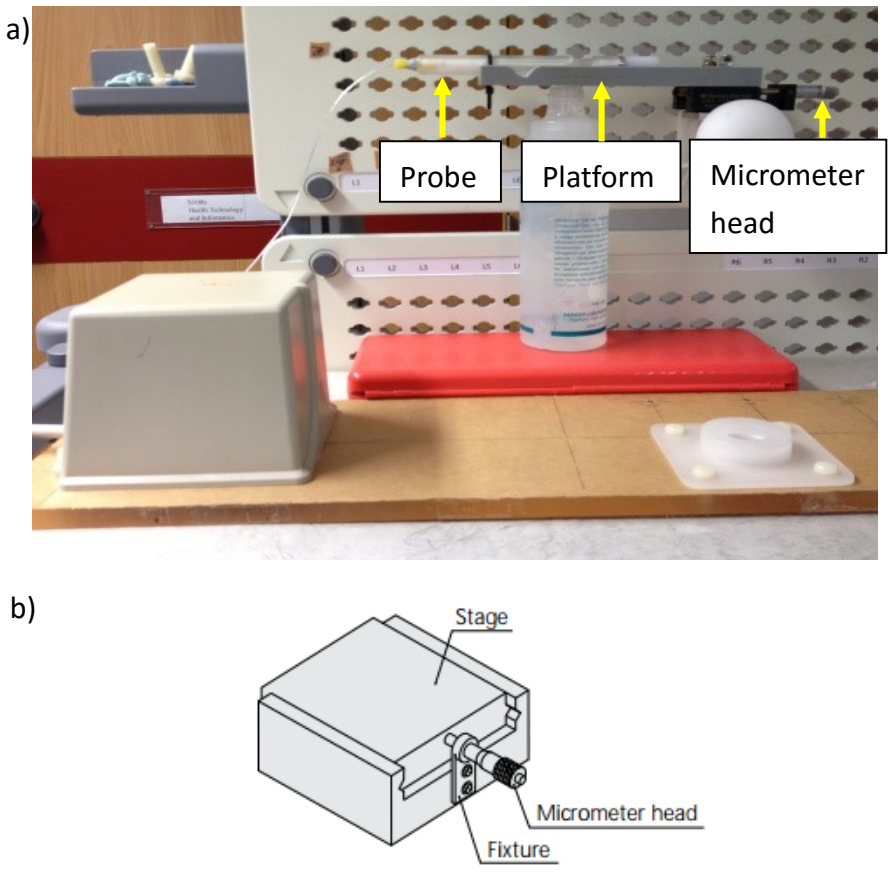

Figure 3-9 (a) Setup of the translation platform with the probe attached on. The platform was installed on a movable stage driven by a micrometer head. (b) An enlarged view of the movable stage controlled by the micrometer head. Figure b was adopted from (Mitutoyo, 2012).

3.5.2. Validation of Young's modulus measurement

Young's modulus measurement results obtained by the new manual indentation system were compared and validated with a standard mechanical testing machine (Instron 5569, Norwood, MA, USA) (Figure 3-10). The result obtained by standard mechanical testing machine is considered as the "gold standard" in indentation measurement and has been used as a mean to compare with other manual indentation systems (Zheng and Mak, 1996, Zheng and Mak, 1999, Lu et al., 2009). The material testing machine is referred as "Instron", its brand name in short, in the following sections.

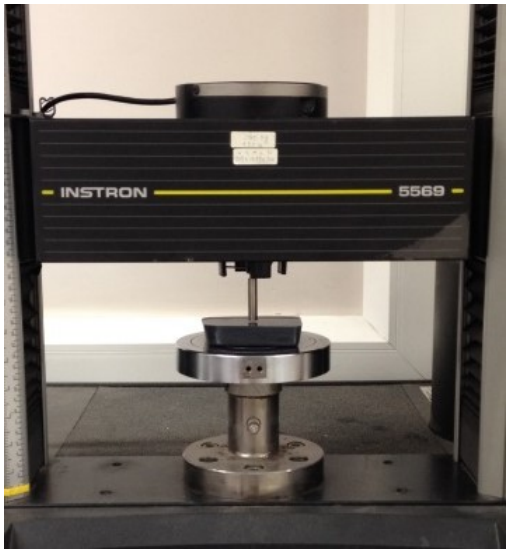

Figure 3-10 The standard mechanical testing machine used in this study. A silicone phantom (black in color) was placed on the flat platform readied to be indented. A flat-ended steel rod with 9 mm diameter was used as the indentation probe and connected to the force actuator of the machine.

Stiffness of the same set of phantoms was measured by both Instron and the manual indentation system and the measurement results were compared. The phantoms were fabricated in our laboratory by mixing silicone oil and curing agent at variant ratios. A smaller portion of curing agent with the same amount of silicone oil increases stiffness of the phantom. The mixture was well combined, then degassed in a vacuum chamber and cured at temperature of 60˚C until it was set (Wang et al., 2014). Nine silicone phantoms of different stiffness mimicking human soft tissue were made for this test.

The settings of indentation measurement performed by Instron followed the settings of the manual indentation system as explained in Section 3.4. A 9mm diameter cylindrical flat-ended steel indenter was inserted to Instron to indent the phantoms. The phantoms were indented by Instron for 6 cycles at a rate of 4 mm/s with a pre-load at 0.5N. As Instron required a fixed indentation rate, the rate was set in the middle of the acceptable range of indentation rate defined in Section 3.4. The indentation was limited to a maximum loading of 10N or a maximum deformation of 20% initial thickness whichever reached earlier. The middle of each phantom was repeatedly tested for 5 times and the results were averaged. A few minutes of "resting time" was given in between measurements to allow the phantom to recover to its original shape. The phantoms were tested again by the manual indentation system in the same sites following the operation settings mentioned in Section 3.4. Measurement results from both methods were analyzed using the MATLAB program. Young's moduli of all phantoms measured by the manual indentation system and Instron were correlated.

3.5.3. Location dependency of measured Young's modulus to the location from the field transmitter

In order to confirm stiffness of an object measured by the manual indentation system was independent of location within the electromagnetic field, an object was repeatedly tested at different distances relative to the field transmitter. Silicone phantoms of different stiffness were used in this test. This location dependency analysis was only carried out along the positive x-axis of the transmitter as the design of the frame used for para-spinal muscle stiffness measurement *in vivo* only allowed the subject to be stood on the right side (i.e. direction of positive x-axis) of the transmitter.

Six phantoms were in turn placed vertically in 3 different positions (28 cm, 35 cm and 42 cm) at separations of about 7 cm along the positive x-axis of the transmitter (Figure 3-11). This was to match the separations between lateral measurement sites on para-spinal muscles at the same vertebral level in later stiffness measurements. The stiffness results of each phantom measured at different locations along the same axis were compared.

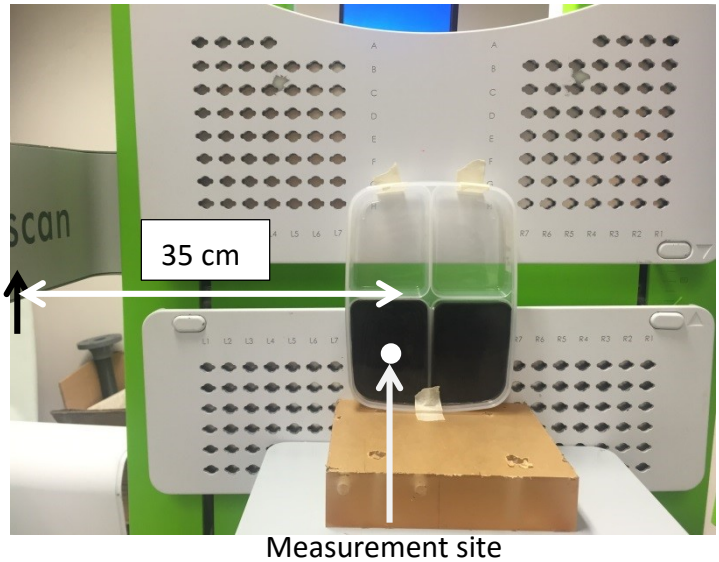

Figure 3-11 The setup of location dependency test.

3.5.4. Intra- and inter- operator reliability of Young's modulus measurement on phantoms

Since the indentation probe was driven manually, precise control on indentation rate or probe alignment could not be guaranteed. Therefore it is important to keep any inconsistency between or within operators to be low. Operator dependency on Young's modulus measurements using the manual indentation system were analyzed by intra- and inter- operator correlation coefficients.

Three operators including the system's developer participated in this test. All operators were familiarized with the system's operation and the indentation test before actual data recording. Each operator performed 5 indentations on a phantom following the same indentation protocol described in Section 3.4. The same number of measurements was performed on each measurement site in a reported para-spinal muscle stiffness analysis and would be used in this study as well (Oliva-Pascual-Vaca et al., 2014). The test was repeated on another 4 phantoms of different stiffness.

Calculations of Young's modulus using force-deformation data were performed by the system's developer. Intra-operator reliability was used to compare the Young's modulus of each phantoms measured repeatedly by the system's developer. Meanwhile, inter-operator reliability was used to compare the average Young's modulus of the same phantom measured by different operators. The reliabilities were calculated based on intraclass correlation coefficient (ICC) and were interpreted as very high for ICC from 1.00 to .90; high from .89 to .70; moderate from .69 to .50; low from .49 to .26; and poor for less than .25 (Leonard et al., 2003).

3.6. Stiffness measurement on para-spinal muscles *in vivo*

The second half of the study focused on para-spinal muscle stiffness measurement. Quantitative analysis of para-spinal muscles stiffness was conducted using the manual indentation system developed in this study. Muscle stiffness at each vertebral level was expected to be varying due to the complexity of spinal musculoskeletal structure. Stiffness measurements aimed at identifying the para-spinal muscle stiffness distribution along and across the spine in standing position. Normal healthy subjects and IS subjects were recruited for measurements and their results were compared.

3.6.1. Recruitment of normal and scoliosis subjects

Before the study, ethical approval was obtained from the University Human Ethics Committee for this study (reference no.: HSEARS20140812002). Normal subjects and some IS subjects were recruited from the campus through poster announcement. The rest of the IS subjects were referred by a practicing Chinese Medical doctor registered in Hong Kong who is specialized in spinal orthopedics. All participants who had responded to our recruitment were screened verbally according to our inclusion and exclusion criteria (see List A to D). Those who did not pass the screening were excluded from subsequent procedures. Successful participants were required to understand the details regarding this study and to sign an informed consent prior to the next stage (see Appendices I to V). Participants who entered the next stage were instructed to be refrained from physical exercises for at least 3 days before the measurement. On the day of measurement, all participants received a radiation-free spine scan using a 3D ultrasound imaging system developed by our research team (Cheung et al., 2013, Cheung et al., 2015) in order to confirm their spinal deformity. Details of the spine scan are elaborated in the next section.

A. Inclusion criteria for normal subjects

1. Age between 17-30.
2. Cobb angle less than 10 degrees.

B. Exclusion criteria for normal subjects

1. History of diagnosed musculoskeletal disease or disorder on back and spinal region.
2. Received musculoskeletal surgical intervention performed on back and spinal region.
3. Performed excessive training on either side of para- spinal muscles.
4. Had back pain.
5. Contraindicate to magnetic field.
6. Pregnant female subjects.
7. Unable to stand for over 10 minutes

C. Inclusion criteria for scoliosis subjects

1. Age between 17-30.
2. Cobb angle greater than 10 degrees.
3. Clinically diagnosed with idiopathic scoliosis.

D. Exclusion criteria for scoliosis subjects

1. Clinically diagnosed with any known cause for scoliosis
2. History of diagnosed musculoskeletal disease or disorder on back and spinal region besides IS.
3. Scoliosis with more than two curvatures.
4. With cervical scoliosis.
5. Received musculoskeletal surgical intervention performed on back and

spinal region.

6. Performed excessive training on either side of para- spinal muscles.
7. Had back pain.
8. Contraindicate to magnetic field.
9. Pregnant female subjects.
10. Unable to stand for over 10 minutes

3.6.2. Scoliosis assessment using 3D ultrasound imaging system

Before measurement, subjects were asked to take a radiation free 3D ultrasound scan on back region using a system developed by the same research group (Cheung and Zheng, 2010, Cheung et al., 2013, Cheung et al., 2015). The design of the 3D ultrasound imaging system is shown in Figure 3-12.

Figure 3-12 The 3D ultrasound imaging system. Patients are required to stand on the anti-fatigue mat and face the patient monitor during scanning.

Subjects were required to stand on the anti-fatigue mat and face the patient monitor during scanning (Figure 3-13). Four adjustable supporters were placed at the locations of the subject's acromia and lateral anterior superior iliac spines to facilitate a stable posture (Figure 3-13). Subjects' arms should be hung at the sides with palms facing the body. The free-hand scanning began from L5 and continued upwards until C7 was reached while a stack of cross-sectional ultrasound images covering the thoracic and lumbar spine were collected.

Inside the ultrasound probe was an electromagnetic spatial sensor, which is the same model as used in the manual indentation system, to record the positions and orientations of all B mode images taken relative to the magnetic field transmitter. After scanning, the image stack was automatically reconstructed into a 3D image volume based on their coordinates by a computer algorithm. Volume projection imaging method was used to generate a 2-dimensional spine image in frontal view from the resulted image volume (Figure 3-14 a) (Cheung et al., 2015).

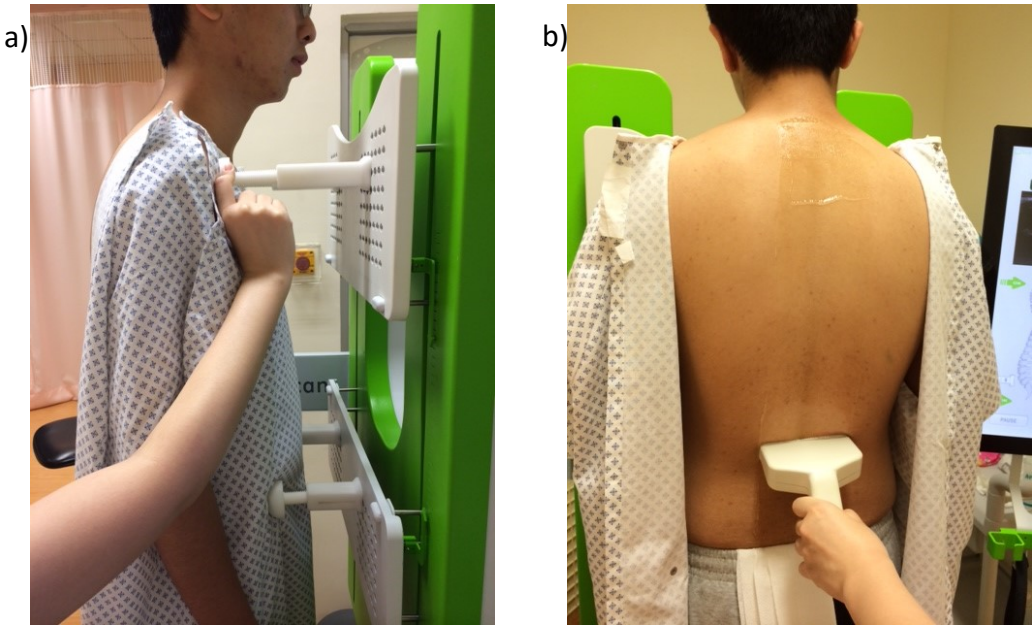

Figure 3-13 (a) A patient stood on the mat and four supporters were placed at his acromia and lateral anterior superior iliac spines. (b) The patient was being scanned. The spine from L5 up to C7 would be scanned.

The final image, which was similar to a posterior-anterior plain radiograph, was used to confirm the severity of spinal curvature in all subjects as well as to identify curve types in scoliosis subjects. The lateral spinal curvature was determined by the spinous process angle (SPA) measured on the resulted image instead of Cobb angle. Although SPA gave a slight overestimation on the curve severity than Cobb angle (i.e. SPA =1.07* Cobb angle), the results from two measurement methods showed high correlation and agreement (R^2= .79) (Cheung et al., 2015). Therefore, it was expected that participants with SPA greater than 10 degrees had scoliosis. To measure SPA, two lines were drawn manually on the spinous process shadows of the two most deviated vertebrae and the angle between the two lines was automatically calculated (Figure 3-14 b) (Li et al., 2010, Cheung et al., 2015). The SPA measurement was performed by an experienced operator of the 3D ultrasound scanning system who was independent of this study.

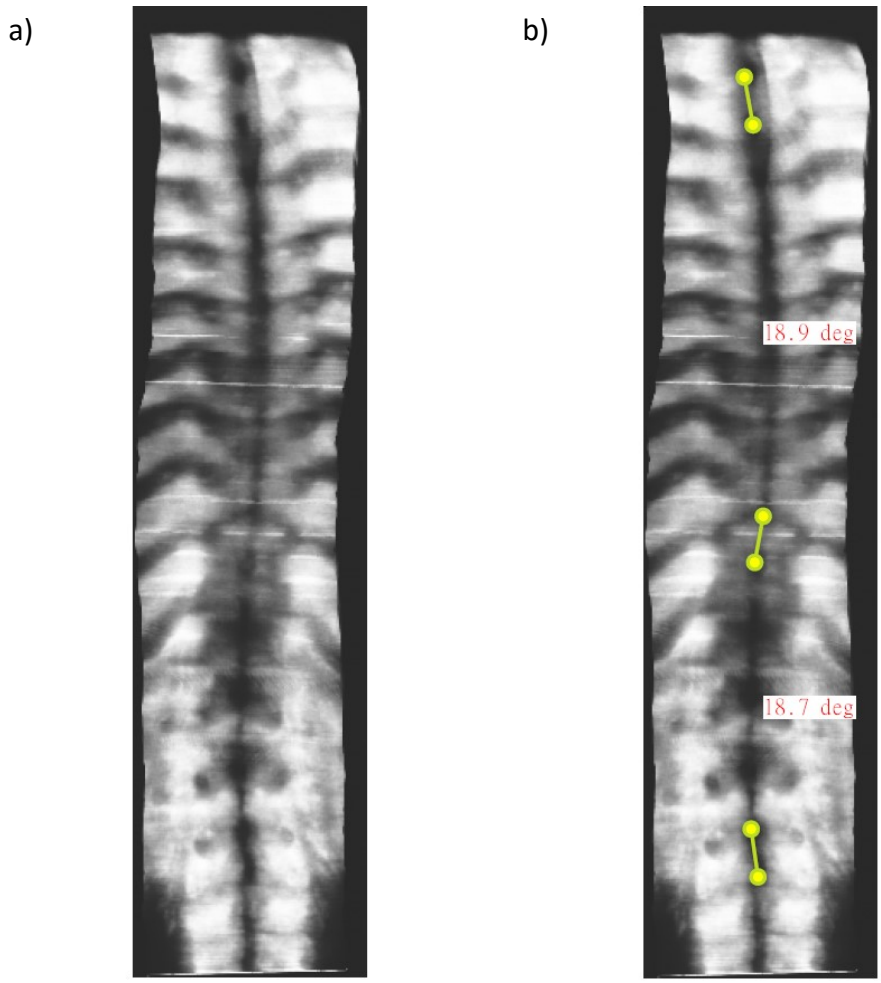

Figure 3-14 (a) A typical 2-dimensional spine image in frontal view obtained from a scoliosis subject which is similar to a posterior-anterior radiograph. (b) The measurement of SPA to indicate spinal deformity on the spine image. A pair of lines were drawn on the shadow of spinous processes of the most tilted vertebrae along the curve. The angle was calculated automatically after the lines were drawn. If there are two curves, a third line could be drawn at the lower end vertebra of the second curve to calculate the second angle.

3.6.3. Young's modulus measurement on para-spinal muscles of normal subjects

Normal subjects were further divided into two groups (Normal_1.5cm and Normal_3cm). Para-spinal muscle stiffness measurements were conducted on muscles at different separations from the spinous processes of subjects from different groups. Group Normal_1.5cm had measurement sites at 1.5 cm bilateral to the spinous processes at all vertebral levels while group Normal_3cm had measurement sites at 3 cm bilateral to the spinous processes at the same horizontal level. Bilateral para-spinal muscles at 4 vertebral levels (i.e. T3, T7, T11, and L4) between T3 to L4 were selected for measurement. The locations of the vertebrae were found by manual palpation with the help of anatomical landmarks (i.e C7 and iliac crests). All measurement sites were marked on skin with a marker pen. The vertebral levels for measurements of the normal subjects are indicated in Figure 3-15.

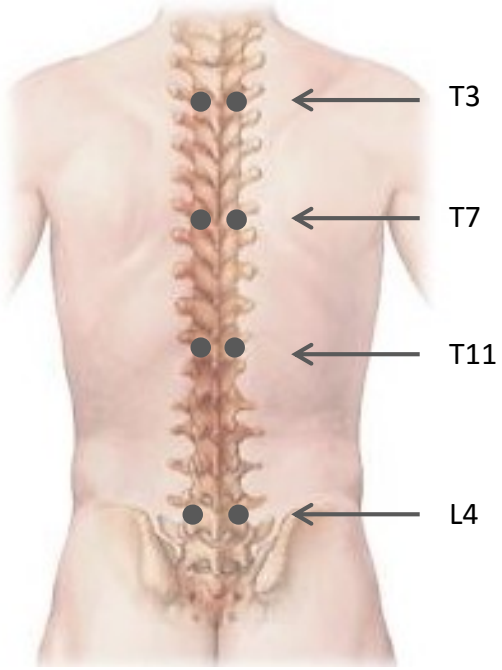

Figure 3-15 The 8 locations for measurements on normal subjects were labelled by dots. Measurements were taken at different separations from the spinous process of the same vertebral level for groups Normal_1.5cm and Normal_3cm. Picture was adopted and modified from (Department of Nursing and Orthopaedic Surgery, 2011).

The initial tissue thickness at each measurement site was measured with ultrasound imaging (EUB-8500, Hitachi Ltd., Japan) in transverse direction (Figure 3-16). Initial tissue thickness and para-spinal muscle stiffness measurements were taken in standing posture. Subjects were required to stand in front of the 3D ultrasound scanning system as shown in Figure 3-12 with the same posture as in the previous spine scanning during stiffness measurement. The locations of the four supporters were not moved during the whole measurement so as to guide the subject to stand in the same posture every time he returned to the standing platform.

Manual indentation was performed on all 8 sites following the protocol presented in Section 3.4. The test was repeated 5 times at the same measurement site for an average. For measurements at T7 and T11, subjects were asked to hold their breath during the indentation process. They were instructed to take a deep breath then exhale up to the functional residual capacity and hold until the end of indentation (Nicholson et al., 2001). Resting time was given to subjects in-between measurements to avoid fatigue.

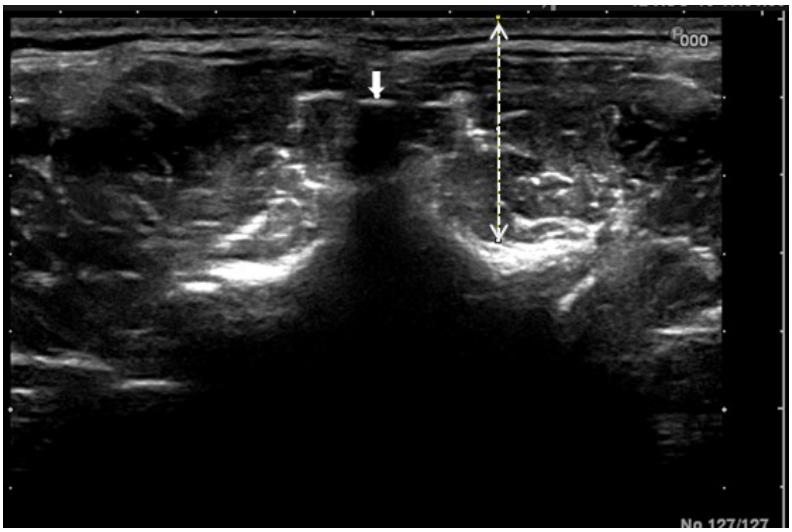

Figure 3-16 An ultrasound image taken at L4 in transverse direction. The arrow indicated the spinous process. The up-down arrow indicated the initial tissue thickness 1.5 cm from spinous process at L4.

3.6.4. Young's modulus measurement on para-spinal muscles of scoliosis subjects

Subjects with IS were also divided into two groups (Scoliosis_1.5cm and Scoliosis_3cm). Scoliosis_1.5cm had measurements at 1.5 cm bilateral to spinous processes and Scoliosis_3cm at 3 cm. Para-spinal muscles at the vertebral levels of apex, upper end and lower end of the curve with the greatest deviation were selected for measurements. Those special vertebrae were visualized and identified from the two-dimensional spine image obtained before measurement. In addition to the three special levels, para-spinal muscles at T3, T7, T11, and L4 vertebral levels were also measured. At most 7 vertebral levels were measured for scoliosis subjects (Figure 3-17). All the procedures of para-spinal muscle stiffness measurement in scoliosis subjects were the same as mentioned in previous subsection for normal subjects.

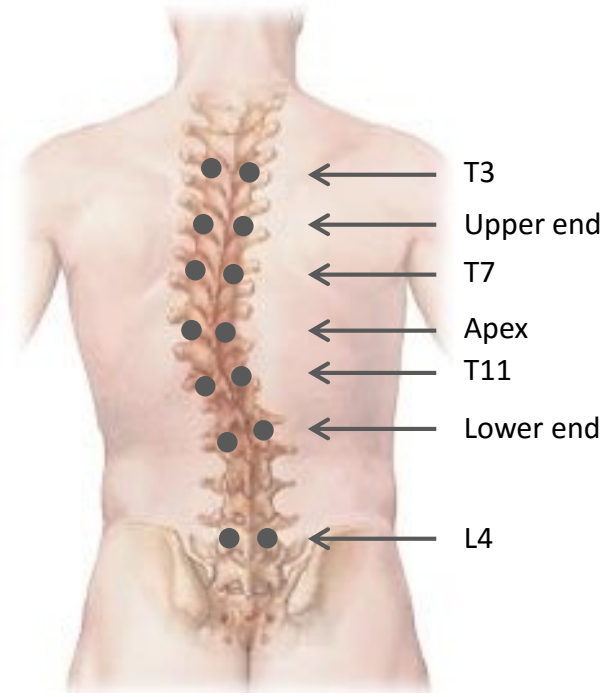

Figure 3-17 The 14 locations for measurements on scoliosis subjects were labelled by dots. Measurements were taken at different separations from the spinous process of the same vertebral level for groups Scoliosis_1.5cm and Scoliosis_3cm. Picture was adopted and modified from (Department of Nursing and Orthopaedic Surgery, 2011).

3.7. Intra- and inter-operator reliability of Young's modulus measurement of para-spinal muscles *in vivo*

Normal subjects regardless of their subgroup were invited to join the repeatability study of muscle stiffness measurement. Subjects who agreed to join the repeatability study were instructed to keep refrained from physical exercise until the second visit. They would receive another measurement on the second day after the first visit and the measurement was repeated on the same locations as in the first test at T3 and L4 in order to reduce measurement duration. The measurement procedures also followed the descriptions in subsection 3.6.3. Intra-operator correlation coefficients were used to compare the reliability of repeated measurement results by the same operator between two visits.

3.8. Statistical analysis on Young's modulus measurement *in vivo*

Statistical analyses were performed using the statistical package SPSS (version 21.0, SPSS Inc., Chicago, IL). Level of significance for all comparisons was set at $p = 0.05$. A comparison result with a p-value less than 0.05 means it was statistical significant. For some comparison results which its p-value was shown to equal to 0.000, the statistical result would be listed as statistical significant and p=.001.

Mean and standard deviation for age, height, weight and BMI of each group were calculated. Normality of each clinical data for each group was analyzed by Shapiro-Wilk test. One-way ANOVA test was used to detect the presence of significant difference in subjects' characteristics between the 4 groups.

Young's modulus was calculated for all the measurements. Normality of Young's modulus measured at different levels along the spine in individual groups was tested

with Shapiro-Wilk test. Two independent factors “side” (left and right or convex and concave) and “level” (different vertebral level measured) might affect muscle stiffness measured within a group. Two-way ANOVA test was performed using “side” and “level” as the fixed factors while the absolute Young’s modulus value measured was regarded as the dependent variable. Interaction between the two factors and the significance of each factor in the muscle stiffness results obtained were identified. Paired t-test was performed to look for between-side differences at each vertebral level tested. More than one Paired t-test was carried out to compare all combinations of measurements performed at different vertebral levels on the same side of the spine. Comparison of muscle stiffness at different locations from the spine between groups Normal_1.5cm and Normal_3cm were made by independent sample t-test.

Para-spinal muscle stiffness with or without scoliosis was also compared. Scoliosis subjects from both groups were separated by major apex location (i.e. thoracic or lumbar) and their para-spinal muscle stiffness results of the convex and the concave sides at the apex were compared with the results of the corresponding spinal region in the normal groups. To represent the normal para-spinal muscle stiffness at a selected spinal region, a value was calculated by averaging the results measured in normal subjects at the two vertebral levels nearest to that spinal region on the same side assuming that the change was linear. The obtained values were used as the test value for the corresponding one sample t-test performed to identify the significance between muscle stiffness at the scoliotic apex and normal muscle stiffness.

CHAPTER 4 RESULTS

In this chapter, verification results of the manual indentation system are first reported. The result of repeatability of para-spinal muscle stiffness measurement *in vivo* using the verified system is included. Main findings including the normal para-spinal muscle stiffness distribution, the muscle stiffness presentation along major curve of scoliosis subjects and the comparisons between the muscle stiffness of normal and scoliosis subjects are followed.

4.1. Probe displacement measurement after calibration

The displacement of the indenter was calculated from the reported coordinates of ${}^{C}T_{R}$ at each check point and compared with the displacement of the platform in a single trial. The displacement of the indenter reported by the calibrated system was demonstrated to be highly correlated with the translation platform controlled by the micrometer (R^2=.9983, p=.001) (Figure 4-1).

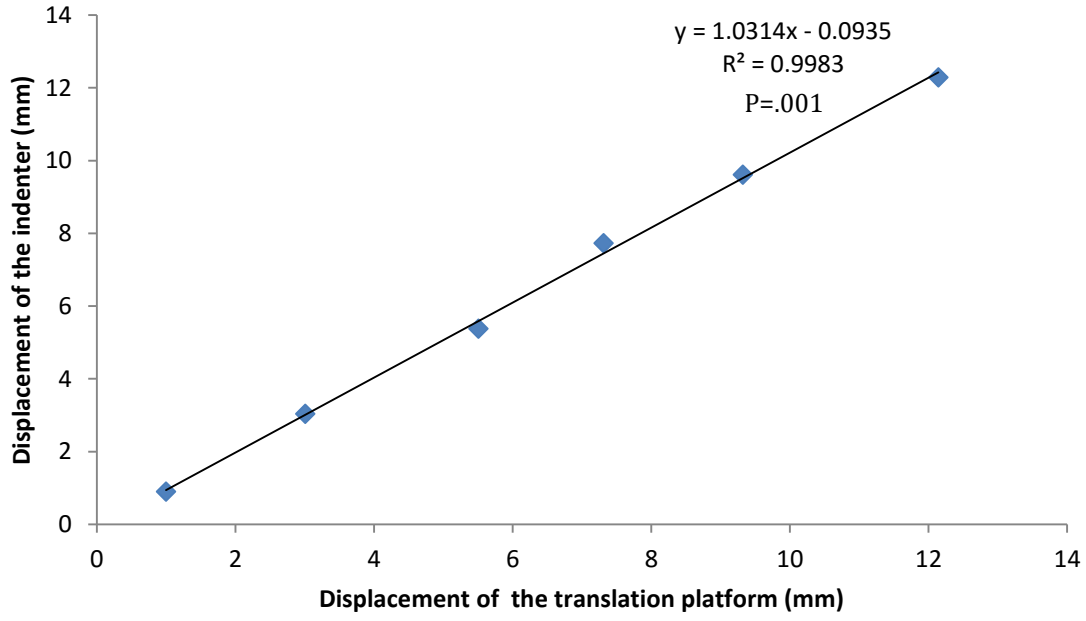

Figure 4-1 The correlation between displacement of the indenter reported by the calibrated system and displacement of the translation platform controlled by the micrometer.

4.2. Correlation between Young's moduli measured by the new method and the reference method

The average Young's modulus of 9 phantoms with different stiffness measured by both Instron and the manual indentation system are shown in Figure 4-2. Measurements made by the manual indentation system had a similar trend as those from Instron. The manual indentation system was able to distinguish different levels of stiffness using silicone phantoms. The Young's modulus measured by the manual indentation system was found to be comparable with that by Instron with excellent correlation (R^2 =.9903, p=.001) (Figure 4-3). The Young's modulus measured by the manual indentation system was smaller than Instron as the correlation curve had a linear slope less than one. Larger deviation of measurement was found when measuring phantoms stiffer than 100 kPa using the manual indentation system.

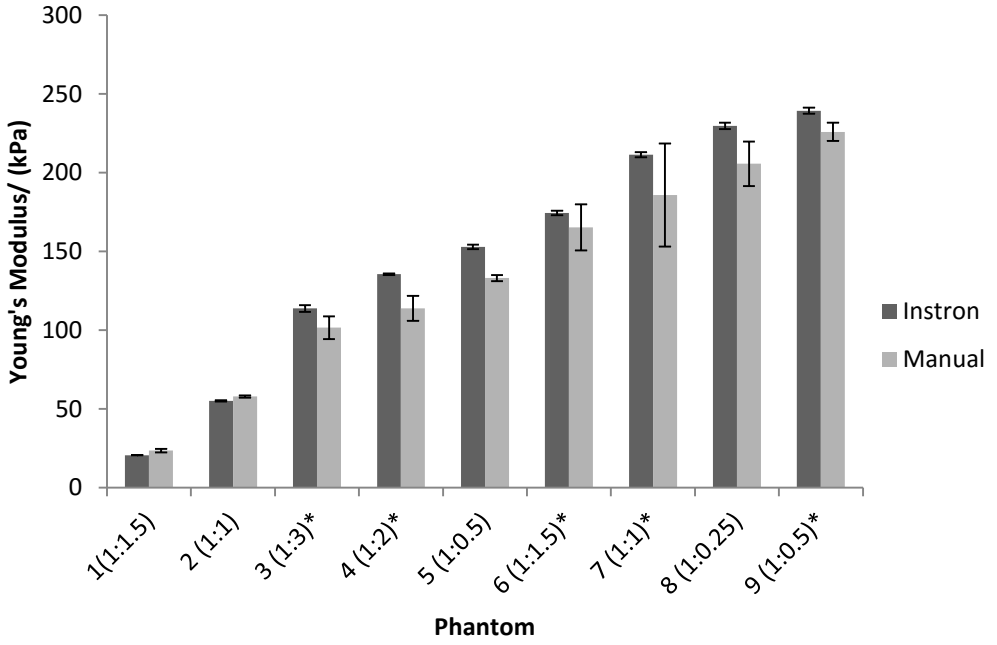

Figure 4-2 Young's modulus of the phantoms measured by Instron and the manual indentation system. The asterisk "*" signs marked the phantoms that were fabricated with chemicals from another brand.

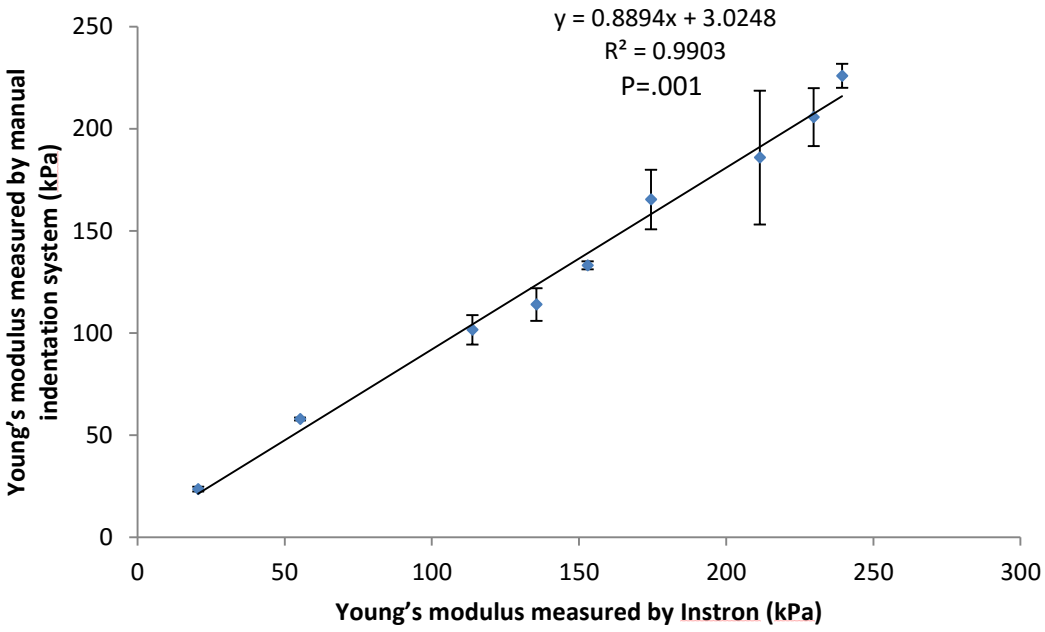

Figure 4-3 The correlation between Young's moduli of the phantoms measured by Instron and the manual indentation system.

4.3. Location dependency of Young's modulus measurement with reference to the electromagnetic transmitter

The Young's modulus of the different phantoms measured repeatedly at three locations along positive x-axis from the field transmitter is plotted in Figure 4-4. Reliability test showed that the measurements at different locations for the same phantom were highly repeatable with ICC(3,k) value of .989 (p=.001). This result suggested that Young's modulus of silicone phantoms measured by the manual indentation system was independent of the location of the measurement site.

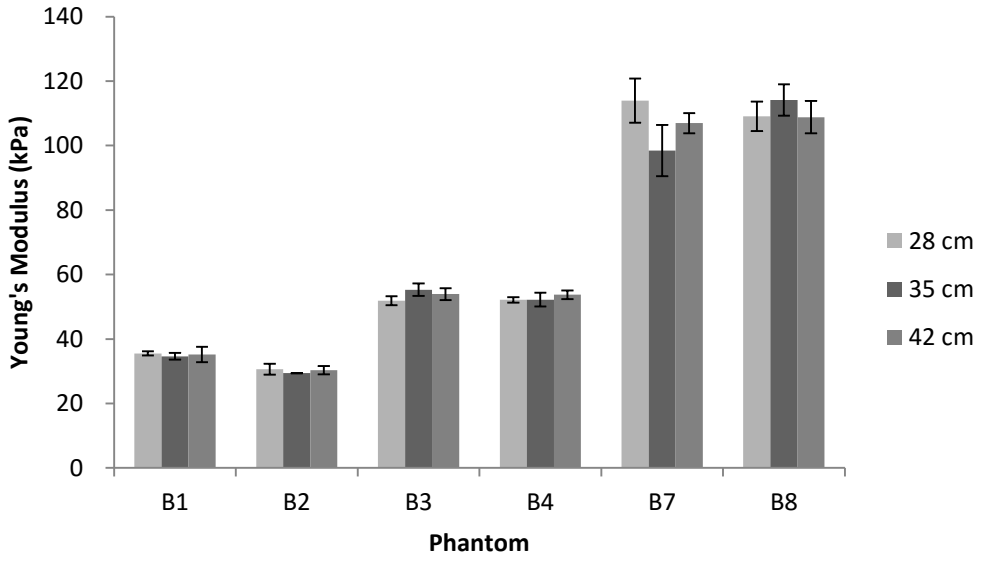

Figure 4-4 Young's modulus of the phantoms measured by the manual indentation system at three separations from the origin of the field transmitter along its positive x-axis.

4.4. Intra and inter-operator reliability of Young's modulus measurement on phantoms

Reliabilities of the measurements using the manual indentation system were shown to be excellent and operator-independent using silicone phantoms. Very high correlation values for intra-operator reliability (ICC (3,1)=.999) and inter-operator reliability (ICC (2,k)=.983) were found with significance less than 0.001.

4.5. Para-spinal muscle stiffness measured *in vivo*

A total of 58 participants were recruited for this study, 33 were normal subjects and 25 had IS. They were separated into 4 groups for measurements. Physical characteristics of each group are summarized in Table 4-1 and Table 4-2. Age, height, weight and BMI of subjects between groups were compared independently using One-way ANOVA test and no significant difference was found.

Table 4-1 Physical characteristics of normal subjects measured at 1.5 cm and 3 cm bilateral to the spinous processes.

	Normal_1.5cm	Normal_3cm
Total (n)	22	11
Male: Female (n:n)	9:13	4:7
Mean Age (years)	25.2±2.9	24.0±4.2
Mean Height (m)	1.67±.07	1.65±.07
Mean Weight (kg)	58.2±10.2	57.0±12.2
Mean BMI	20.8±2.4	20.9±3.1
Dominant hand	All Right	All Right

Table 4-2 Physical characteristics of scoliosis subjects measured at 1.5 cm and 3 cm bilateral to the spinous processes. For apex location, T, TL and L stand for thoracic, thoracolumbar and lumbar respectively.

	Scoliosis_1.5cm	Scoliosis_3cm
Total (n)	13	12
Male: Female (n:n)	3:10	4:8
Mean Age (years)	23.2±6.1	23.0±6.3
Mean Height (m)	1.63±.06	1.64±0.10
Mean Weight (kg)	54.6±6.5	51.6±5. 9
Mean BMI	20.5±2.0	19.3±1.4
Dominant hand	All Right	All Right
SPA (degree)	18.9±7.1	20.6±6.5
S-shape: C-shape	7:6	7:5
Major to Left: Right	6:7	6:6
Apex location	T:7 TL:1 L:5	T:5 TL:3 L:4

4.6. Intra- and inter-operator reliability of para-spinal muscle stiffness measured *in vivo*

Nine normal subjects agreed to participate in the repeatability test. The average Young's modulus at a location measured on the first visit was compared with the result from the second visit. Reliability test showed strong agreement of para-spinal muscle stiffness measured at T3 with ICC (3,k) of .800 and excellent agreement of stiffness measured at L4 with ICC (3,k) of .845. This indicated that para-spinal muscle stiffness measurement *in vivo* using the manual indentation system was repeatable.

4.7. Normal para-spinal muscle stiffness distribution

The normality of measurements at all measurement sites were confirmed with significance greater than .05. No interaction was found between stiffness measured between "side" and "level" for muscles at 1.5 cm [$F(3,168) = .416$, $p=.742$] as well as at 3 cm from spinous process [$F(3,56) = .367$, $p=.777$]. Figure 4-5 illustrates the average Young's modulus measured at the 4 vertebral levels at different locations from spinous process on the normal subjects.

The Young's modulus measured at all locations and the significance of between "side" comparisons are summarized in Table 4-3. Muscles on the left hand side at 1.5 cm from the spinous process had Young's modulus significantly larger than the right hand side at all levels tested. For Normal_3cm group, Young's modulus of muscles on the left hand side was consistently larger than the lateral side but only showed significant difference at level T3 ($p=.001$) and T7 ($p=.006$). Asymmetry of the lateral para-spinal muscle stiffness was observed in normal subjects and the variance reduced gradually when muscles were located further aside from the spine in horizontal directions.

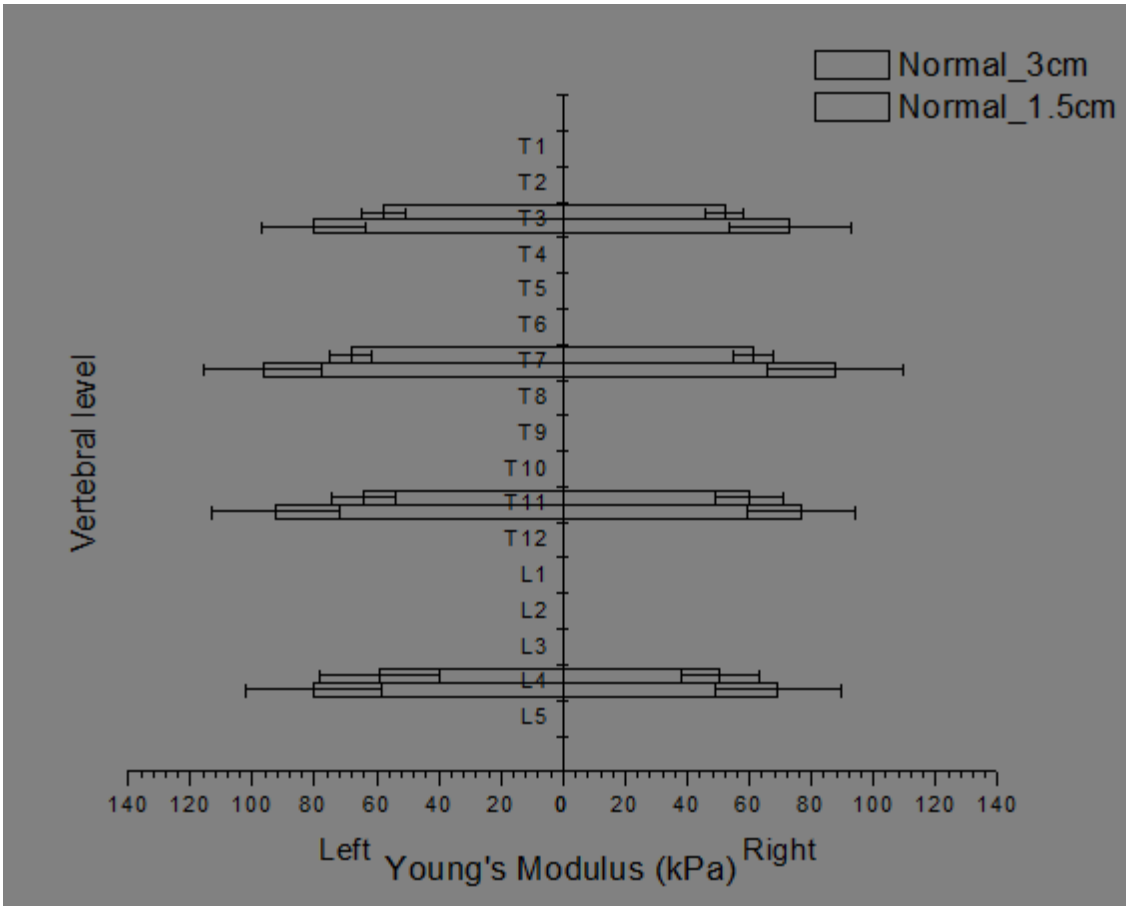

Figure 4-5 The average Young's modulus of para-spinal muscles measured at 1.5 cm and 3 cm bilateral to the spinous processes at vertebral level T3, T7, T11 and L4 of normal subjects.

Table 4-3 Average Young's modulus of muscles measured on different vertebral levels and locations from the spine. Results of statistical comparisons between "side" are included. Bold P-value shows a significant difference between the Young's moduli of lateral sides at that vertebral level.

	Normal_1.5cm			Normal_3cm		
Vertebral level	Left	Right	Effect of side (p-value)	Left	Right	Effect of side (p-value)
T3	80.3±16.6	73.1±13.9	**.001**	57.7±7.1	52.0±6.1	**<.001**
T7	96.5±19.0	87.7±21.8	**.002**	68.3±6.6	61.3±6.5	**.006**
T11	92.4±20.6	76.5±17.3	**<.001**	64.3±10.2	60.0±10.7	.229
L4	80.6±21.8	69.3±20.1	**.004**	59.1±19.3	50.4±12.5	.109

At 1.5 cm from the spine, the average Young's modulus at T7 and T11 was larger than that at T3 and L4. Paired t-tests showed muscle stiffness on the left hand side at T3 and L4 was significantly different from that at T7 and T11. However, muscle stiffness was not significantly different within pair T7 and T11 (p=.310) nor pair T3 and L4 (p=.952). On the opposite side, the average Young's modulus at T7 was significantly larger than T3 (p=.001), T11 (p=.013) and L4 (p=.001). Additional paired-t tests were ran between measurements at T3, L4 and the average result of T7 and T11. Both T3 and L4 were found to be significantly different from the average value with p-values of .008 and .007 which represent that T3 and L4 had lower muscle stiffness than the mid thoracic region. In general, muscles at 1.5 cm from spinous process were less stiff at the upper thoracic and lumbar regions compared with the mid and lower thoracic regions.

For muscles at 3 cm from the spinous processes, larger average Young's modulus was also found on both sides at T7 and T11. On the left hand side, Young's modulus measured at T3 was significantly lower than that at T7 (p=.007). Young's modulus at T3 was found to be significantly different from the average result of T7 and T11 in further statistical test (p=.002). Young's modulus at L4 was not significantly different compared with results at T3, T7 and T11 or with the average result of T7 and T11. On the opposite side, stiffness at T3 and L4 were significantly different from that at T7 and T11 respectively but there was not significant difference within the pairs.

Statistical analyses results between muscle stiffness at two vertebral levels on one side for normal groups are separated into Table 4-4 and Table 4-5. Although statistical analyses did not generate identical results for all combinations, it was expected that muscles in thoracic region were stiffer than the superior and inferior regions along a normal spine in standing posture regardless of the measurement locations.

Table 4-4 P-values generated by statistical analyses on the Young's moduli of any two vertebral levels in Normal_1.5cm group. Bold P-value shows a significant difference between Young's moduli of the two levels.

	Normal_1.5cm							
	Left				Right			
Vertebral level	T3	T7	T11	L4	T3	T7	T11	L4
Young's Modulus (kPa)	80.3±16.6	96.5±19.0	92.4±20.6	80.6±21.8	73.1±13.9	87. 7±21.8	76.5±17.3	69.3±20.1
T3	---	**<.001**	**.028**	.952	---	**.001**	.403	.431
T7	**<.001**	---	.310	**.012**	**.001**	---	**.013**	**.001**
T11	**.028**	.310	---	**.003**	.403	**.013**	---	.065
L4	.952	**.012**	**.003**	---	.431	**.001**	.065	---

Table 4-5 P-values generated by statistical analyses on the Young's moduli of any two vertebral levels in Normal_3cm group. Bold P-value shows a significant difference between Young's moduli of the two levels.

	Normal_3cm							
	Left				Right			
Vertebral level	T3	T7	T11	L4	T3	T7	T11	L4
Young's Modulus (kPa)	57.7±7.1	68.3±6.6	64.3±10.2	59.1±19.3	52.0±6.1	61.3±6.5	60.0±10.7	50.4±12.5
T3	---	**.007**	.066	.812	---	**.005**	**.046**	.696
T7	**.007**	---	.260	.202	**.005**	---	.656	**.029**
T11	.066	.260	---	.313	**.046**	.656	---	**.032**
L4	.812	.202	.313	---	.696	**.029**	**.032**	---

Young's moduli measured bilaterally at 1.5 cm at all levels were larger than the results measured at 3 cm. When comparing the measurements at different lateral locations from spinous process on the same side of a vertebral level, Young's modulus measured at the two locations were significantly different at all 4 vertebral levels (all $p<.05$) (Table 4-6). The results indicated that muscles further away from the spine were relatively less stiff.

Table 4-6 Average Young's modulus of muscles measured on different lateral locations from the spinous process on the same side of a vertebral level in normal subjects. Results of statistical comparisons between locations are included. Bold P-value shows a significant difference between the Young's moduli of different locations at that vertebral level.

	Left			Right		
Vertebral level	1.5 cm	3 cm	Effect of location (p-value)	1.5 cm	3 cm	Effect of location (p-value)
T3	80.3±16.6	57.7±7.1	**<.001**	73.1±13.9	52.0±6.1	**<.001**
T7	96.5±19.0	68.3±6.6	**<.001**	87.7±21.8	61.3±6.5	**<.001**
T11	92.4±20.6	64.3±10.2	**<.001**	76.5±17.3	60.0±10.7	**.008**
L4	80.6±21.8	59.1±19.3	**.011**	69.3±20.1	50.4±12.5	**.009**

4.8. Para-spinal muscle stiffness distribution in presence of scoliosis

Para-spinal muscle stiffness at the same 4 vertebral levels (i.e. T3, T7, T11 and L4) was also measured on scoliosis subjects and the results are presented in

Figure 4-6. Young's moduli measured at each sites of both scoliosis subgroups were normally distributed. No interaction was found in Young's modulus results when comparing between "side" or "level" in Scoliosis_1.5cm [$F(3, 96) = .582$, $p = .629$], nor in Scoliosis_3cm [$F(3, 88) = 1.307$, $p = .277$] group.

The average Young's modulus was found higher on the left hand side at 1.5 cm of spinous process and the between-side imbalance was significant at 3 vertebral levels except T7 ($p = .071$). For muscles at 3 cm from spinous process, Young's modulus on the left was not consistently larger than on the right. Significant difference in Young's modulus measured on left and right was only found at level T7 ($p = .001$) and L4 ($p = .001$). Similar to normal subjects, para-spinal muscle stiffness of the overall scoliosis subjects was still significantly larger on the right hand side in most locations measured. Table 4-7 summarizes the average Young's modulus measured on left and right hand side at different levels of scoliosis subjects and the statistical significances of between-side comparisons.

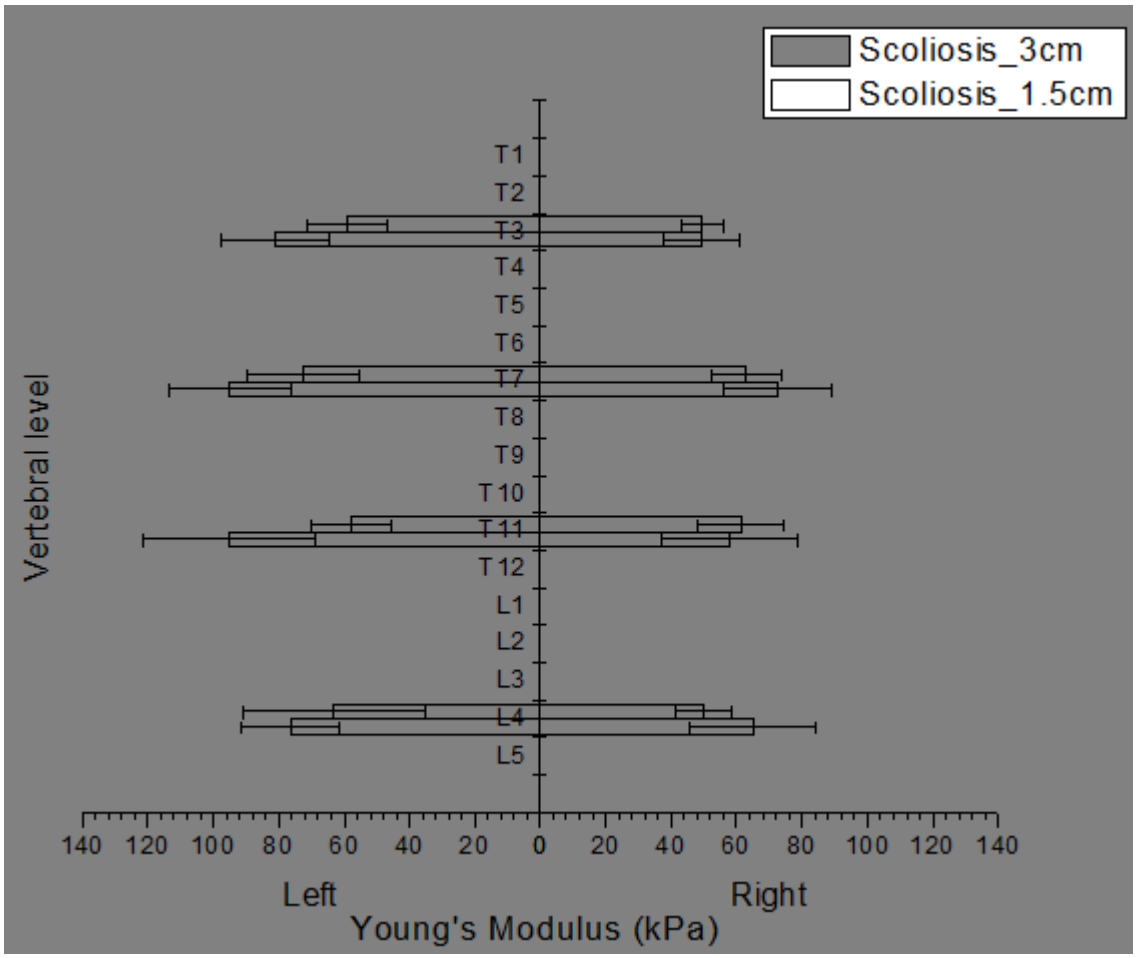

Figure 4-6 The average Young's modulus of para-spinal muscles measured at 1.5 cm and 3 cm bilateral to the spinous processes at vertebral level T3, T7, T11 and L4 of scoliosis subjects.

Table 4-7 Average Young's modulus of muscles measured on different vertebral levels and locations from the spine of scoliosis subjects. Results of statistical comparisons between "side" are included. Bold P-value shows significant difference between "side" at that vertebral level.

	Scoliosis_1.5cm			Scoliosis_3cm		
Vertebral level	Left	Right	Effect of side (p-value)	Left	Right	Effect of side (p-value)
T3	81.0±16.3	49.5±11.6	**.007**	59.2±12.3	49.5±6.4	.447
T7	95.1±18.6	72.5±16.5	.071	72.5±17.0	63.0±10.7	**<.001**
T11	95.3±26.4	57.8±20.8	**.004**	57.8±12.3	61.2±13.0	.616
L4	76.4±15.1	65.1±19.4	**.016**	63.1±27.8	50.2±8.6	**<.001**

Table 4-8 P-values generated by statistical analyses on the Young's moduli of any two vertebral levels in Scoliosis_1.5cm group. Bold P-value shows a significant difference between Young's moduli of the two levels.

	Scoliosis_1.5cm							
	Left				Right			
Vertebral level	T3	T7	T11	L4	T3	T7	T11	L4
Young's Modulus (kPa)	81.0±16.3	95.1±18.6	95.3±26.4	76.4±15.1	49.5±11.6	72.5±16.5	57.8±20.8	65.1±19.4
T3	---	**.036**	.092	.359	---	**.001**	.595	.323
T7	**.036**	---	.979	**.002**	**.001**	---	**.014**	**.004**
T11	.092	.979	---	**.007**	.595	**.014**	---	.058
L4	.359	**.002**	**.007**	---	.323	**.004**	.058	---

Table 4-9 P-values generated by statistical analyses on the Young's moduli of any two vertebral levels in Scoliosis_3cm group. Bold P-value shows a significant difference between Young's moduli of the two levels.

	Scoliosis_3cm							
	Left				Right			
Vertebral level	T3	T7	T11	L4	T3	T7	T11	L4
Young's Modulus (kPa)	59.2±12.3	72.5±17.0	57.8±12.3	63.1±27.8	49.5±6.4	63.0±10.7	61.2±13.0	50.2±8.6
T3	---	**.035**	.686	.619	---	**<.001**	**.002**	.773
T7	**.035**	---	**.025**	.264	**<.001**	---	.604	**.001**
T11	.686	**.025**	---	.447	**.002**	.604	---	**.010**
L4	.619	.264	.447	---	.773	**.001**	**.010**	---

The average Young's moduli measured at T7 and T11 in scoliosis subjects were not consistently higher than the other two vertebral levels similar to the case in normal subjects (Table 4-8 and Table 4-9). Along the left hand side at 1.5 cm, Young's modulus at L4 was significantly different from T7 (p=.002) and T11 (p=.007) while T3 was only significantly different from T7 (p=.036). Young's modulus at T7 on the lateral side was significantly different from T3 (p=.001), T11 (p=.014) and L4 (p=.004). At 3 cm from the spinous process, Young's modulus measured on the left of T7 was significantly different from T3 (p=.035) and T11 (p=.025). On the opposite side, T3 and L4 were each significantly different from T7 and T11.

Young's modulus measured at different lateral locations from the spinous process of the same vertebral level in scoliosis subjects also showed significant difference except on the left of L4 (p=.164) and the right side of T11 (p=.127) (Table 4-10).

Table 4-10 Average Young's modulus of muscles measured on different lateral locations from the spinous process on the same side of a vertebral level in scoliosis subjects. Results of statistical comparisons between locations are included. Bold P-value shows a significant difference between the Young's moduli of different locations at that vertebral level.

	Left			Right		
Vertebral level	1.5 cm	3 cm	Effect of location (p-value)	1.5 cm	3 cm	Effect of location (p-value)
T3	81.0±16.3	59.2±12.3	**.001**	49.5±11.6	49.5±6.4	**<.001**
T7	95.1±18.6	72.5±17.0	**.006**	72.5±16.5	63.0±10.7	**.002**
T11	95.3±26.4	57.8±12.3	**<.001**	57.8±20.8	61.2±13.0	.127
L4	76.4±15.1	63.1±27.8	.164	65.1±19.4	50.2±8.6	**.025**

4.9. Para-spinal muscle stiffness distribution along major curve of scoliosis

Since the para-spinal muscle stiffness was shown to vary according to vertebral level, the effect of scoliosis on local muscle stiffness was analyzed based on the curve's apex location. Vertebral levels between T3 and T11 were categorized as thoracic region while below T11 to L4 were categorized as lumbar region in this analysis. Thus, subjects with apex located at thoracolumbar region were grouped into lumbar curve in this study.

Table 4-11 and Table 4-12 listed the average Young's modulus measured at different locations on scoliosis subjects separated by the curve's apex location. Although larger Young's modulus was observed on the convex side of lumbar curve, Young's moduli of the lateral sides at the upper end, the apex and the lower end vertebrae did not show significant differences for subjects from both Scoliosis_1.5cm and Scoliosis_3cm groups. For subjects with thoracic curve, higher Young's modulus was found mostly on the concave side of the curve. However, between "side" comparisons were only found significant at the lower end vertebra for subjects in Scoliosis_1.5cm group and at the upper and apex vertebrae for Scoliosis_3cm group. The significant difference observed in lateral para-spinal muscle stiffness of normal subjects seemed to have become more balanced between the convex and concave sides in scoliosis subjects separated according to curve's apex.

Figure 4-7 shows the Young's modulus measured on different levels and locations of scoliosis subjects with thoracic and lumbar curves. For subjects with lumbar curve, Young's modulus at the upper end was larger than those at the apex and the lower end for both convex and concave sides (a and b). Significance was found between the upper end and the apex at both locations from the spinous processes (1.5 cm: p=.043; 3 cm: p=.017) and between the upper end and the lower end (p=.025) at 1.5 cm of the concave side. For subjects with thoracic curve, the highest Young's modulus was at the apex level on convex and concave sides (c and d). Significance was only found between the apex and the upper end on lateral sides (convex: p=.007; concave: p=.006) as well as between the apex and the lower end (p=.002) at 3 cm concave side.

Table 4-11 The average Young's modulus measured at different locations of subjects from group Scoliosis_1.5cm separated according to curve's apex location. Results of statistical comparisons between "side" at the 3 levels are included. Bold P-value shows significant difference between "side" at that vertebral level.

	Lumbar (n=6)			Thoracic (n=7)		
Vertebral level	Convex	Concave	Effect of convex and concave (p-value)	Convex	Concave	Effect of convex and concave (p-value)
Upper end	92.5±31.7	84.7±19.5	.499	78.5±19.9	84.6±11.6	.207
Apex	79.4±23.8	68.4±13.7	.145	82.3±16.5	98.0±25.3	.078
Lower end	77.8±20.0	68.8±21.2	.328	71.9±17.3	87.7±16.7	**.022**

Table 4-12 The average Young's modulus measured at different locations of subjects from group Scoliosis_3cm separated according to curve's apex location. Results of statistical comparisons between "side" at the 3 levels are included. Bold P-value shows significant difference between "side" at that vertebral level.

	Lumbar (n=7)			Thoracic (n=5)		
Vertebral level	Convex	Concave	Effect of convex and concave (p-value)	Convex	Concave	Effect of convex and concave (p-value)
Upper end	63.0±13.1	58.5±11.0	.379	48.4±8.0	57.6±13.0	.018
Apex	55.2±21.8	46.3±7.4	.266	66.3±14.5	85.7±15.2	.015
Lower end	60.4±34.8	50.9±12.3	.395	57.9±15.4	54.2±15.1	.484

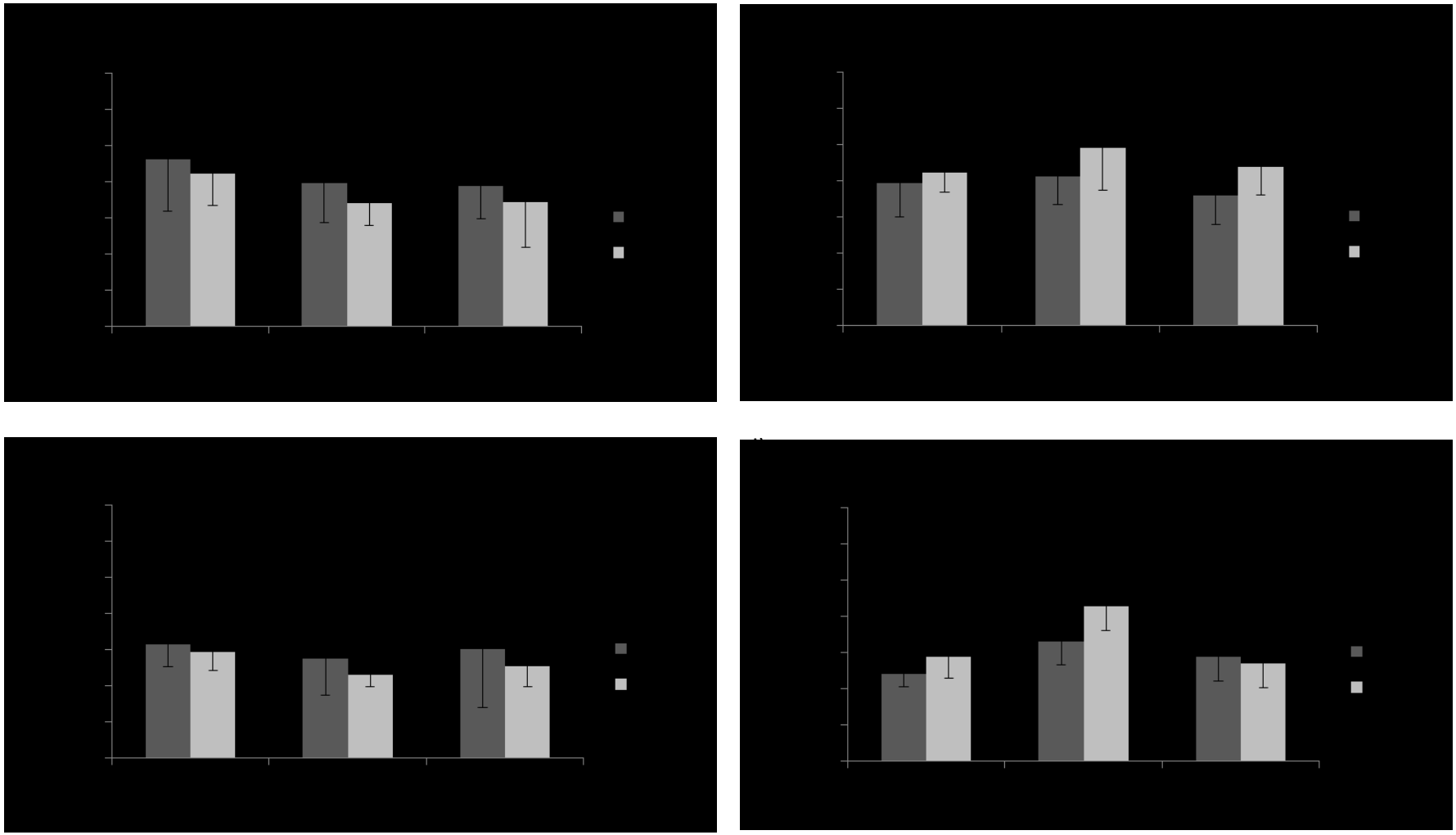

Figure 4-7 The average Young's modulus measured at different locations of scoliosis subjects. (a) Results of 1.5 cm group with lumbar curve. (b) Results of 1.5 cm group with thoracic curve. (c) Results of 3 cm group with lumbar curve. (d) Results of 3 cm group with thoracic curve. A pair with significant difference is marked by an asterisk "*" on top.

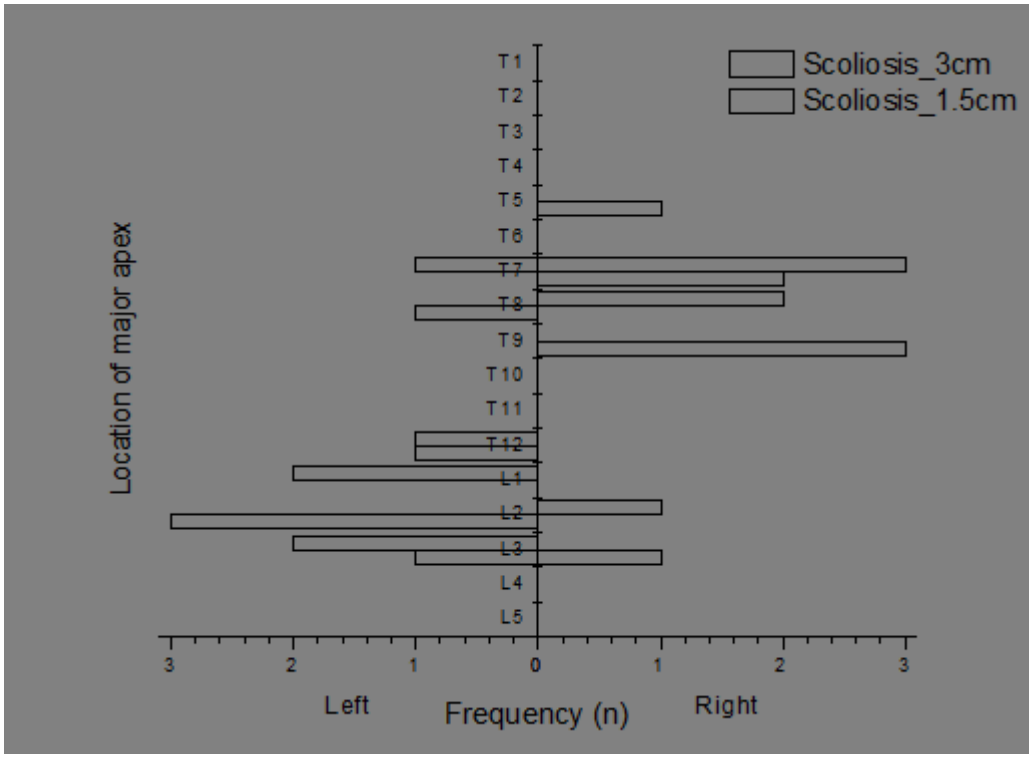

Figure 4-8 The apexes locations and the curves' direction of scoliosis subjects in this study. The apexes of lumbar curves were in between T11-L4 while the apexes of thoracic curves were mostly in between T7-T11. Lumbar curves mainly convexed to the left while thoracic curves mainly convexed to the right.

The final comparison between normal and scoliosis muscle stiffness was to identify if para-spinal muscle stiffness in the same spinal region altered between normal and scoliosis subjects. The apexes of thoracic curves were concentrated between T7 and T11 except for one subject and the apexes of lumbar curves were concentrated between T11 and L4 as illustrated in Figure 4-8. Therefore, average Young's modulus at lumbar region bounded by T11 and L4 of normal subjects was used to compare with Young's modulus at lumbar apex of scoliosis subjects. Similarly, average Young's modulus at thoracic region bounded by T7 and T11 of normal subjects was used to compare with Young's modulus at thoracic apex of scoliosis subjects. The Young's modulus representing normal muscle stiffness of lumbar and thoracic region

was averaged from the Young's moduli of the bounding levels and listed in Table 4-13 and Table 4-14.

From Figure 4-8, the majority of subjects with lumbar curve had the convexity to the left and those with thoracic curve had the convexity to the right. So the Young's modulus of lumbar para-spinal muscles on the left of normal subjects was used to compare with the Young's modulus of para-spinal muscles on the apex's convex of lumbar curve. Meanwhile, the Young's modulus of thoracic para-spinal muscles on the right of normal subjects was used to compare with that of para-spinal muscles on the apex's convex of thoracic curve. The comparison results between Young's moduli of normal and scoliosis subjects at the same spinal region are depicted in Figure 4-9.

For comparisons in lumbar region as shown in Figure 4-9a and b, Young's moduli of normal subjects were larger than that of scoliosis subjects on both lateral sides and in both muscle groups from spinous process. However, the result was only significant at the right (concave) side at 3 cm muscle group ($p=.019$). For thoracic curve comparisons as shown in Figure 4-9c and d, Young's moduli of normal subjects were mostly smaller than that of scoliosis subjects but only at left (concave) at 3 cm muscle group was significant ($p=.047$). Para-spinal muscle stiffness at scoliosis apex appeared to be different from the normal para-spinal muscle stiffness at the same spinal region. The direction of asymmetry was not consistent between the two curve types. Para-spinal muscle stiffness difference between normal and scoliosis subjects were more obvious and significant when comparing at muscle groups 3 cm away from spinous process.

Table 4-13 The average Young's modulus on both sides at apex level of group Scoliosis_1.5cm and on the corresponding spinal region of group Normal_1.5cm. Results of statistical analysis between groups are included. Bold P-value shows significant difference between groups at that vertebral level.

	Left			Right		
Spinal region	Normal_1.5cm	Scoliosis_1.5cm	Effect of group (p-value)	Normal_1.5cm	Scoliosis_1.5cm	Effect of group (p-value)
Lumbar	86.5±22.0	79.4±21.7	.494	72.9±19.1	68.4±12.5	.458
Thoracic	94.5±19.9	98.0±23.4	.099	82.1±20.5	82.3±15.3	.147

Table 4-14 The average Young's modulus on both sides at apex level of group Scoliosis_3cm and on the corresponding spinal region of group Normal_3cm. Results of statistical analysis between groups are included. Bold P-value shows significant difference between groups at that vertebral level.

	Left			Right		
Spinal region	Normal_3cm	Scoliosis_3cm	Effect of group (p-value)	Normal_3cm	Scoliosis_3cm	Effect of group (p-value)
Lumbar	61.7±14.9	55.2±20.2	.462	55.2±12.0	46.3±6.8	**.019**
Thoracic	66.4±8.4	85.7±13.6	**.047**	60.6±8.4	66.3±12.9	.427

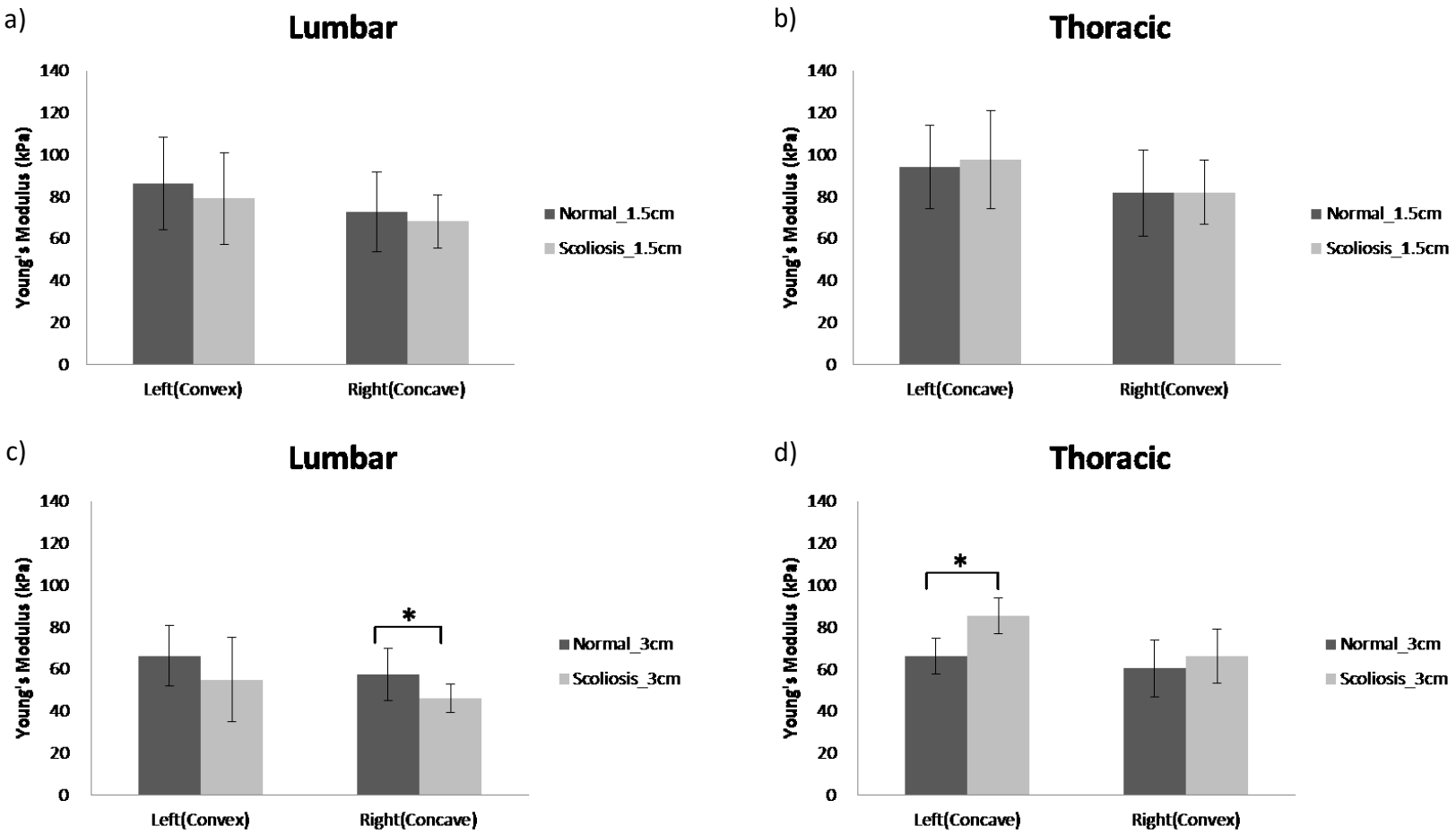

Figure 4-9 The average Young's modulus at different locations on the corresponding spinal regions between normal and scoliosis groups. (a) Comparison at lumbar at 1.5 cm. (b) Comparison at thoracic 1.5 cm. (c) Comparison at lumbar 3 cm. (d) Comparison at thoracic 3 cm. A pair with significant difference is marked by an asterisk "*".

CHAPTER 5 DISCUSSION

Based on the findings presented in last chapter, discussions about the rationale behind and study limitations are made in this chapter. The performance of the manual indentation system is briefly discussed. The main focus of this chapter is placed on discussing the possible causes of between-side and between-level para-spinal muscle stiffness imbalance considering the structural and functional usages of the spinal musculoskeletal system. Our findings on para-spinal muscle stiffness distribution in scoliosis subjects in contrast with the related past studies are also discussed. Limitations for this study and future study directions are included at the end.

5.1. Performance of the manual indentation system

Reliability of stiffness measurement using the newly developed manual indentation system has been demonstrated through a series of measurements on phantoms. Displacement of the probe reported by the calibrated electromagnetic spatial sensor showed excellent correlation with the displacement measured by the micrometer. Although the probe was displaced to limited points in the test, the results obtained suggested the reported displacement could reflect actual tissue deformation.

The manual indentation system was able to distinguish phantoms of different stiffness made from various compositions of silicone oil and curing agent. A smaller Young's modulus indicating lower stiffness was measured in phantoms made with higher portion of curing agent. For silicone phantoms with stiffness lower than 250 kPa, the Young's moduli measured by the manual indentation system formed a significant linear correlation with the results of the same measurements using Instron. As the stiffness of phantom increased, Young's modulus measured by the manual indentation system was apparently lower than that measured by Instron. Such a systemic

discrepancy in the measurement results could be due to non-identical indentation settings in the two measurement systems i.e. probe alignment and indentation rate.

Stress distribution within a layered material can be affected by probe misalignment during indentation. The resultant load on the material recorded by the load cell could have slight changes from the actual load when indention was not applied perpendicularly (Zheng and Mak, 1999). Indentation measurements using Instron was controlled along a perpendicular direction but the alignment control in the manual indentation system might be difficult to maintain. Probe misalignment up to 15 degrees was still tolerable in previous manual indentation study (Zheng et al., 1999). Meanwhile, the silicone phantoms used in this study were added with carbon particulates for another purpose irrelevant to this study. Phantoms were assumed to be homogenous but clumps could exist inside due to non-uniform mixing. This could cause a further change in stress distribution inside the phantoms when manual indentation is misaligned. Therefore in our phantom study using the manual indentation system, a lower force might have been detected for the same tissue deformation and resulted in a smaller Young's modulus when compared with Instron.

Mechanical response of silicone under indentation is time dependent due to its viscoelastic nature. Young's modulus measured by indentation tends to increase with higher indentation rate under the stiffening effect (Koo et al., 2011). During measurements with Instron, the indenter was moved up and down at a steady rate with motor control. However in the case of manual indentation, constant indentation rate could not be well controlled and might fluctuate during indentation. The overall indentation rate applied manually could be lower than the desired rate and thus led to a smaller Young's modulus. The effect of indentation rate on Young's modulus measurement was also reported in other studies (Lu et al., 2009, Zheng et al., 1999).

Young's moduli measured at a range of indentation rates (2.5-8.3mm/s in Lu et al., 2009 and 0.7-7.5 mm/s in Zheng et al., 1999) were compared and found no significant difference between the results. So the range of indentation rate used in this study was chosen to be in the middle of the values used by previous studies.

Probe misalignment and inconsistent indentation rate between measurements using manual indentation could also cause the results to have larger standard deviation compared with measurement results using Instron. Phantom 7 showed a particularly large variation in Young's modulus measured using the manual indentation system. This could be due to structural inhomogeneity in the phantom itself which caused the variation of stiffness at different points. In addition, indentation probe might not be placed at the exactly same site as in the previous test. So, Young's moduli obtained from repeated measurements on Phantom 7 could have greater variation when the indentation probe was misplaced from previous location.

Young's modulus measured by different means of indentation methods was not expected to be identical, but the difference could be reduced by applying a preload on the tissue before indentation or when tissue thickness is increased. Since the target of this study was to compare the para-spinal muscle stiffness between sides and levels of the human spine, it was not necessary to find out the absolute muscle stiffness at each point. With an excellent correlation when compared with the standard mechanical testing machine and operator independent performance, the manual indentation system developed in this study was confirmed to be reliable for para-spinal muscle stiffness measurement in the later stage of this study. Nevertheless, optimization of the manual indentation system is needed, for examples to include indications in the software to remind the operator about the current indentation rate and alignment.

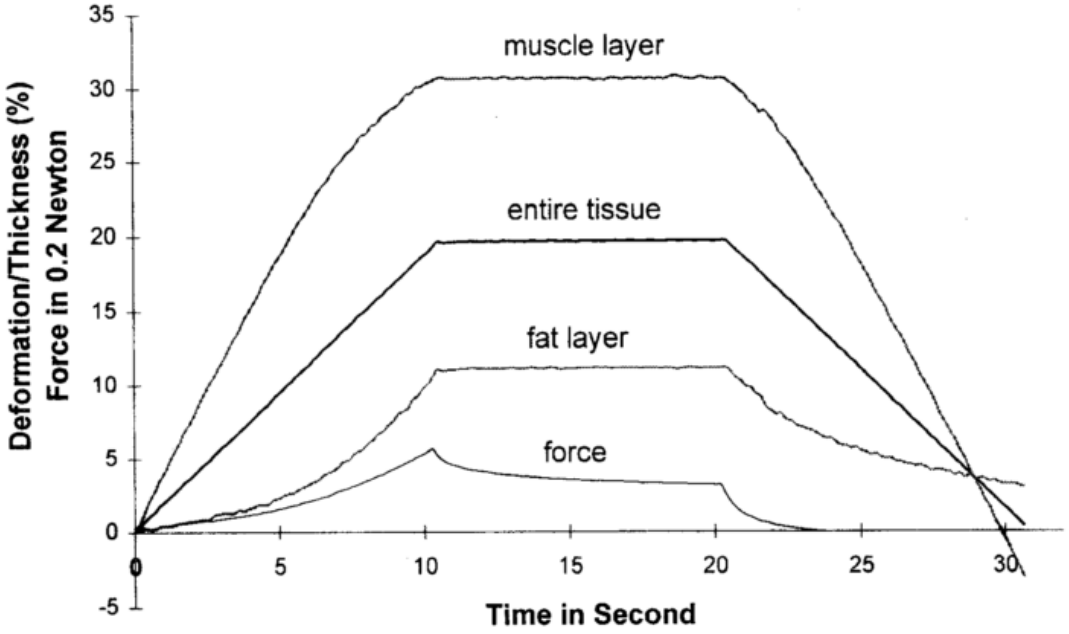

Figure 5-1 the deformation relative to the intial thickness of each layer in a porcine tissue during indentation. Tissue deformation was monitored with ultrasound. Figure was adopted from (Zheng and Mak, 1996).

It should be noted that Young's modulus measured using the manual indentation system in this study was a resultant stiffness of all soft tissue layers from skin to bone surface (Lu et al., 2009). Absolute stiffness of each muscle layer could not be extracted from our results. Zheng and Mak (1996) examined the deformation of muscle and adipose of a skinless porcine tissue specimen using indentation while the deformation of each layer was measured using ultrasound. They found muscle deformed more relative to their original thickness than the adipose layer on top provided that the size of the indenter was large enough to compress the entire tissue layer (Figure 5-1). Also Ylinen et al. (2006) investigated the effect of tissue thickness on stiffness using indentation and did not find correlations between skin or subcutaneous tissues thickness and the overall stiffness value. Considering that the geometry of the indenter in the current system was comparable to the indenter used in Zheng and Mak (1996) 's study, we could deduce that Young's moduli of para-spinal muscles obtained in this study mainly reflected stiffness of the muscle layer.

5.2. Para-spinal muscle stiffness distribution in normal subjects

Para-spinal muscle stiffness at two locations from the spinous process was measured on normal subjects in standing posture. Situated along those lateral lengths of the spine are two different muscle groups: transversospinalis and erector spinae group. Both muscle groups are extensor muscles but contribute differently to the structural functions of the spine. Transversospinalis group, which is made up of multifidus, rotatores and other small muscles, is situated at the closet to the spine and critical for the spinal stability and movements in erect posture. By alternate contraction and relaxation of the lateral muscles, the human spine can rotate and bend sideway while remaining at equilibrium. Meanwhile, the erector spinae muscles, which are further away from the spine, contract to against the body weight in front of the spine and maintain an erect torso.

Although the etiology of IS is still inconclusive, a lot of researchers support the idea that an anterior vertebral torsion resulting from an asymmetric loading or vertebral growth initiates the v*icious cycle* of scoliosis development (Burwell, 2003) (Figure 5-2). The role of para-spinal muscle in this cycle is still unclear. Para-spinal muscle could have changed to induce the asymmetric vertebral growth or to adapt to the asymmetric growth and counter the vertebral rotation. Previous studies which attempted to identify the asymmetrical changes in para-spinal muscles of scoliosis subjects focused on both transversospinalis (typically multifidus) and erector spinae. Therefore, the stiffness of both muscle groups was our interest in this study. However, any stiffness abnormality found in a pathological condition should be confirmed by comparing with a normal baseline value. Therefore, normal para-spinal stiffness distribution was first investigated in this study.

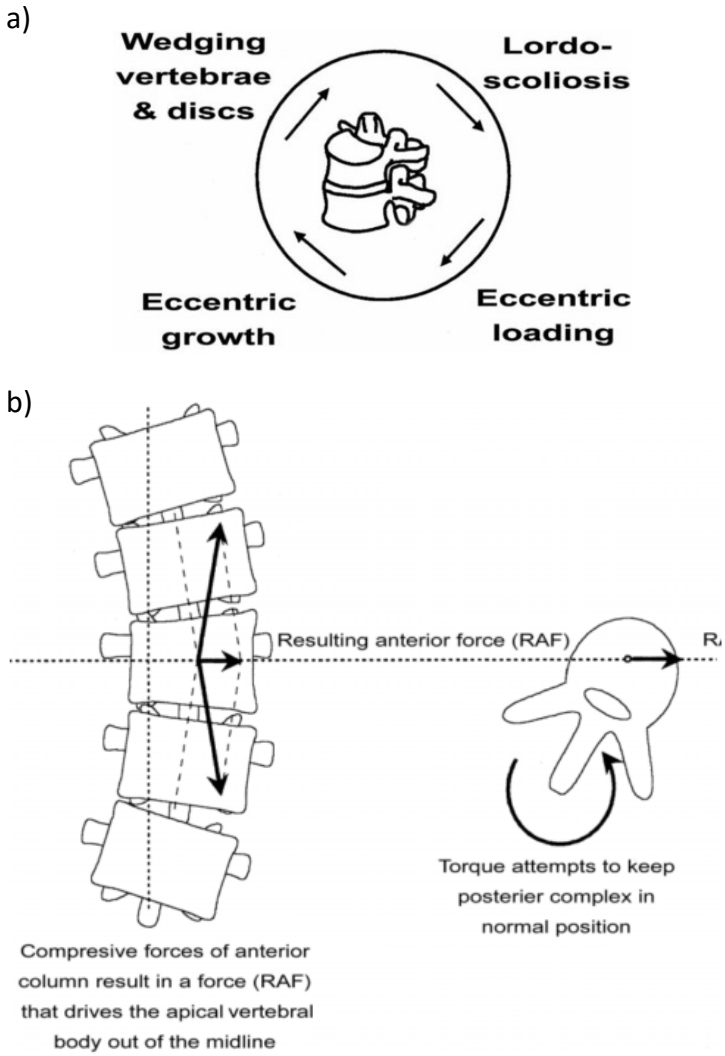

Figure 5-2 (a) An eccentric loading on a vertebral body caused asymmetric growth on the vertebrae. (b) The reaction froce applied to the superior and inferior normal vertebrae resulted in a force vector in the vertebrae with asymmetric growth and ld to deviation to one side. Figures were adopted from (Burwell, 2003).

5.2.1. Para-spinal muscle stiffness imbalance between lateral sides

In our study, transversospinalis on the left hand side was found to be consistently stiffer than the same muscle group on the lateral side for the majority of our normal subjects. For erector spinae, muscles of the left hand side also had larger stiffness than the right hand side but the asymmetry was only significant at level T3 and T7.

The design of the experimental setup was initially accused of causing the systemic difference between left and right para-spinal muscle stiffness. The magnetic field transmitter of the 3D ultrasound scanning system was fixed horizontally on the left hand side of subjects during indentation measurements. It was uncertain whether the magnetic field density at different locations covered by the field transmitter would introduce error to the measurement results when the measurement sites were farther away from the transmitter.

If this explanation was true, left para-spinal muscle stiffness of Normal_3cm group would have been significantly greater than right para-spinal muscle stiffness of the same group if the measurement was influenced by the location from the transmitter; otherwise this explanation would not make sense. Furthermore, the results of location dependency test indicated that stiffness of phantoms measured was independent of the separation from the transmitter. Therefore, the difference in side stiffness found was not introduced by experimental setup but caused by other factors within subjects.

Considering that exercise can cause muscle stiffness change and affect measurement results, subjects were refrained from physical exercise for a few days before measurement. Any change of muscle stiffness from short-term training before the cool down period should return to normal level at the time of measurement (Chen et al., 2014). We understood through verbal conversations that most of our normal subjects had not been involved in any regular and or intensive exercise for over one week before the measurement. As a result, the imbalance of muscle stiffness found between-side was unlikely to be caused by physical exercise.

Intrinsic factors such as physiological pressure inside the human trunk can also be relevant to the para-spinal muscle imbalance between sides (Kouwenhoven et al., 2006). Due to the anatomical position of the human heart, a steady aortic pressure is developed in the left of the thoracic cavity by the pumping heart. The internal pressure in the body could be an action force on para-spinal muscles to against the external indentation force. In this sense, muscles on the left hand side required a larger force to be deformed to the same degree compared to muscle on the right hand side. However, this could not explain why lumbar para-spinal muscles on the left hand side were also stiffer as intense physiological pressure is absent in that region.

Muscle stiffness change could also be related to the skeletal structure. As vertebral rotation coexists with scoliosis, Kouwenhoven et al. (2006) performed a study to understand the vertebral rotation pattern in healthy non-scoliotic spines using computer tomography scan. They concluded there was a vertebral rotation pre-existed in the human spine where the mid and lower thoracic vertebral bodies significantly rotated to the right by a maximum of 2 degrees (Figure 5-3a). Right rotation was predominant in the left-right vertebral rotation distribution. Vertebral bodies in lumbar spine also slightly rotated to the right but the result was not significant.

Kouwenhoven et al. (2007) further discovered the thoracic vertebral bodies also rotated but to the reverse direction (i.e. left) in a group of normal nonscoliotic subjects with situs inversus totalis such that their internal organs were arranged in mirror image of the normal anatomy (Figure 5-3b). Left-handed subjects were included in that study in a proportion close to the ratio of left-right handedness in the general population but the overall subjects showing left rotation were still predominated. However, a large scale school screening (n=8245) revealed that trunk asymmetry at mid-thoracic levels was significantly correlated to the handedness which signaled a right vertebral rotation in right-handed population (Grivas et al., 2006). Although the reason for this pre-existed vertebral rotation was inconclusive, arrangement of thoracic organs and handedness could influence vertebral rotation and para-spinal muscle stiffness.

Stiffer muscles on the side of dominant hand were more likely to be expected as it is a common belief that muscle stiffness tends to increase after prolonged use or training (Lam et al., 2015). On the other hand, the increased in muscle stiffness on the left hand side of our right-handed subjects could also be viewed as a biomechanical compensation to the repetitive use of the right human trunk.

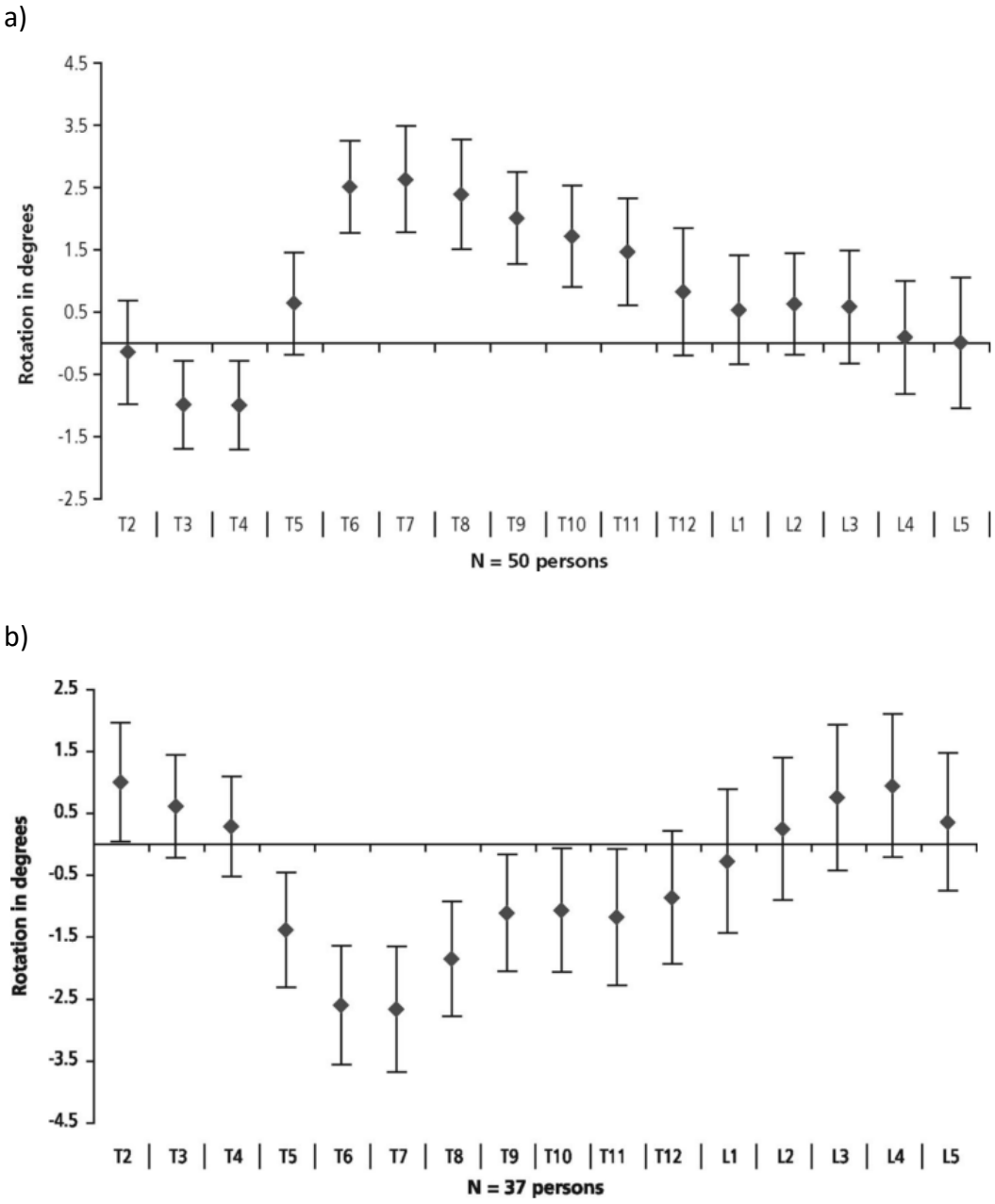

Figure 5-3 (a) Mean rotation angle at each vertebral level from T2 to L5 of normal subjects without scoliosis. (b) Mean rotation angle at each vertebral level from T2 to L5 of subjects with situs inversus totalis and without scoliosis. Figure were adopted from (Kouwenhoven et al., 2007).

Two left-handed normal subjects participated in our study but their results were not included in the findings presented in Chapter 4 in order to maintain consistency in hand dominancy. Their para-spinal muscles also tended to be stiffer on the left hand side than the right (Table 5-1). One study focused on the biomechanical property of biceps brachii of healthy older males and did not identify consistent asymmetry between muscles on the dominant limb and the non-dominant limb (Bailey et al., 2013). We cannot give a solid conclusion on whether hand dominance affects para-spinal muscle stiffness on a particular side at this moment due to limited sample size studied. Nevertheless, more analysis should be performed on left-handed subjects before determining the relationship between handedness and para-spinal muscle stiffness.

Higher stiffness of para-spinal muscle groups on the left hand side could be an influence from the pre-existed vertebral rotation along the spine. It should be noted that in Kouwenhoven's studies, the rotation was discovered under supine posture, which the testing posture was different from the posture used in this study. However, the chance for the vertebral rotation to remain under standing posture could not be neglected since the rotation was a structural change.

Table 5-1 Young's Modulus results for left handed normal subjects at 4 vertebral levels.

	Subject L1		Subject L2	
Vertebral level	Left	Right	Left	Right
T3	58.9±3.6	68.9±1.2	56.7±3.6	56.9±3.4
T7	82.3±4.4	69.0±6.0	84.2±5.2	75.8±3.4
T11	124.5±6.2	67.5±3.3	54.1±1.0	43.8±2.8
L4	79.0±6.0	73.5±4.2	36.1±1.5	44.2±2.7

We assumed none of our subjects had the condition of situs inversus totalis as the chance of occurrence is rare (1 per 20000 in normal population). Considering that pre-existed vertebral body rotation might be found in our normal subjects, their spinous process and transverse processes at the posterior could be rotated to the left. Larger para-spinal muscle stiffness on the left side could be associated with the vertebral rotation as a cause, a progressive factor or an effect. The existence of vertebral rotation in normal subjects should be treated as an assumption in the current discussion. It would be unethical to ask subject to take an unnecessary X-ray scan in order to demonstrate the case. Theoretically, the spinal curvature assessment taken by all subjects using the 3D ultrasound imaging system could provide vertebral rotation information. However, the existing analyzing software, image quality and resolution were not yet capable to provide such information in the transverse plane.

Muscles stiffness on the vertebra's left hand side could be increased by contracting more than the lateral side which subsequently pulls the vertebral arch to the left. An increase in contraction could be due to physiological stimulus or hormonal imbalance e.g. melatonin and serotonin (Machida, 1999). Such a kind of muscle contraction might not be detected through EMG signals, as contraction can occur in form of contracture or spasm (Simons and Mense, 1998). The formation of scoliosis under the effect of para-spinal muscle imbalance was performed by Carpintero et al. (1997) using rabbits. As a result of surgical tethering a few levels of spinous and transverse apophysis on one side of the rabbits' spines, the affected vertebral bodies rotated to the opposite side of the tether in all animals. Surgical tethering simulated the possible asymmetric para-spinal muscle contraction in our normal subjects as a form of muscle imbalance. Larger stiffness could represent higher muscle contraction on the left which served as a progressive factor in developing the right vertebral rotation.

Para-spinal muscle stiffness increased on the left could also appear after the formation of vertebral rotation. Distance between the bony prominences of adjacent vertebrae for muscle attachment was changed after vertebral rotation so that para-spinal muscles in between the bony prominences could be either shortened or lengthened. Para-spinal muscles such as multifidus and longissimus could be regarded as a straight line between the assertion points as these muscles were found to orientate linearly from dissection studies (Bogduk et al., 1992).

Muscle is stretched when the distance between bony prominences increases. According to Davis' law, new material is generated in muscle's micro-structure for elongation to fill the lengthened gap (Marusiak et al., 2011). Muscle stiffness might increase due to the addition of collagenous content for the lengthening. On the contrary, when the bony assertion points came closer muscle atrophy could occur by dissolving its original structure and in turn increased the stiffness at the muscle tendon (Marusiak et al., 2011). Since different muscle groups were overlapping at the back, there might be a possibility that the overall indentation result of a random measurement site at one vertebral level had included stiffness of muscle tendon originated from other vertebral levels and resulted in a larger overall stiffness value (Bojadsen et al., 2000).

Therefore, the association between the incident of vertebral arch rotated to the left and para-spinal muscle stiffness increased on the same side in normal subjects might be related to the three mechanisms mentioned above. However, the above explanations for larger muscle stiffness on the left hand side observed in our study could only be a speculation. Presentation of the lateral para-spinal muscle lengths and muscle content other than muscle fiber could not be concluded as no previous study was noticed for the investigations of these related para-spinal muscle properties in normal subjects.

5.2.2. Para-spinal muscle stiffness variation between spinal regions

There was also a discrepancy between the para-spinal muscle stiffness in thoracic and lumbar regions. Our study revealed that para-spinal muscle stiffness at the mid and the lower thoracic spine was in generally larger than that at the upper thoracic and the lumbar spine. Both muscle groups on the left and right hand sides exhibited the same trend. This result was consistent with the findings reported in previous studies but lacked discussion by other researchers (Waldorf et al., 1991, Williams II et al., 2007). The difference of muscle stiffness between the two regions could be explained in two aspects: muscular composition and function.

Different histologic compositions of the thoracic para-spinal muscles from the lumbar muscles might be required to adapt to its specific functions. Širca and Kostevc (1985) used human muscle specimens from autopsy and biopsy and found greater percentage of type I fiber (about 74%) than type II fiber in thoracic longissimus muscle, whereas the percentage of type I fiber in lumbar multifidus was lower. From this result, the authors suggested a possible functional difference might exist in para-spinal muscles at separate regions (Širca and Kostevc, 1985). Type I fiber is stiffer than type II fiber so muscle stiffness might increase with higher proportion of type I fiber content (Gajdosik, 2001). It is then reasonable to link the muscle stiffness variation along the spine to the different muscle fiber contents in para-spinal muscles.

However, Mannion et al. (1997) challenged that inter-individual variability could induce difference in fiber type ratio in the study performed by Širca and Kostevc (1985) as the authors did not specify whether or not the thoracic and lumbar samples compared were from the same subject. Mannion et al. (1997) repeated the histologic analysis using normal erector spinae biopsy samples from the thoracic and lumbar

regions but could not obtain the same results as in the previous study. The percentage distribution of type I fiber either by number, by relative muscle area occupied, or by fiber size was not found to be different from type II fiber in both regions. Only the mean fiber size in the thoracic region was found greater than that in the lumbar region. From their point of view, para-spinal muscles in the thoracic and lumbar regions might not display difference in their functions but only dissimilar force generation capabilities.

The level of para-spinal muscles participation on both spinal regions in standing posture was looked into following this direction. In erect standing posture, the lumbar stability was maintained by both the thoracic and lumbar muscles (Bogduk et al., 1992). Bogduk et al. (1992) calculated and compared the magnitude of force exerted by the lumbar back muscles through mathematical algorithms. Thoracic erector spinae which were based at the lumbar segments contributed half of the total extensor force on L4 and L5 while the rest was supported by lumbar multifidi and erector spinae. The thoracic muscles generated a higher level of muscle force than the lumbar muscles (e.g. multifidus) in normal human in standing posture was also demonstrated in a thoraco-lumbar spine computer model (Han et al., 2012). O'Sullivan et al. (2002) also obtained a similar conclusion that muscle activity in the thoracic erector spinae was higher than the superficial lumbar multifidus in healthy subjects in standing posture using surface EMG detection (Figure 5-4).

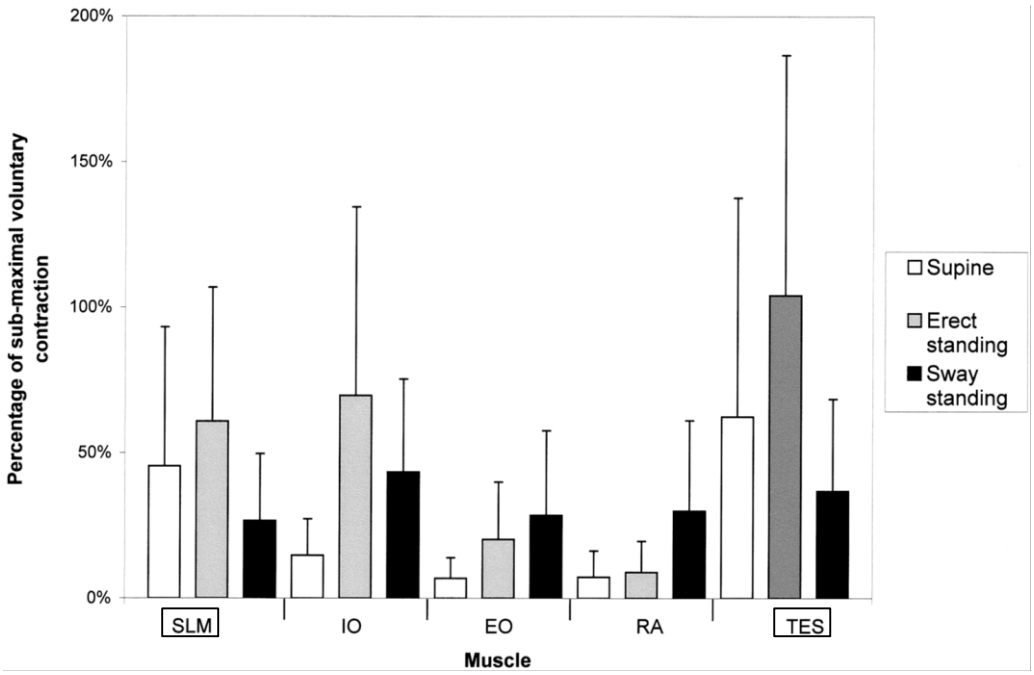

Figure 5-4 Muscle activity levels normalized to the baseline activity of some muscles groups in human in erect standing (in the middle of 3 columns). In this discussion, only the relationship between superficial lumbar multifidus (SLM) and thoracic erector spinae (TES) was focused (in brackets). TES had a higher activity than SLM. Figure was adopted from (O'Sullivan et al., 2002).

We had suspected that the difference in para-spinal muscle stiffness along the spine was because muscles in the two regions were responsible for specific tasks in maintaining the overall spine stability. However, histologic studies on the muscles could not provide precise evidence. At the same time, muscle activity studies consistently demonstrated a higher muscle activity level in the thoracic region. Since muscles with higher muscle activity or force generation show larger stiffness, the larger stiffness of the same para-spinal muscle group in the thoracic region compared with the upper and the lower regions found in this study could simply be a result of higher thoracic muscle activities during standing.

5.2.3. Para-spinal muscle stiffness variation between muscle groups

Para-spinal muscle stiffness measured at different lateral distances from the midline of vertebra was found to have different levels of stiffness in our study. Stiffness was lower when the muscle group was laterally away from the spine. Measuring sites at 1.5 cm and 3 cm in this study corresponded to the transversospinalis group notably multifidi and the erector spinae, respectively.

The difference in muscle stiffness could once again be argued due to their fiber compositions. Since the two muscle groups showed dissimilar function in maintaining spinal stability as mentioned in previous sections, different fiber contents between these two muscle groups might not be impossible. However, relevant studies which supported this notion were not identified.

Meanwhile, it was noticed that muscle stiffness increased during activation and was inversely proportional to muscle length (Granata and Marras, 2000, Gardner-Morse and Stokes, 1998). Erector spinae and multifidi apparently have different morphologies including muscle length. Muscle length of erector spinae is taken as distance between the most proximal fibers to the most distal fibers. Average muscle length was about one-fourth of the human body height converted from the measurement results in a cadaver study conducted by Delp et al. (2001). On the contrary, multifidus muscles which were divided into many smaller muscle-tendon units only connected across several (3-6) vertebral levels (Bojadsen et al., 2000, Maruyama, 1999). Muscle length of a unit of multifidus muscle is much shorter than erector spinae.

Muscle activates to generate the extension force and maintain the spinal stability during erect posture. Both muscle groups should activate to a similar degree when standing as their relative activities were close when performing different isometric back exercises (Ng and Richardson, 1994). Other than relevancy to the level of muscle activity, muscle stiffness is also governed by its morphology and varies indirectly with its length (Equation 5-1). Therefore, erector spinae in standing posture should have lower stiffness than multifidus as it had longer muscle length and similar activation force generated (Gardner-Morse and Stokes, 1998).

$$\mathrm{k} = \mathrm{q}\frac{F}{L} \tag{5-1}$$

where k is muscle stiffness (N/mm), q is a dimensionless coefficient assumed to be the same for all muscles, F is active muscle force (N) and L is muscle length (mm). (Gardner-Morse and Stokes, 1998)

5.3. Para-spinal muscle stiffness distribution in scoliosis subjects

Para-spinal muscle stiffness at vertebral levels T3, T7, T11 and L4 of scoliosis subjects was also measured in order to observe the average stiffness distribution along the spine of both groups. Considering that the scoliosis curve might have changed the local muscle stiffness, Young's modulus on each vertebral level between normal and scoliosis subjects should not be compared directly.

Since the locations of apexes of our scoliosis subjects were distributed evenly in both thoracic and lumbar regions, muscle stiffness at one vertebral level could be increased by one type of curve and decreased by another type of curve. Therefore, the average results of two groups might compensate each other and generate a less variable muscle stiffness distribution along the spine as in the case of normal subjects. However, even in the presence of scoliosis, the overall muscle stiffness distribution of scoliosis subjects in terms of side, level and lateral locations still matched with the distribution profile of normal subjects. In other words, para-spinal muscle stiffness remained larger on the left hand side, at mid thoracic region, and in the muscle group closer to spine.

Statistics from a number of national scale surveys in IS population showed that thoracic curves and thoracolumbar curves were the most common (above 70% in total) curve types (Wong 2005 and Suh, 2011). It is reasonable to assume that the majority of IS patients examined by those MTs had apex at the thoracic region. Before knowing the para-spinal muscle stiffness distribution in normal condition, some MTs proposed that muscles around apex usually had stiffer feeling than other vertebral levels. MT conducted manual palpation examination on para-spinal muscles for the patient in prone posture most of the time. Although the posture of subjects when being

examined is different from the posture during our measurement, para-spinal muscle stiffness along the spine remained varied at least in normal subjects (Waldorf et al., 1991). Since our results demonstrated that thoracic muscle stiffness was larger in both normal and scoliosis subjects, the impression of larger para-spinal muscle stiffness at thoracic apex from manual palpation on IS patients could simply be a reflection of the inherent larger muscle stiffness at the thoracic region.

Para-spinal muscle stiffness of scoliosis subjects was further analyzed according to the location of apex. For subjects with apex at the lumbar region, the muscle stiffness on the concave side was consistently lower than that on the convex side of all levels for both muscle groups. While for subjects with apex at the thoracic region, muscle stiffness on the concave side was larger when compared with the convex side. Since para-spinal muscle stiffness had already been demonstrated to be asymmetric in normal spines without scoliosis, the results from scoliosis subjects could not be used to conclude that para-spinal muscle stiffness imbalance in different curve types was due to scoliosis.

Looking back on the curve pattern of each subject, the curve convexity was mostly on the left for lumbar group subjects and on the right for thoracic group subjects. When the stiffness results were viewed with direction of convexity in consideration, muscle stiffness on the convex side (i.e. left hand side) of lumbar group should be higher than the concave side as the left side muscle stiffness was supposed to be larger. Similar trend should be applicable to the thoracic group with the concave side (i.e. left hand side) having larger stiffness.

A similar study related to para-spinal muscle stiffness in scoliosis found larger stiffness on the concave side of the curve despite lacking statistical significance in the results (Oliva-Pascual-Vaca et al., 2014). The authors reported that the majority of

their subjects had thoracolumbar curve but did not indicate the direction of convexity of the subjects (i.e. towards left or right hand side). However, we speculated the convexity was mainly to the right based on past clinical observations (Goldberg and Dowling, 1991, Saito et al., 1998). Thus, the concave side of the curves had a higher possibility to be on the left hand side of those subjects and thus the muscle stiffness on the concave side should be larger based on our findings. However, whether the stiffness imbalance observed by the authors was due to the intrinsic between-side muscle stiffness imbalance or associated with scoliosis remains unknown.

From our results, para-spinal muscle stiffness along the lumbar curve was gradually lowered from upper end to lower end. Muscle stiffness along the thoracic curve increased then decreased with the peak at apex level. Referring to the curve pattern of each subject, the upper end of lumbar curves and the apex of thoracic curves lied at the mid thoracic region mostly. The para-spinal muscle stiffness distribution along the curved spine of both curve types seemed to follow the distribution pattern of normal subjects in which the largest stiffness was found at mid thoracic region (T7-T11) compared with the superior and inferior regions. Therefore, the above results were still insufficient to demonstrate whether the significant change in local muscle stiffness at a specific vertebral level was caused by scoliosis or not.

Para-spinal muscle stiffness at a corresponding location of normal and scoliosis subjects was further compared. Para-spinal muscle stiffness on the concave side of the thoracic apex was on average larger than normal stiffness while the convex side remained similar to normal stiffness. At the lumbar curve, muscle stiffness on both the convex and concave sides was lower than normal stiffness. Compared with the normal muscle stiffness, the result was not consistently larger or lower on the same side of curvature for both curve types. As the role of para-spinal muscle was complex, there

was no direct evidence to draw a definite conclusion on whether muscle stiffness change was a cause or effect in the development of scoliosis. Our findings might have suggested the interactions between para-spinal muscle and scoliosis could be in multiple ways (Kennelly and Stokes, 1993).

Under one of the presumptions that para-spinal muscle on the left hand side might be contracting more in normal subjects and thus be associated with the vertebral body rotation to the right, para-spinal muscles on the concave side (i.e. left) of the thoracic curve could be under a similar scenario. Normal subjects with relatively higher muscle contraction on the left during growth period might have caused vertebral rotation and developed into right thoracic scoliosis. This explanation also followed the explanation of scoliosis development under “bowstring” effect (Du et al., 2013).

The muscle contraction as mentioned earlier might not be electromyogenic. If EMG activity was involved, the result would have been contradicted to the observation of higher muscle activities on the convex side of curves reported in previous studies. However, Zoabli et al. (2007) discovered that the skinfold thickness on the convex side around the apex level was always thinner than that on the concave side (Figure 5-5). A shorter distance between the muscle layer and the surface electrodes (used by scoliosis EMG studies observed so far) might lead to larger EMG signal detected on the convex side. Thus, it gave an impression that convex muscles contracted stronger. This might also be related to the feelings of larger muscle stiffness on the convex side to some MTs when using manual palpation as muscle (relatively stiffer than soft tissues) were sensed quickly without compressing too deep. At the same time, the increase in EMG detected on the convex side could also be interpreted as a signal of positive corrective mechanism in para-spinal muscles against the curve progression (Chwala et al., 2014).

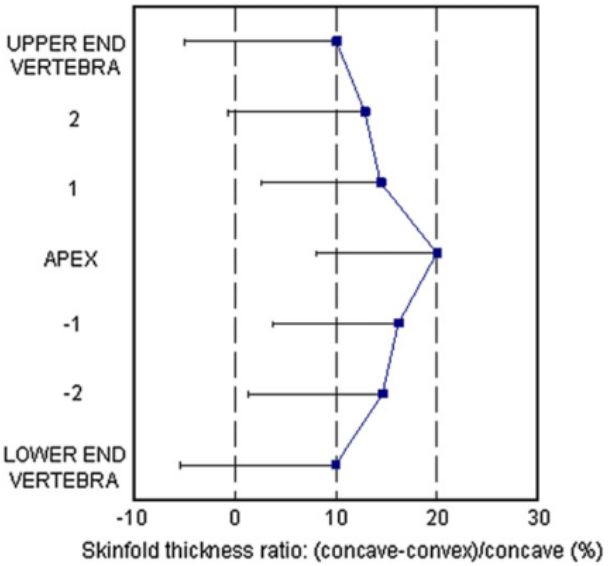

Figure 5-5 The percentage change of skinfold thickness between the convex side and the concave side along the curvature. The greatest change was identified at the apex level. Figure was adopted from (Zoabli et al., 2007).

In contrast, lower para-spinal muscle stiffness on both sides of the lumbar curve than the normal stiffness could be a result of muscle disuse under the compression of the scoliosis curve. Lumbar curve in S-shape deformity is mainly a compensatory curve due to higher flexibility of the lumbar spine (Lenke et al., 1999). Such a compensatory curve might not be a structural deformity like most of the thoracic curves. Most of the subjects in lumbar curve group had S-shape deformity with the largest deformation happened to be in lumbar region. Unfortunately, medical knowledge was lack to diagnose compensatory curve in this study. If the lumbar curve was a compensatory curve and para-spinal muscle was the cause of scoliosis, the lumbar muscles did not need to take an active role in the formation of compensatory curve. Para-spinal muscles in lumbar spine could be affected after the curve had formed and result in stiffness reduction with prolonged disuse. Further functional studies such as investigating the contractile function of lumbar para-spinal muscles in subjects with or without lumbar scoliosis could be performed to verify such a speculation.

5.4. Limitations of the study

The accuracy of our results on the para-spinal muscle stiffness in normal and scoliosis subjects could be hindered by several limitations.

Among all the pairs for comparison of spinal muscle stiffness, some did not show statistical difference. Limited number of subjects used in this study could be a reason. The number of subject included in each group simply followed the average number of 10 – 15 subjects reported in previous studies. In addition, scoliosis curve characteristics, such as severity and location of apex also had large variations among individuals. The number of results separated by apex location that was used for comparisons with normal subjects was further reduced by half.

Comparisons between muscle groups from the spinous process might be confounded by the between-individual variations in non-matched subjects as the results obtained in 1.5 cm and 3 cm groups were not from the same subjects. In our initial study design, we intended to measure muscles at 1.5 cm from spinous processes. We included another measurement at 3 cm from spinous processes in the middle of the study considering that a large number of past researches demonstrated that erector spinae also exhibited imbalance in scoliosis. For subjects recruited at the later stage, measurements should have been taken on both separations from the spinous process. However by doing so, the duration of measurement would be too long for each subject (i.e. more than 2 hours). Given that subjects might feel discomfort for a long-hour study, an additional set of measurements at another separation was not included.

Para-spinal muscle stiffness distribution in both normal and scoliosis subjects found in our study should be interpreted as relative results. The absolute Young's modulus measured might not be able to represent muscle stiffness of the general population at that level. The absolute values might have a systemic difference from true value as the boundary conditions in our measurement sites did not completely follow the assumptions set by Hayes' model (Hayes et al., 1972). Moreover, the vertebral levels for para-spinal muscle stiffness measurement were located by manual palpation with the help of anatomical landmarks (i.e C7 and iliac crests). Although the identified landmarks may be shifted by one level compared with the true anatomy (Grivas et al., 2013), the overall para-spinal muscle stiffness distribution measured on the palpated sites was not expected to be differed much.

Also the stiffness measurements might be affected by the subject's body movement during indentation although we had tried to control the posture by placing restraints at some locations. Placement of center of gravity inside the subject's body was also not recorded and controlled in our measurements. The position of center of gravity might affect the overall para-spinal muscle activity and stiffness as well. Some scoliosis subjects had received treatments such as physiotherapy, MT or bracing before they participated in our research. It was not sure if these treatments had altered the para-spinal muscle stiffness and influenced our results.

Indentation might elicit muscle contraction in some subjects (Kawchuk and Fauvel, 2001). EMG activity on para-spinal muscles was not measured during measurement so as to monitor any occurrence of sudden voluntary muscle contraction. Muscle contraction during relaxed standing could affect our measurement and should have been neglected in the analysis.

5.5. Future studies

In order to clarify whether the para-spinal muscles stiffness distribution was not caused by some uncertain conditions mentioned in the discussion; further studies should be continued along those directions.

More left handed subjects with or without scoliosis could be recruited to understand the effect of handedness on para-spinal muscle stiffness distribution. In case para-spinal stiffness distribution of left handed subjects is reversed, such that the right side muscle stiffness is higher, then muscle stiffness might not be solely associated with spinal structure or scoliosis. At the same time, pre-existed vertebral rotation in future normal subjects should be verified by extracting information from the 3D ultrasound image volume of their spines in transverse plane.

Para-spinal muscle stiffness may be altered at different ages. Normal subjects from a variety of age groups can be involved and the correlation between muscle stiffness distribution and age can be determined. Likewise, para-spinal muscle stiffness may change in different postures. In this study, only standing posture was investigated. Activation of various muscle groups may change with static or dynamic postures and present a different level of stiffness. Understanding the effect of age and posture on para-spinal muscle stiffness can allow deeper understanding on the muscle activation pattern in maintaining trunk stability.

Study on the para-spinal muscle stiffness change in subjects with scoliosis should be carried out on subjects with matched deformation pattern. Direct comparison of muscle stiffness on the same vertebral level with normal subjects can give a better understanding on the change caused by scoliosis. Also the muscle stiffness distribution in normal subjects can be measured at each vertebral level to enhance the

resolution of current results.

The current indentation measurements could only provide stiffness information of the combined soft tissue. Although Han et al. (2003) attempted to obtain stiffness of individual layers using indentation method, the best solution they could achieve was only identifying the relative stiffness of multiple layers in ratio form. Other stiffness measurement techniques such as shear wave elastography in the elastography may be applied to provide absolute stiffness measurement for multilayer tissue with standardized operation protocol. Understanding the stiffness of each tissue layer could help identify which tissue layer has the most significant stiffness change and leads to the imbalance we observed in this study. The association between scoliosis and para-spinal muscle or other soft tissues such as tendon can be also specified.

CHAPTER 6 CONCLUSIONS

A manual indentation system was developed in this study to measure para-spinal muscle stiffness in human subjects *in vivo*. The performance of the system in stiffness measurement was proved to be reliable and repeatable with excellent correlation with the standard mechanical testing machine and very good intra- and inter-operator reliability. Muscle stiffness was indicated by the value of Young's modulus and calculated using the Haye's model.

Para-spinal muscle stiffness measurement in this study was carried out using the manual indentation system. To our knowledge, this was the first study to systematically demonstrate the presence of para-spinal muscle stiffness imbalance in normal subjects. Para-spinal muscle stiffness at contralateral sides of 4 vertebral levels which were evenly located along the normal spine was measured in relaxed standing.

Preliminary results showed that para-spinal muscle stiffness imbalance existed in a group of normal right-handed subjects with higher muscle stiffness on the left hand side. Such imbalance maintained but diminished in muscle groups more distant from the spinous processes along the spine. Muscle stiffness imbalance between sides in normal subjects had a possibility to be associated with a pre-existed vertebral rotation. Three possible mechanisms for increasing the muscle stiffness on the left hand side were proposed. Muscle stiffness at the mid and the lower thoracic levels was higher than the superior and inferior vertebral levels on both left and right sides. Different physiological requirements to muscles groups in maintaining the overall trunk stability during standing were discussed and considered as strongly related to the stiffness imbalance along the spine.

Measurements were repeated on scoliosis subjects at the same 4 vertebral locations together with the contralateral sides of the upper limit, the apex, and the lower limit vertebrae of the curvature. Overall muscle stiffness distribution along and across the deformed spines resembled the pattern in normal spines. Significant para-spinal muscle stiffness imbalance was not unique to scoliosis subjects, which was different from our hypothesis. It was unable to conclude that muscle stiffness imbalance was mainly associated with the spinal deformity in scoliosis subjects.

Comparisons between para-spinal muscle stiffness of normal and scoliosis subjects revealed higher muscle stiffness at the concave of thoracic apexes than that at the normal left hand side. However, lower muscle stiffness was found at both sides of the lumbar apexes. In coherence with the mechanisms for para-spinal muscle stiffness change with the spine's structural alternation discussed in this report, there was a chance that para-spinal muscles engaged differently in the development of scoliosis. Thoracic muscles could contract and subsequently formed a vertebral rotation and further developed into the concave side of the curvature following the "bowstring" effect. Meanwhile, lumbar muscles around the lumbar curve, which is commonly a compensatory curve, could be changed passively after prolonged disuse. Nonetheless, all hypotheses generated to explain the results in this study require further investigations to support.

In this study, para-spinal muscle stiffness distributions in both normal and scoliosis populations were reported and compared. Discussions were made in hopes to relate the observed stiffness change to the structural presentation of the spine. It was not intended to explain the etiology of scoliosis through the change of para-spinal muscle stiffness. The cause of para-spinal muscle stiffness change observed in this study remained unknown.

In summary, the major findings of this study are listed as follow:

- In normal subjects, para-spinal muscle stiffness on the left hand side was larger than the right hand side.
- In normal subjects, para-spinal muscle stiffness at the mid-thoracic region was larger than the superior and inferior regions.
- In normal subjects, para-spinal muscle stiffness on the muscle groups closer to the spinous processes was larger than distant muscle groups at the same vertebral level.
- In scoliosis subjects, para-spinal muscle stiffness was also larger on the left hand side, at the mid-thoracic region, and on the muscle groups closer to the spinous processes.
- In scoliosis subjects, para-spinal muscle stiffness at the concave side of thoracic apex was larger compared with on the left hand side of normal thoracic spine. Para-spinal muscle stiffness at the convex and concave sides of the lumbar apex was lower than that on both sides of normal lumbar spine.

APPENDICES

I English version of information sheet

Information Sheet

Project Title: Correlation between Spinal Deformity and back muscle stiffness distribution

You are invited to participate on a study conducted by Ms Connie Cheng, an MPhil student of Prof. Yongping Zheng, who is the Head and Professor of the Interdisciplinary division of Biomedical Engineering in The Hong Kong Polytechnic University. The project has been approved by the Human Subjects Ethics Sub-committee (HSESC) (or its Delegate) of the University (HSESC Reference Number: HSEARS20140812002).

You are required to read the information sheet carefully and sign the attached Consent form before taking any test of this study. You have every right to withdrawn from the study before or during the measurement without penalty of any kind.

The aim of this study is to establish a relationship between para-spinal muscle stiffness in normal subjects and subjects with scoliosis. With the information obtained from this experiment, it is hoped that muscle stiffness distribution along spine and across same spinal level of a subject with or without posture effect can be identified.

The above experiment will be divided into two parts. You will first be required to take a radiation free 3-D ultrasound scan on the whole spinal region. Second part of the experiment requires you to stay in standing position while the research will perform manual indentation on selective points along the para-spinal muscles with a small self developed indentation probe. The whole experiment should last for about two hour.

During the experiment, you may experience some slight discomfort. Some subjects may feel itchy during the scanning and have temporary skin redness after the scanning. This is caused by the use of ultrasound coupling gel, and will disappear very soon after the test. You may also feel tired while maintaining upright for a period of time.

Sufficient resting time will be given to subject between each test in the experiment and upon request.

If you have any complaints about the conduct of this research study, please do not hesitate to contact Miss Cherrie Mok, Secretary of the Human Subjects Ethics Sub-Committee of The Hong Kong Polytechnic University in writing (c/o Research Office of the University) stating clearly the responsible person and department of this study.

Thank you for your interest in participating in this study.

II Chinese version of information sheet

資料單

項目名稱：背部肌肉硬度分佈與脊柱變形關係的研究

您已被邀請參加上述的一項研究，負責人鄭樂勤小姐是香港理工大學生物醫學工程跨領域學部系主任鄭永平教授的碩士生。此項目已獲香港理工大學人類課題道德下屬委員會審批（檔案編號：HSEARS20140812002）。

請在參與任何測試前細閱本資料單並簽署附頁的知情同意書。本項研究的目的是爲了確立脊柱兩側肌肉硬度在普通人和脊柱側彎的患者之間的關係。其後利用是次實驗獲得的數據，分析兩組參加者的脊柱上下和兩側的脊柱肌肉硬度分佈。閣下完全有權利在測試進行前或過程中終止測試而不受任何形式的懲罰。

測試會分為兩個部分。首先您需要接受一個無輻射傷害的三維脊柱超聲掃描。然後研究員會請您保持站立姿勢。期間，在背部上多個指定位置利用自行研發的儀器進行按壓測試。 整個實驗過程大概需要兩小時。

測試過程中，您可能會感到輕微不適。由於測試中會用到超聲耦合劑有部分參加者會在實驗過程中感到皮膚痕癢或事後皮膚出現紅點，但情況不會持續。參加者需要在一段短時間中，保持站立姿勢，您有機會因而感到疲倦。每個測試之間，會提供足夠的休息時間。您亦可以在實驗過程中要求休息。

如果您有任何關于此項研究行爲的控訴，請當面或者書信聯繫香港理工大學人類課題道德下屬委員會的秘書 Ms. Cherrie Mok。

非常感謝您對本研究的支持並參與是次實驗。

III English version of informed consent for participants above 18

CONSENT FORM

Project Title: Correlation between Spinal Deformity and Back Muscle Stiffness distribution

I, _____ (name of participant), hereby consent to participate as a subject for the above captioned project.

Before signing this document,

- I am clear about the experimental procedures presented to me.
- I understand the details presented in a separate information sheet attached with this form.
- I have given opportunity to ask question(s) about the experiment, and the response is up to my satisfaction.
- I understand that I can withdraw from the experiment with no reasons given and no penalty received anytime during the process.
- I understand that my personal information will not be disclosed to people who are irrelevant to this study.
- I understand that results will be obtained from this experiment may be used in future research and publication(s). Meanwhile my information will be kept confidential.
- I understand that results of this experiment will be property of The Hong Kong Polytechnic University.

Subject name:_____ Signature: _____

Investigator name:_____Signature: _____

Date:_____

IIII Chinese version of informed consent for participants above 18

同意書

研究課題：背部肌肉硬度分佈與脊柱變形之關係

本人，_____（參加者姓名）在此同意作為受試者參加上述研究課題。

在簽署本同意書前，

- 本人已明白此研究測試的步驟。
- 本人已明白在附頁的資料單上列出的所有內容
- 本人已給予機會詢問有關研究的細節，並已獲得滿意的回答。
- 本人已明白在實驗中，本人可以隨時終止研究測試而無需給予任何理由，或因此而受到任何懲罰。
- 本人已明白所有個人資料將不會向與本研究無關之人仕公開。
- 本人已得悉是次研究測試所獲的資料及結果，日後有機會用於其他研究及學術發表。當中有關本人的個人資料亦將獲得保密
- 本人已清楚是次測試的結果將屬香港理工大學所擁有。

參加者姓名:_____ 簽署:_____

研究員姓名:_____ 簽署:_____

日期: _____

IV English version of informed consent for parents or guardians of participants below 18

CONSENT FORM

Project Title: Correlation between Spinal Deformity and Back Muscle Stiffness distribution

I, _____ (name of parent/guardian), hereby consent to allow my child _____ (name of participant) to participate as a subject for the above captioned project.

Before signing this document,

- I am clear about the experimental procedures presented to me and my child.
- I understand the details presented in a separate information sheet attached with this form.
- I and my child have given opportunity to ask question(s) about the experiment, and the response is up to my satisfaction.
- I understand that I and my child can withdraw from the experiment with no reasons given and no penalty received anytime during the process.
- I understand that my child's personal information will not be disclosed to people who are irrelevant to this study.
- I understand that results will be obtained from this experiment may be used in future research and publication(s). Meanwhile my child's information will be kept confidential.
- I understand that results of this experiment will be property of The Hong Kong Polytechnic University.

Subject name:_____

Parent/ guardian name: _____Signature: _____

Investigator name:_____Signature: _____

Date:_____

V Chinese version of informed consent for parents or guardians of participants below 18

同意書

研究課題：背部肌肉硬度分佈與脊柱變形之關係

本人，_____(參加者家長/監護人姓名）在此同意讓敝子弟_____(參加者姓名）作為受試者參加上述研究課題。
在簽署本同意書前，

- 本人已明白此研究測試的步驟。
- 本人已明白在附頁的資料單上列出的所有內容
- 本人及敝子弟已給予機會詢問有關研究的細節，並已獲得滿意的回答。
- 本人已明白在實驗中， 本人及敝子弟可以隨時終止研究測試而無需給予任何理由，或因此而受到任何懲罰。
- 本人已明白所有個人資料將不會向與本研究無關之人仕公開。
- 本人已得悉是次研究測試所獲的資料及結果，日後有機會用於其他研究及學術發表。當中有關敝子女的個人資料亦將獲得保密
- 本人已清楚是次測試的結果將屬香港理工大學所擁有。

參加者姓名:_____

家長/監護人姓名:_____ 簽署:_____

研究員姓名:_____ 簽署:_____

日期: _____

REFERENCES

ANDERSEN, M. O., CHRISTENSEN, S. B. & THOMSEN, K. 2006. Outcome at 10 Years After Treatment for Adolescent Idiopathic Scoliosis. *Spine (Phila Pa 1976),* 31**,** 350-354.

Anatomy human Body 2016, Muscles of the head by label axial muscles of the head neck and back anatomy and physiology, online image, Anatomy –diagram, accessed August 2016,
<http://www.anatomy-diagram.info/wp-content/uploads/2016/08/muscles-of-the-head-by-label-axial-muscles-of-the-head-neck-and-back-anatomy-and-physiology-i.jpg>.

Ascension Technology Corporation 2016, 3D Guidance, online image, accessed June 2016, <http://www.ascension-tech.com/products/>.

ARDA, K., CILEDAG, N., AKTAS, E., ARIBAS, B. K. & KOSE, K. 2011. Quantitative assessment of normal soft-tissue elasticity using shear-wave ultrasound elastography. *AJR Am J Roentgenol,* 197**,** 532-6.

AROKOSKI, J. P., SURAKKA, J., OJALA, T., KOLARI, P. & JURVELIN, J. S. 2005. Feasibility of the use of a novel soft tissue stiffness meter. *Physiol Meas,* 26**,** 215-28.

ASHER, M. A. & BURTON, D. C. 2006. Adolescent idiopathic scoliosis: natural history and long term treatment effects. *Scoliosis,* 1**,** 2.

ASPEGREN, D. D. & COX, J. M. 1987. Correction of progressive idiopathic scoliosis utilizing neuromuscular stimulation and manipulation: a case report. *Journal of manipulative and physiological therapeutics,* 10**,** 147-156.

AVIKAINEN, V. J., REZASOLTANI, A. & KAUHANEN, H. A. 1999. Asymmetry of paraspinal EMG_time charateristics in idiopathic scoliosis. *Journal of Spinal Disorders,* 12**,** 61-67.

BAILEY, L., SAMUEL, D., WARNER, M. & STOKES, M. 2013. Parameters Representing Muscle Tone, Elasticity and Stiffness of Biceps Brachii in Healthy Older Males: Symmetry and Within-Session Reliability Using the Myotonpro. *J Neurol Disord,* 1**,** 116.

BERCOFF, J., TANTER, M. & FINK, M. 2004. Supersonic Shear Imaging: A New Technique for Soft Tissue Elasticity Mapping *IEEE Trans on Ultrasonics, Ferroelectrics, and Frequency control* 51**,** 396-409.

BETTANY-SALTIKOV, J., WEISS, H., CHOCKALINGAM, N., TARANU, R., SRINIVAS S, HOGG J, WHITTAKER V & RV, K. 2013. Surgical versus non-surgical interventions in patients with adolescent idiopathic scoliosis (Protocol). *The Cochrane Library*.

BOCTOR, E. M., FICHTINGER, G., TAYLOR, R. H. & CHOTI, M. A. 2003. Tracked 3D Ultrasound in Radio-Frequency Liver Ablation. *Proc. SPIE, Medical Imaging:Ultrasonic Imaging and Signal Processing,* 5035**,** 174-182.

BOGDUK, N., MACINTOSH, J. E. & PEARCY, M. J. 1992. A Universal Model of the Lumbar Back Muscles in the Upright Position. *Spine (Phila Pa 1976),* 17**,** 898-913.

BOJADSEN, T. W. A., SILVA, E. S., RODRIGUES, A. J. & AMADIO, A. C. 2000. Comparative study of Mm. Multifidi in lumbar and thoracic spine *Journal of Electromyography and Kinesiology* 10**,** 143-149.

British Columbia Children's Hospital 2016, Scoliosis, online image, Provincial Health Services Authority, accessed June 2016, <http://www.bcchildrens.ca/our-services/clinics/orthopaedics/spine-conditions/scoliosis>.

BURWELL, R. G. 2003. Aetiology of idiopathic scoliosis: current concepts. *Pediatr Rehabil,* 6**,** 137-70.

C SPEDES, I., OPHIR, J., PONNEKANTI, H. & MAKLAD, N. 1993. Elastography: Elasticity Imaging Using Ultrasound with Application to Muscle and Breast in Vivo. *Ultrasonic Imaging,* 15**,** 73-88.

CARPINTERO, P., MESA, M., GARCIA, J. & CARPINTERO, A. 1997. Scoliosis Induced by Asymmetri Lordosis and Rotation. *Spine (Phila Pa 1976),* 22**,** 2202-2206.

CASSELLA, M. C. & HALL, J. E. 1991. Current Treatment Approaches in the Nonoperative and Operative Management of Adolescent Idiopathic Scoliosis *Physical Therapy,* 71**,** 897-909.

CHAN, S. T., FUNG, P. K., NG, N. Y., NGAN, T. L., CHONG, M. Y., TANG, C. N., HE, J. F. & ZHENG, Y. P. 2012. Dynamic changes of elasticity, cross-sectional area, and fat infiltration of multifidus at different postures in men with chronic low back pain. *Spine J,* 12**,** 381-8.

CHAN, Y.-L., CHENG, J. C. Y., GUO, X., KING, A. D., GRIFFITH, J. F. & METREWELI, C. 1999. MRI evaluation of multifidus muscles in adolescent idiopathic scoliosis. *Pediatric Radiology,* 29**,** 360-363.

CHEN, T. C., CHEN, H. L., LIU, Y. C. & NOSAKA, K. 2014. Eccentric exercise-induced muscle damage of pre-adolescent and adolescent boys in comparison to young men. *Eur J Appl Physiol*.

CHENG, J. C., CASTELEIN, R. M., CHU, W. C., DANIELSSON, A. J., DOBBS, M. B., GRIVAS, T. B., GURNETT, C. A., LUK, K. D., MOREAU, A., NEWTON, P. O., STOKES, I. A., WEINSTEIN, S. L. & BURWELL, R. G. 2015. Adolescent idiopathic scoliosis. *Nature Reviews Disease Primers,* 1**,** 15030.

CHEUNG, C.-W. J. & ZHENG, Y. Development of 3-D Ultrasound System for Assessment of Adolescent Idiopathic Scoliosis (AIS) WCB 2010, IFMBE Proceedings 31, 2010. 584-587.

CHEUNG, C. W. J., SIU-YIN, L. & YONG-PING, Z. Development of 3-D ultrasound system for assessment of adolescent idiopathic scoliosis (AIS): And system validation. Engineering in Medicine and Biology Society (EMBC), 2013 35th Annual International Conference of the IEEE, 3-7 July 2013. 6474-6477.

CHEUNG, C. W. J., ZHOU, G. Q., LAW, S. Y., MAK, T. M., LAI, K. L. & ZHENG, Y. P. 2015. Ultrasound Volume Projection Imaging for Assessment of Scoliosis. *IEEE International on Medical Imaging,* 34**,** 1760-1768.

CHEUNG, J., HALBERTSMA, J. P., VELDHUIZEN, A. G., SLUITER, W. J., MAURITS, N. M., COOL, J. C. & VAN HORN, J. R. 2005. A preliminary study on electromyographic analysis of the paraspinal musculature in idiopathic scoliosis. *Eur Spine J,* 14**,** 130-7.

CHINO, K., AKAGI, R., DOHI, M., FUKASHIRO, S. & TAKAHASHI, H. 2012. Reliability and Validity of Quantifying Absolute Muscle Hardness Using Ultrasound Elastography. *PLoS ONE,* 7**,** e45764.

CHWALA, W., KOZIANA, A., KASPERCZYK, T., WALASZEK, R. & PLASZEWSKI, M. 2014. Electromyographic assessment of functional symmetry of paraspinal muscles during static exercises in adolescents with idiopathic scoliosis. *Biomed Res Int,* 2014**,** 573276.

CORTEZ, D. C., HERMITTE, L., RAMAIN, A., MESMANN, C., LEFORT, T. & PIALAT, J. B. 2016. Ultrasound shear wave velocity in skeletal muscle: A reproducibility study. *Diagnostic and Interventional Imaging,* 97**,** 71-79.

DANBERT, R. J. 1989. Scoliosis: Biomechanic and Rationale for Manipulative Treatment. *Journal of Manipulative and Physiological Therapeutics,* 12**,** 38-45.

DE OLIVEIRA, A. S., GIANINI, P. E., CAMARINI, P. M. & BEVILAQUA-GROSSI, D. 2011. Electromyographic analysis of paravertebral muscles in patients with idiopathic scoliosis. *Spine (Phila Pa 1976),* 36**,** E334-9.

DELP, S. L., SURYANARAYANAN, S., MURRAY, W. M., UHLIR, J. & TRIOLO, R. J. 2001. Architecture of the rectus abdominis, quadratus lumborum and erector spinae. *Journal of Biomechanics,* 34**,** 371-375.

Department of Nursing and Orthopaedic Surgery 2011, Treating scoliosis with posterior spinal fusion with instrumentation, online image, University of Iowa Children's Hospital, accessed June 2016,

<https://www.uichildrens.org/treating-scoliosis-with-posterior-spinal-fusion/>.

DIMON, T., JR. 2008. *Anatomy of the Moving Body: A Basic Course in bones, Muscles. and Joints*, North Atlantic Books.

DRAKONAKI, E. E., ALLEN, G. M. & WILSON, D. J. 2012. Ultrasound elastography for musculoskeletal applications. *Br J Radiol,* 85**,** 1435-45.

DU, H.-G., YE, S.-L., XU, J.-Y., JIANG, Z., SONG, H.-Q. & YU, J. 2013. 表面肌电图在中医脊柱平衡法治疗青少年特发性脊柱侧凸症中的应用[Application of surface electromyography in the treatment of adolescent idiopathic scoliosis with traditional spinal balanced therapy]. *China J Orthop Trauma,* 26**,** 914-917.

EBY, S. F., CLOUD, B. A., BRANDENBURG, J. E., GIAMBINI, H., SONG, P., CHEN, S., LEBRASSEUR, N. K. & AN, K.-N. 2015. Shear wave elastography of passive skeletal muscle stiffness: Influences of sex and age throughout adulthood. *Clinical Biomechanics,* 30**,** 22-27.

ERIKSSON CROMMERT, M., LACOURPAILLE, L., HEALES, L. J., TUCKER, K. & HUG, F. 2015. Massage induces an immediate, albeit short-term, reduction in muscle stiffness. *Scandinavian Journal of Medicine & Science in Sports,* 25**,** e490-e496.

EVERAERT, D. G., STAPPAERTS, K. H., VAN LEEMPUTTE, M. F. & OOSTENDORP, R. A. B. 1997. Towards a Measurement of Paraspinal Soft Tissue Mobility: Development of a Method and Preliminary Results. *The Journal of Manual & Manipulative Therapy* 5**,** 12-19.

FAN, Y.-Z. & WU, Y.-C. 2014. Effect of electroacupuncture combined with tuina on lumbar muscle tone in patients with acute lumbar sprain. *Journal of Acupuncture and Tuina Science,* 12**,** 310-315.

FIDLER, M. W. & JOWETT, R. L. 1976. Muscle Imbalance in the aetiology of scoliosis. *The Journal of Bone and Joint Surgery* 58-B**,** 200-201.

FISCHER, A. A. 1987a. Clinical use of tissue compliance meter for documentation of soft tissue pathology. *The Clinical Journal of Pain,* 3**,** 23-30.

FISCHER, A. A. 1987b. Tissue compliance meter for objective, quantitative documentation of soft tissue consistency and pathology. *Archives of physical medicine and rehabilitation,* 68**,** 122-125.

FONG, D. Y., CHEUNG, K. M., WONG, Y. W., WAN, Y. Y., LEE, C. F., LAM, T. P., CHENG, J. C., NG, B. K. & LUK, K. D. 2015. A population-based cohort study of 394,401 children followed for 10 years exhibits sustained effectiveness of scoliosis screening. *Spine J,* 15**,** 825-33.

FORD, D. M., BAGNALL, K. M., MCFADDEN, K. D., GREENHILL, B. J. & RASO, V. J. 1984. Paraspinal Muscle Imbalance in Adolescent Idiopathic Scoliosis *Spine (Phila Pa 1976),* 9**,** 373-376.

GAJDOSIK, R. L. 2001. Passive extensibility of skeletal muscle: review of the literature with clinical implications. *Clinical Biomechanics,* 16**,** 87-101.

GAMMON, S. R., MEHLMAN, C. T., CHAN, W., HEIFETZ, J., DURRETT, G. & WALL, E. J. 2010. A Comparison of Thoracolumbosacral Orthoses and SpineCor Treatment of Adolescent Idiopathic Scoliosis Patients Using the Scoliosis Research Society Standardized Criteria. *Journal of Pediatric Orthopaedics,* 30**,** 531-538.

GARDNER-MORSE, M. G. & STOKES, I. A. 1998. The Effects of Abdominal Muscle Coactivation on Lumbar Spine Stability. *Spine (Phila Pa 1976),* 23**,** 86-92.

GENNISSON, J.-L., DEFFIEUX, T., MAC , E., MONTALDO, G., FINK, M. & TANTER, M. 2010. Viscoelastic and Anisotropic Mechanical Properties of in vivo Muscle Tissue Assessed by Supersonic Shear Imaging. *Ultrasound in Medicine & Biology,* 36**,** 789-801.

GENNISSON, J. L., DEFFIEUX, T., FINK, M. & TANTER, M. 2013. Ultrasound elastography: Principles and techniques. *Diagnostic and Interventional Imaging,* 94**,** 487-495.

GOLDBERG, C. J. & DOWLING, F. E. 1991. Idiopathic scoliosis and asymmetry of form and function. *Spine (Phila Pa 1976),* 16**,** 84-87.

GONYEA, W., J., MOORE-WOODARD, C., MOSELEY, B., HOLLMANN, M. & WENGER, D. R. 1985. An Evaluation of Muscle Pathology in Idiopathic Scoliosis. *Journal of Pediatric Orthopaedics,* 5**,** 323-329.

GRANATA, K. P. & MARRAS, W. S. 2000. Cost-Benefit of Muscle Cocontration in Protecting Against Spinal Stability. *Spine (Phila Pa 1976),* 25**,** 1398-1404.

GRIVAS, T. B., VASILIADIS, E. S., MIHAS, C. & SAVVIDOU, O. 2007. The effect of growth on the correlation between the spinal and rib cage deformity: implications on idiopathic scoliosis pathogenesis. Scoliosis, 2, 11.

GRIVAS, T. B., VASILIADIS, E. S., POLYZOIS, V. D. & MOUZAKIS, V. 2006. Trunk asymmetry and handedness in 8245 school children. Pediatric Rehabilitation, 9, 259-266.

GRIVAS, T., TSILIMIDOS, G., VERRAS, C., BOTSIOS, K. & CHATZISAROGLOU, M. 2013. Which is the most prominent spinous process in the cervico-thoracic spinal junction? A radiological study in a Mediterranean population sample. Scoliosis, 8, O40.

HACQUEBORD, J. H. & LEOPOLD, S. S. 2012. In brief: The Risser classification: a classic tool for the clinician treating adolescent idiopathic scoliosis. *Clin Orthop Relat Res,* 470**,** 2335-8.

HAN, K. S., ZANDER, T., TAYLOR, W. R. & ROHLMANN, A. 2012. An enhanced

and validated generic thoraco-lumbar spine model for prediction of muscle forces. *Med Eng Phys,* 34**,** 709-16.

HAN, L., NOBLE, J. A. & BURCHER, M. 2003. A novel ultrasound indentation system for measuring biomechanical properties of in vivo soft tissue. *Ultrasound Med Biol,* 29**,** 813-823.

HANELINE, M. T. & YOUNG, M. 2009. A review of intraexaminer and interexaminer reliability of static spinal palpation: a literature synthesis. *J Manipulative Physiol Ther,* 32**,** 379-86.

HAYES, W. C., KEER, L. M., HERRMANN, G. & MOCKORS, L. F. 1972. A Mathematical Analysis for Indentation Tests of Articular Cartilage *J Biomechanics* 5**,** 541-551.

HEDEQUIST, D. & EMANS, J. B. 2007. Congenital Scoliosis: A Review and Update. *Journal of Pediatric Orthopaedics,* 27**,** 106-116.

HIDES, J. A., COOPER, D. H. & STOKES, M. J. 1992. Diagnostic ultrasound imaging for measurement of the lumar multifidus muscle in normal young adults. *physiotherapy theory and practice* 8**,** 19-26.

HORIKAWA, M. 2001. Effect of visual display terminal height on the trapezius muscle hardness: quantitative evaluation by a newly developed muscle hardness meter. *Applied Ergonomics,* 32**,** 473-478.

HRESKO, M. T. 2013. Clinical practice. Idiopathic scoliosis in adolescents. *N Engl J Med,* 368**,** 834-41.

IIVARINEN, J. T., KORHONEN, R. K., JULKUNEN, P. & JURVELIN, J. S. 2011. Experimental and computational analysis of soft tissue stiffness in forearm using a manual indentation device. *Med Eng Phys,* 33**,** 1245-53.

IIVARINEN, J. T., KORHONEN, R. K. & JURVELIN, J. S. 2013. Experimental and numerical analysis of soft tissue stiffness measurement using manual indentation device – significance of indentation geometry and soft tissue thickness. *Skin Research and Technology***,** n/a-n/a.

IKEZOE, T., ASAKAWA, Y., FUKUMOTO, Y., TSUKAGOSHI, R. & ICHIHASHI, N. 2012. Associations of muscle stiffness and thickness with muscle strength and muscle power in elderly women. *Geriatr Gerontol Int,* 12**,** 86-92.

JANSEN, R. D., NANSEL, D. D. & SLOSBERG, M. 1990. Normal paraspinal tissue compliance: the reliability of a new clinical and experimental instrument. *Journal of manipulative and physiological therapeutics,* 13**,** 243-246.

JAROCKA, E., MARUSIAK, J., KUMOREK, M., JASKOLSKA, A. & JASKOLSKI, A. 2012. Muscle stiffness at different force levels measured with two myotonometric devices. *Physiol Meas,* 33**,** 65-78.

KAWCHUK, G. & HERZOG, W. 1995. The reliability and accuracy of a standard

method of tissue compliance assessment. *Journal of manipulative and physiological therapeutics,* 18**,** 298-301.

KAWCHUK, G. N. & FAUVEL, O. R. 2001. Sources of variation in spinal indentation testing: indentation site relocation, intraabdominal pressure, subject movement, muscular response, and stiffness estimation. *J Manipulative Physiol Ther,* 24**,** 84-91.

KEISAKU, K., YASUHARU, W., MASAHIRO, U., YOSHITAKA, A., TADASHI, W. & SHOJI, S. 2007. Quantitative analysis of the relation between soft tissue stiffness palpated from the body surface and tissue hemodynamics in the human forearm. *Physiological Measurement,* 28**,** 1495.

KENNELLY, K. P. & STOKES, M. J. 1993. Pattern of Asymmetry of Paraspinal Muscle Size in Adolescent Idiopathic Scoliosis Examined by Real-Time Ultrasound Imaging: A Prelimary Study *Spine (Phila Pa 1976),* 18**,** 913-917.

KOO, T. K., COHEN, J. H. & ZHENG, Y. 2011. A mechano-acoustic indentor system for in vivo measurement of nonlinear elastic properties of soft tissue. *J Manipulative Physiol Ther,* 34**,** 584-93.

KOO, T. K., COHEN, J. H. & ZHENG, Y. 2012. Immediate effect of nimmo receptor tonus technique on muscle elasticity, pain perception, and disability in subjects with chronic low back pain. *J Manipulative Physiol Ther,* 35**,** 45-53.

KORR, I. M. 1978. Neurobiologic Mechanisms in Manipulative Therapy. Plenum Press.

KOT, B. C. W., ZHANG, Z. J., LEE, A. W. C., LEUNG, V. Y. F. & FU, S. N. 2012. Elastic Modulus of Muscle and Tendon with Shear Wave Ultrasound Elastography: Variations with Different Technical Settings. *PLoS ONE,* 7**,** e44348.

KOTWICKI, T. 2008. Evaluation of scoliosis today: examination, X-rays and beyond. *Disabil Rehabil,* 30**,** 742-51.

KOUWENHOVEN, J.-W. M., BARTELS, L. W., VINCKEN, K. L., VIERGEVER, M. A., VERBOUT, A. J., DELHAAS, T. & CASTELEIN, R. M. 2007. The Relation Between Organ Anatomy and Pre-existent Vertebral Rotatin in the Normal Spine: Magnetic Resonance Imaging Study n Humans With Situs Inversus Totalis *Spine (Phila Pa 1976),* 32**,** 1123-1128.

KOUWENHOVEN, J.-W. M., VINCKEN, K. L., BARTELS, L. W. & CASTELEIN, R. M. 2006. Analysis of Preexistent Vertebral Rotation in the Normal Spine. *Spine (Phila Pa 1976),* 31**,** 1467-1472.

KWAN, R. L.-C., ZHENG, Y.-P. & CHEING, G. L.-Y. 2010. The effect of aging on the biomechanical properties of plantar soft tissues. *Clinical Biomechanics,* 25**,** 601-605.

KWON, D. R. & PARK, G. Y. 2012. Diagnostic Value of Real-time Sonoelastography in Congential Muscular Torticollis *J Ultrasound Med* 31**,** 721-727.

LAM, W. K., MOK, D., LEE, W. C. & CHEN, B. 2015. Reliability and Asymmetry Profiles of Myotonometric Measurements in Healthy Skeletal Muscles. *Journal of Novel Physiotherapies,* 05.

LANTZ, C. A. & CHEN, J. 2001. Effect of chiropractic intervention on small scoliotic curves in younger subjects: a time-series cohort design. *J Manipulative Physiol Ther,* 24**,** 385-93.

LEE, S. S. M., GAEBLER-SPIRA, D., ZHANG, L.-Q., RYMER, W. Z. & STEELE, K. M. 2016. Use of shear wave ultrasound elastography to quantify muscle properties in cerebral palsy. *Clinical Biomechanics,* 31**,** 20-28.

LEHNERT-SCHROTH, C. 1992. Introduction to the Three-dimensional Scoliosis Treatment According to Schroth *Physiotherapy,* 78**,** 810-821.

LENKE, L. G., BETZ, R. R., BRIDWELL, K. H., HARMS, J., CLEMENTS, D. H. & LOWE, T. G. 1999. Spontaneous Lumbar Curve Coronal Correction After Selective Anterior or Posterior Thoracic Fusion in Adolescent Idiopathic Scoliosis. *Spine,* 24**,** 1663.

LENKE, L. G., BETZ, R. R., HARMS, J., BRIDWELL, K., CLEMENTS, D. H., LOWE, T. & BLANKE, K. 2001. Adolescent Idiopathic Scoliosis: A new classification to determine extent of spinal arthrodesis. *The Journal of Bone & Joint Surgery,* 83-A**,** 1169-1181.

LEONARD, C. T., DESHNER, W. P., ROMO, J. W., SUOJA, E. S., FEHRER, S. C. & MIKHAILENOK, E. L. 2003. Myotonometer Intra- and Interrater Reliabilities. *Arch Phys Med Rehabil,* 84**,** 928-932.

LEONARD, C. T. & MIKHAILENOK, E. L. 2000. Apparatus for measuring muscle tone. Google Patents.

LEONG, H.-T., NG, G. Y.-F., LEUNG, V. Y.-F. & FU, S. N. 2013. Quantitative Estimation of Muscle Shear Elastic Modulus of the Upper Trapezius with Supersonic Shear Imaging during Arm Positioning. *PLoS ONE,* 8**,** e67199.

LEOTTA, D. F., DETMER, P. R., GILJA, O. H., JING-MING, J., MARTIN, R. W., PRIMOZICH, J. F., BEACH, K. W. & STRANDNESS, D. E. 1995. Three-dimensional ultrasound imaging using multiple magnetic tracking systems and miniature magnetic sensors. *Ultrasonics Symposium, 1995. Proceedings., 1995 IEEE.*

LEUNG, S. F., ZHENG, Y., CHOI, C. Y., MAK, S. S., CHIU, S. K., ZEE, B. & MAK, A. F. 2002. Quantitative measurement of post-irradiation neck fibrosis based on the young modulus: description of a new method and clinical results. *Cancer,* 95**,** 656-62.

LI, M., CHENG, J., YING, M., NG, B., ZHENG, Y. P., LAM, T. P., WONG, W. Y. & WONG, M. S. Application of 3-D ultrasound in assisting the fitting procedure of spinal orthosis to patients with adolescent idiopathic scoliosis. 2010 Montreal, QC. 34-37.

LI, Y. 2001. 脊柱推拿的历史[History of Spinal Manipulation]. *The Journal of Cervicodynia and Lumbodynia,* 22**,** 169-171.

LI, Y. & SNEDEKER, J. G. 2011. Elastography: modality-specific approaches, clinical applications, and research horizons. *Skeletal Radiology,* 40**,** 389-397.

LIANG, D. 1991. Investigation of mechainsm in deformation correction of scoliosis *Chin J Surg,* 29**,** 228-230.

LONSTEIN, J. E. & CARLSON, J. M. 1984. The Prediction of Curve Progression in Untreated Idiopathic Scoliosis during grwoth. *The Journal of Bone and Joint Surgery,* 66-A**,** 1061-1071.

LOWE, T. G., EDGAR, M., MARGULIES, J. Y., MILLER, N. H., RASO, V. J., REINKER, K. A. & RIVARD, C.-H. 2000. Etiology of Idiopathic Scoliosis: Current Trends in Research*. *The Journal of Bone & Joint Surgery,* 82**,** 1157-1157.

LU, M. H., YU, W., HUANG, Q. H., HUANG, Y. P. & ZHENG, Y. P. 2009. A Hand-Held Indentation System for the Assessment of Mechanical Properties of Soft Tissue In vivo. *IEEE Transactions on Instrumentation and Measurement* 58**,** 3079-3085.

LU, W. W., HU, Y., LUK, K. K. D., M.C., C. K. & C.Y., L. J. 2002. Paraspinal muscle activities of patients with scoliosis after spine fusion- An electromyographic study. *Spine (Phila Pa 1976),* 27**,** 1180-1185.

LUK, K. D. K., LEE, C. F., CHEUNG, K. M. C., CHENG, J. C. Y., NG, B. K. W., LAM, T. P., MAK, K. H., YIP, P. S. F. & FONG, D. Y. T. 2010. Clinical effectiveness of school screening for adolescent idiopathic scoliosis: A large population-based retrospective cohort study. *Spine (Phila Pa 1976),* 35**,** 1607-1614.

LV, F., TANG, J., LUO, Y., BAN, Y., WU, R., TIAN, J., YU, T., XIE, X. & LI, T. 2012. Muscle Crush Injury of Extremity: Quantitative Elastography with Supersonic Shear Imaging. *Ultrasound in Medicine & Biology,* 38**,** 795-802.

MACHIDA, M. 1999. Causes of Idiopathic Scoliosis. *Spine (Phila Pa 1976),* 24**,** 2576-2583.

MAKHSOUS, M., VENKATASUBRAMANIAN, G., CHAWLA, A., PATHAK, Y., PRIEBE, M., RYMER, W. Z. & LIN, F. 2008. Investigation of Soft Tissue Stiffness Alteration in Denervated Human Tissue Using an Ultrasound Indentation System. *journal of Spinal Cord Medicine* 31**,** 88-96.

MANNION, A. F., DUMAS, G. A., COOPER, R. G., ESPINOSA, F. J., FARIS, M. W. & STEVENSON, J. M. 1997. Muscle fibre size and type distribution in thoracic and lumbar regions of erector spinae in healthy subjects without low back pain: normal values and sex differences. *Journal of Anatomy,* 190**,** 505-513.

MANNION, A. F., MEIER, M., GROB, D. & M NTENER, M. 1998. Paraspinal muscle fibre type alterations associated with scoliosis: an old problem revisited with new evidence. *Eur Spine J,* 1998**,** 289-293.

MARTINI, F. H. & NATH, J. L. 2009. *Fundamentals of Anatomy & Physiology*, Pearson Education.

MARUSIAK, J., JASKOLSKA, A., BUDREWICZ, S., KOSZEWICZ, M. & JASKOLSKI, A. 2011. Increased muscle belly and tendon stiffness in patients with Parkinson's disease, as measured by myotonometry. *Mov Disord,* 26**,** 2119-22.

MARUYAMA, T. 1999. Length of the Multifidus Muscle in Adolescent Idiopathic Scoliosis. *STUDIES IN HEALTH TECHNOLOGY AND INFORMATICS***,** 231-233.

MCKEE, C. T., LAST, J. A., RUSSELL, P. & MURPHY, C. J. 2011. Indentation versus tensile measurements of Young's modulus for soft biological tissues. *Tissue Eng Part B Rev,* 17**,** 155-64.

MEIER, M. P., KLEIN, M. P., KERBS, D., GROB, D. & M NTENER, M. 1997. Fiber Transformations in Multifidus Muscle of Young Patients With Idiopathic Scoliosis *Spine (Phila Pa 1976),* 22**,** 2375-2364.

Mitutoyo 2012, Micrometer Heads E1006, catalogue, Mitutoyo Japan, accessed June 2016,
<http://www.mitutoyo.com/wp-content/uploads/2012/11/E1006MicrometerHeads.pdf>.

MORAIS, T., BERNIER, M. & TURCOTTE, F. 1985. Age- and Sex-specific Prevalence of Scoliosis and the Value of School Screening Programs. *Am J Public Health,* 75**,** 1377-1380.

MUSCOLINO, J. E. 2015. *Manual Theraphy for the Low Back and Pelvis: A Clinical Orthopedic Approach*, Wolters Kluwer Health.

National Institute of Arthritis and Musculoskeletal and Skin Diseases (NIAMS) 2015, Question and Answers about Scoliosis in Children and Adolescents, online image, National Institutes of Health, accessed June 2016,
<http://www.niams.nih.gov/Health_Info/Scoliosis/#normal>.

NEGRINI, S., AULISA, A. G., AULISA, L., CIRCO, A. B., DE MAUROY, J. C., DURMALA, J., GRIVAS, T. B., KNOTT, P., KOTWICKI, T., MARUYAMA,

T., MINOZZI, S., O'BRIEN, J. P., PAPADOPOULOS, D., RIGO, M., RIVARD, C. H., ROMANO, M., WYNNE, J. H., VILLAGRASA, M., WEISS, H.-R. & ZAINA, F. 2012. 2011 SOSORT guidelines: Orthopaedic and Rehabilitation treatment of idiopathic scoliosis during growth. *Scoliosis,* 7**,** 1-35.

NG, J. & RICHARDSON, C. 1994. EMG study of erector spinae and multifidus in two isometric back extension exercises. *Australian Journal of Physiotherapy,* 40**,** 115-121.

NICHOLSON, L., MAHER, C., ADAMS, R. & PHAN-THIEN, N. 2001. Stiffness properties of the human lumbar spine: A lumped parameter model. *Clinical Biomechanics* 16**,** 285-292.

O'SULLIVAN, P. B., GRAHAMSLAW, K. M., KENDELL, M., LAPENSKIE, S. C., M LLER, N. E. & RICHARDS, K. V. 2002. The Effect of Different Standing and Sitting Postures on Trunk Muscle Activity in a Pain-Free Population. *Spine (Phila Pa 1976),* 27**,** 1238-1244.

OLIVA-PASCUAL-VACA, Á., HEREDIA-RIZO, A. M., BARBOSA-ROMERO, A., OLIVA-PASCUAL-VACA, J., RODR GUEZ-BLANCO, C. & TEJERO-GARC A, S. 2014. Assessment of Paraspinal Muscle Hardness in Subjects With a Mild Single Scoliosis Curve: A Preliminary Myotonometer Study. *Journal of Manipulative and Physiological Therapeutics,* 37**,** 326-333.

PARK, G.-Y. & KWON, D. R. 2012. Sonoelastographic Evaluation of Medial Gastrocnemius Muscles Intrinsic Stiffness After Rehabilitation Therapy With Botulinum Toxin A Injection in Spastic Cerebral Palsy. *Archives of Physical Medicine and Rehabilitation,* 93**,** 2085-2089.

Performance Analysis Laboratory 2015, Equipment Myotonometer, online image, School and Graduate Institute of Physical Therapy National Taiwan University, accessed June 2016,
<http://www.pt.ntu.edu.tw/english/index2.asp?main_id=4&sub_id=1#>.

POLAK, J. 2013. Adolescent Idiopathic Scoliosis: A 71 Cases Study Ascertaining that Straightening Is Possible, and a New Etiological Hypothesis. *Asian Spine J,* 7**,** 282-8.

ROMANO, M. & NEGRINI, S. 2008. Manual therapy as a conservative treatment for adolescent idiopathic scoliosis: a systematic review. *Scoliosis,* 3**,** 2.

ROUSSOULY, P., GOLLOGLY, S., BERTHONNAUD, E. & DIMNET, J. 2005. Classification of the normal variation in the sagittal alignment of the human lumbar spine and pelvis in the standing position. *Spine,* 30**,** 346-353.

ROWE, D. E., FEISE, R. J., CROWTHER, E. R., GROD, J. P., MENKE, J. M., GOLDSMITH, C. H., STOLINE, M. R., SOUZA, T. A. & KAMBACH, B.

2006. Chiropractic manipulation in adolescent idiopathic scoliosis: a pilot study. *Chiropr Osteopat,* 14**,** 15.

SAITO, N., EBARA, S., OHOTSUKA, K., KUMETA, H. & TAKAOKA, K. 1998. Natural history of scoliosis in spastic cerebral palsy. *The Lancet,* 351**,** 1687-1692.

SANDERS, G. E. & LAWSON, D. A. 1992. Stability of paraspinal tissue compliance in normal subjects. *Journal of manipulative and physiological therapeutics,* 15**,** 361-364.

SCHL SSER, T., VAN DER HEIJDEN, G., VERSTEEG, A. & CASTELEIN, R. 2014. How 'Idiopathic' Is Adolescent Idiopathic Scoliosis? A Systematic Review on Associated Abnormalities. *PLoS One,* 9.

SCHMID, A. B., DYER, L., B NI, T., HELD, U. & BRUNNER, F. 2010. Paraspinal Muscle Activity During Symmetrical and Asymmetrical Weight Training in Idiopathic Scoliosis. *Journal of Sport Rehabilitation,* 19**,** 315-327.

SCHULTZ, A. B. 1984. Biomechanical Factors in The Progression of Idiopathic Scoliosis. *Annals of Biomedical Engineering,* 12**,** 621-630.

SEFFINGER, M. A., NAJM, W. I., MISHRA, S. I., ADAMS, A., DICKERSON, V. M., MURPHY, L. S. & REINSCH, S. 2004. Reliability of Spinal Palpation for Diagnosis of Back and Neck Pain: A Systematic Review of the Literature. *Spine (Phila Pa 1976),* 29**,** E413-E425.

SHI, N.-N., SHEN, G.-Q., ZHANG, X.-L. & HE, S.-Y. 2009. Holistic View of Chinese Spinal Manipulation and Its Clinical Application. *J. Acupunct. Tuina. Sci,* 7**,** 288-292.

SHIINA, T. 2014. Ultrasound elastography: Development of novel technologies and standardization. *Japanese Journal of Applied Physics,* 53**,** 07KA02.

SHINOHARA, M., SABRA, K., GENNISSON, J. L., FINK, M. & TANTER, M. 2010. Real-time visualization of muscle stiffness distribution with ultrasound shear wave imaging during muscle contraction. *Muscle Nerve,* 42**,** 438-41.

SIMONS, D. G. & MENSE, S. 1998. Understanding and measurement of muscle tone as related to clinical muscle pain. *Pain,* 75**,** 1-17.

ŠIRCA, A. & KOSTEVC, V. 1985. The fibre type composition of thoracic and lumbar paravertebral muscles in man. *Journal of anatomy,* 141**,** 131-137.

SOUCACOS, P. N., ZACHARIS, K., GELALIS, J., SOULTANIS, K., KALOS, N., BERIS, A., ZENAKIS, T. & JOHNSON, E. O. 1998. Assessment of Curve Progression in Idiopathic Scoliosis. *Eur Spine J,* 7**,** 270-277.

STOKES, I. A., BIGALOW, L. & MORELAND, M. S. 1987. Three-Dimensional Spinal Curvature in Idiopathic Scoliosis *Journal of Orthopaedic Research,* 5**,** 103-113.

STOKES, I. A. F. 1994. Three-Dimensioinal Terminology of Spinal Deformity *Spine (Phila Pa 1976),* 19**,** 236-248.

STOKES, I. A. F., ARMSTRONG, J. G. & MORELAND, M. S. 1988. Spinal deformity and back surface asymmetry in idiopathic scoliosis. *Journal of Orthopaedic Research,* 6**,** 129-137.

STOKES, M., HIDES, J., ELLIOTT, J., KIESEL, K. & HODGES, P. 2007. Rehabilitative ultrasound imaging of the posterior paraspinal muscles. *J Orthop Sports Phys Ther,* 37**,** 581-95.

TANIGUCHI, K., SHINOHARA, M., NOZAKI, S. & KATAYOSE, M. 2013. Acute decrease in the stiffness of resting muscle belly due to static stretching. *Scandinavian Journal of Medicine & Science in Sports***,** n/a-n/a.

TONES, M., MOSS, N. & POLLY, D. W. J. 2006. A Review of Quality of Life and Psychosocial Issues in Scoliosis. *Spine,* 31**,** 3027-3038.

TRIBUS, C. B. 2003. Degeneration Lumber Scoliosis: Evaluation and Management. *J Am Acad Orthop Surg,* 11**,** 174-183.

'Vertebral column', 2015, Wikipedia, wiki article, accessed June 2016,<https://en.wikipedia.org/wiki/Vertebral_column>.

VICKERS, A. & ZOLLMAN, C. 1999. The manipulative therapies: osteopathy and chiropractic *BMJ Case Rep,* 319**,** 1176-1179.

WALDORF, T., DEVLIN, L. & NANSEL, D. D. 1991. The comparative assessment of paraspinal tissue compliance in asymptomatic female and male subjects in both prone and standing positions. *Journal of manipulative and physiological therapeutics,* 14**,** 457-461.

WALLWORK, T. L., HIDES, J. A. & STANTON, W. R. 2007. Intrarater and interrater reliability of assessment of lumbar multifidus muscle thickness using rehabilitative ultrasound imaging. *J Orthop Sports Phys Ther,* 37**,** 608-12.

WANG, C., ZHENG, Y., XIAO, Y., QIU, W. & ZHENG, H. 2012. Using vibro-ultrasound method to assess the vastus intermedius stiffness over the entire range of step isometric contraction of knee extensors. *IEEE International Ultrasonics Symposium Proceedings***,** 1351-1354.

WANG, C. Z., LI, T. J. & ZHENG, Y. P. 2014. Shear modulus estimation on vastus intermedius of elderly and young females over the entire range of isometric contraction. *PLoS One,* 9**,** e101769.

WANG, W. J., YEUNG, H. Y., CHU, C. W. W., TANG, L. S. N., LEE, K. M., QIU, Y., BURWELL, R. G. & CHENG, C. Y. J. 2011. Top Theories for the Etiopathogenesis of Adolescent Idiopathic Scoliosis. *J Pediatr Orthop* 31**,** S14-S27.

WEI, Y. 2006. *Chinese Spinal Orthopeadic,* Beijing, People's Medical Publishing

House.

WEINSTEIN, S. L., DOLAN, L. A., CHENG, J. C. Y., DANIELSSON, A. & MORCUENDE, J. A. 2008. Adolescent idiopathic scoliosis. *The Lancet,* 371**,** 1527-1537.

WEINSTEIN, S. L., DOLAN, L. A., SPRATT, K. F., PETERSON, K. K., SPOONAMORE, M. J. & PONSETI, I. V. 2003. Health and Function of Patients With Untreated Idiopathic Scoliosis: A 50-Year Natural History Study. JAMA, 289, 559-567.

WEINSTEIN, S. L., DOLAN, L. A., WRIGHT, J. G. & DOBBS, M. B. 2013. Effects of bracing in adolescents with idiopathic scoliosis. *N Engl J Med,* 369**,** 1512-21.

WEISS, H. R., NEGRINI, S., RIGO, M., KOTWICKI, T., HAWES, M. C., GRIVAS, T. B., MARUYAMA, T. & LANDAUER, F. 2006. Indications for conservative management of scoliosis (guidelines). *Scoliosis,* 1**,** 5.

WELLS, P. N. & LIANG, H. D. 2011. Medical ultrasound: imaging of soft tissue strain and elasticity. *J R Soc Interface,* 8**,** 1521-49.

WILLIAMS II, R. L., JI, W., HOWELL, J. N. & CONATSER JR., R. R. 2007. In Vivo Measurement of Human Tissue Compliance. *2007 SAE Digital Human Modeling Conference DHM1: Advanced Measuring Methods/3D Human Modeling.* Seattle, Washington, USA.

WONG, M. S., CHENG, J. C. Y., LAM, T. P., NG, B. K. W., SIN, S. W., LEE-SHUM, S. L. F., CHOW, D. H. K. & TAM, S. Y. P. 2008. The Effect of Rigid Versus Flexible Spinal Orthosis on the Clinical Efficacy and Acceptance of the Patients With Adolescent Idiopathic Scoliosis. *Spine (Phila Pa 1976),* 33**,** 1360-1365.

YAMAN, O. & DA LBAYRAK, S. 2014. Idiopathic Scoliosis. *Turkish Neurosurgery,* 24**,** 38-52.

YANAGISAWA, O., NIITSU, M., KURIHARA, T. & FUKUBAYASHI, T. 2011. Evaluation of human muscle hardness after dynamic exercise with ultrasound real-time tissue elastography: A feasibility study. *Clinical Radiology,* 66**,** 815-819.

YANG, Y.-T. & ZUO, G. 2015. Forty-Two Cases of Adolescent Scoliosis Treated with Musculature Massage in Combinatino with Bone-Setting Therapy. *Henan Traditional Chinese Medicine,* 35**,** 1343-1344.

YAROM, R. & ROBIN, G. C. 1979. Studies on Spinal and Peripheral Muscles From Patients With Scoliosis. *Spine,* 4**,** 12-21.

YLINEN, J., TEITTINEN, I., KAINULAINEN, V., KAUTIAINEN, H., VEHMASKOSKI, K. & H KKINEN, A. 2006. Repeatability of a

computerized muscle tonometer and the effect of tissue thickness on the estimation of muscle tone. *Physiological measurement,* 27**,** 787-796.

ZAPATA, K. A., WANG-PRICE, S. S., SUCATO, D. J. & DEMPSEY-ROBERTSON, M. 2015. Ultrasonographic Measurements of Paraspinal Muscle Thickness in Adolescent Idiopathic Scoliosis: A Comparison and Reliability Study. *Pediatric Physical Therapy,* 27**,** 119-125.

ZETTERBERG, C., BJ RK, R., ÖRTENGREN, R. & ANDERSSON, G. B. J. 1984. Electromyography of the paravertebral muscles in idiopathic scoliosis: Measurements of amplitude and spectral changes under load. *Acta Orthopaedica,* 55**,** 304-309.

ZHENG, Y. & MAK, A. F. T. 1999. Effective Elastic Properties for Lower Limb Soft Tissues from Manual Indentation Experiment *IEEE Trans Neural Syst Rehabil Eng* [Online], 7.

ZHENG, Y. P., CHOI, Y. K. C., WONG, K., CHAN, S. & MAK, A. F. T. 2000a. Biomechanical assessment of plantar foot tissue in diabetic patients using an ultrasound indentation system. *Ultrasound Med Biol,* 26**,** 451-456.

ZHENG, Y. P., LEUNG, S. F. & MAK, A. F. T. 2000b. Assessment of neck tissue fibrosis using an ultrasound palpation system: a feasibility study. *Medical & Biological Engineering & Computing,* 38**,** 497-502.

ZHENG, Y. P., LI, Z. M., CHOI, A. P., LU, M. H., CHEN, X. & HUANG, Q. H. 2006. Ultrasound palpation sensor for tissue thickness and elasticity measurement--assessment of transverse carpal ligament. *Ultrasonics,* 44 Suppl 1**,** e313-7.

ZHENG, Y. P. & MAK, A. F. T. 1996. An Ultrasound Indentation System for Biomechanical Properties Assessment of Soft Tissues In-Vivo. *IEEE Trans on Biomedical Engineering* 43**,** 912-918.

ZHENG, Y. P., MAK, A. F. T. & LUE, B. 1999. Objective assessment of limb tissue elasticity: Development of a manual indentation procedure. *Journal of Rehabilitation research and Development* 36**,** 71-85.

ZOABLI, G., MATHIEU, P. A. & AUBIN, C. E. 2007. Back muscles biometry in adolescent idiopathic scoliosis. *Spine J,* 7**,** 338-44.